

AD-A040 033

AERONUTRONIC FORD CORP WILLOW GROVE PA WILLOW GROVE--ETC F/G 17/2
VIDEO IMAGE BANDWIDTH REDUCTION/COMPRESSION STUDY.(U)
FEB 76 E SCHMIDT, W SPICER, H WATKINS F33657-75-C-0353

UNCLASSIFIED

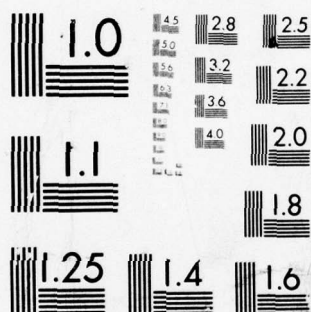
ASD-TR-76-36

NL

1 OF 2

AD
A040033





MICROCOPY RESOLUTION TEST CHART
NATIONAL BUREAU OF STANDARDS-1963-A

(12) 4

AD A 040033

Report F33657-75-C-0353-A005

VIDEO IMAGE BANDWIDTH REDUCTION/COMPRESSION STUDY

FINAL REPORT

Ernest Schmidt
William Spicer
Harry Watkins
Dr. Paul Wintz
Richard Yutz

409 766

Aeronutronic Ford Corporation
~~Western Development Laboratories Division~~
Willow Grove Operation
3900 Welsh Road
Willow Grove, Pennsylvania 19090

1 October 1976

DDC
RECEIVED
MAY 31 1977
RECEIVED

Prepared for

UNITED STATES AIR FORCE
AERONAUTICAL SYSTEMS DIVISION (AFSC)
WRIGHT-PATTERSON AFB, OHIO 45433

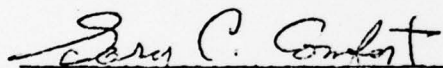
APPROVED FOR PUBLIC
RELEASE
Distribution Unlimited

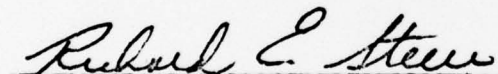
AD No. _____
DDC FILE COPY

When Government drawings, specifications, or other data are used for any purpose other than in connection with a definitely related Government procurement operation, the United States Government thereby incurs no responsibility nor any obligation whatsoever; and the fact that the government may have formulated, furnished, or in any way supplied the said drawings, specifications, or other data, is not to be regarded by implication or otherwise as in any manner licensing the holder or any other person or corporation, or conveying any rights or permission to manufacture, use, or sell any patented invention that may in any way be related thereto.

This report has been reviewed by the Information Office (IO) and is releasable to the National Technical Information Service (NTIS). At NTIS, it will be available to the general public, including foreign nations.

This technical report has been reviewed and is approved for publication.


GARY C. COMFORT, MAJ, USAF
Program Manager


RICHARD E. STEERE, COL, USAF
Director, RPV SPO
Deputy for RPV/ALSM

Unclassified

SECURITY CLASSIFICATION OF THIS PAGE (When Data Entered)

REPORT DOCUMENTATION PAGE		READ INSTRUCTIONS BEFORE COMPLETING FORM	
1. REPORT NUMBER F33657-75-C-0353-A005	2. GOVT ACCESSION NO.	3. RECIPIENT'S CATALOG NUMBER 9 18 ASD 19 TR-76-36	
4. TITLE (and Subtitle) Video Image Bandwidth Reduction/Compression Study, Final Report		5. TYPE OF REPORT & PERIOD COVERED Final Report, for period Jan 1975 - Dec 1975	
7. AUTHOR(s) Ernest/Schmidt, Paul Wintz William/Spicer, Richard Yutz Harry/Watkins		8. CONTRACT OR GRANT NUMBER(s) F33657-75-C-0353 new	
9. PERFORMING ORGANIZATION NAME AND ADDRESS Aeronutronic Ford Corporation 3900 Welsh Road Willow Grove, Pa. 19090		10. PROGRAM ELEMENT, PROJECT, TASK AREA & WORK UNIT NUMBERS CLIN 0002 CDRL A005	
11. CONTROLLING OFFICE NAME AND ADDRESS USAF Aeronautical Systems Division (AFSC) ASD/YMKS Wright-Patterson AFB Ohio 45433		12. REPORT DATE 13 Feb 1976	
14. MONITORING AGENCY NAME & ADDRESS (if different from Controlling Office) 12156p		13. NUMBER OF PAGES 159	
		15. SECURITY CLASS. (of this report) UNCLASSIFIED	
16. DISTRIBUTION STATEMENT (of this Report) ASD/YMRC 5/0 AMRL/HED 1/0 AFAL/AAA 1/0 DDC 12/0 TAC/DRR 1/0		18a. DECLASSIFICATION/DOWNGRADING SCHEDULE	
17. DISTRIBUTION STATEMENT (of the abstract entered in Block 20, if different from Report)		18. SUPPLEMENTARY NOTES	
19. KEY WORDS (Continue on reverse side if necessary and identify by block number) Remotely Piloted Vehicles Computer Simulation Video Bandwidth Compression Digital Processing		<div data-bbox="1193 924 1518 1354"> <p>ABSTRACT for</p> <p>NTIS White Section <input checked="" type="checkbox"/></p> <p>DDC Both Sections <input type="checkbox"/></p> <p>UNANNOUNCED <input type="checkbox"/></p> <p>JUSTIFICATION</p> <p>BY</p> <p>DISTRIBUTION/AVAILABILITY CODES</p> <p>Dist. Point and M. SPECIAL</p> <p>A</p> </div>	
20. ABSTRACT (Continue on reverse side if necessary and identify by block number) This report covers the development, simulation, evaluation, and implementation design of a video bandwidth reduction/compression technique for use in remotely piloted vehicle systems. The bandwidth reduction technique discussed is frame rate reduction. The range of frame rates from 8 per second to 1/4 per second are evaluated.			

DD FORM 1 JAN 73 1473

EDITION OF 1 NOV 65 IS OBSOLETE

409 766
SECURITY CLASSIFICATION OF THIS PAGE (When Data Entered)

20. (Continued)

The bandwidth compression technique selected is cosine transform/DPCM encoding. A range of parameters are evaluated; final parameters which provide satisfactory performance even under high error rate conditions are 512 elements per scan line, 480 scan lines per frame, one frame per second and one bit per picture element. Under these conditions the baseband bandwidth is under 250 kHz using the conservative assumption of one bit per Hertz.

The design of a computer and I/O facility for generation of video tapes simulating compression as applied to USAF provided flight film strips is described. Ten parameter variations were applied to each of ten film strips.

The resultant simulations were each evaluated by 8 observers (military pilots). The results from which optimum parameters are defined are included. Results for the optimum parameters are:

Simulation	Mean (To Target)		Standard Deviation	
	Time (SEC)	Slant Range (FT)	Time (SEC)	Distance (FT)
Baseline (PCM, 24FPS)	18.1	12,579	1.47	1,014
Cosine/DPCM				
512 x 1; BER = 0	15.8	11,005	1.13	780
EL/Line Bit/PEL				
512 x 1; BER = 10^{-4}	15.1	10,526	1.52	1,049
512 x 1; BER = 10^{-3}	14.7	10,253	1.38	952
512 x 1; BER = 10^{-2}	13.0	9,095	0.97	669

An all-digital implementation of the coder is developed which provides high reliability and minimizes the need for maintenance and adjustment under field conditions. With a reasonable amount of LSI circuitry only two 5" x 10" PC boards and a miniature power supply are required. The anticipated volume is 150 cubic inches and power dissipation is 31 watts.

An analog implementation is presently being developed which will require only one 4" x 8" PC board and will consume less than 10 watts.

20. (Continued)

A sensor which can be read out at slow frame rates is recommended, particularly the presently emerging solid state devices. If it is necessary to use the encoder with a conventional TV camera, a frame memory is recommended. This device adds 90 cubic inches and 35 watts to the above estimate.

If target tracking is required, the frame rate should be raised to 8 frames per second, while a reduction in resolution to 256 x 240 appears satisfactory due to the usual decrease in field of view. Therefore, with the same coding algorithm, the baseband bandwidth still remains under 450 kHz.

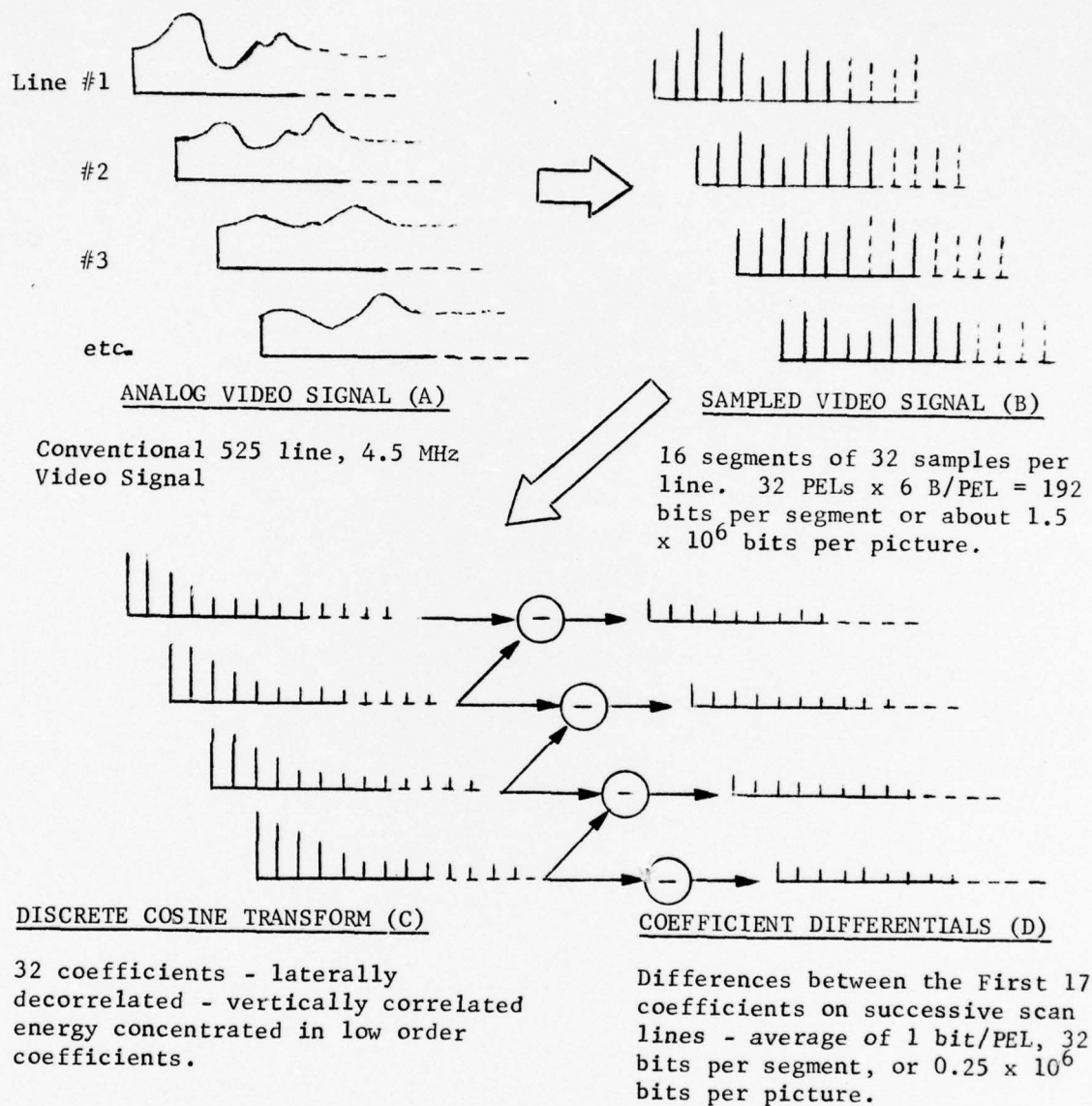
Summary

The program objective was to develop a video bandwidth reduction and compression system which would permit the use of anti-jam protection of the video transmission channel of a remotely piloted vehicle (RPV). The technique which was developed uses low camera frame rate for bandwidth reduction (relative to the conventional T.V. frame rate of 30 per second). A frame rate of one per second was found to be optimum by "flying" simulated missions using Air Force supplied film strips as input material.

The selected bandwidth compression technique uses a combination of Cosine Transform Encoding and Differential Pulse Code Modulation (DPCM). Figure 1 shows how video generated by line scanning (Figure 1-A) is first sampled to form discrete Picture Elements (PELS) as in Figure 1B. Horizontal segments of 32 PELS are subjected to a discrete cosine transform which operates on the PELS with a succession of cosine terms harmonically related to the segment length. The result is a series of cosine term coefficients with an amplitude distribution as shown in Figure 1-C. The statistics of the coefficients is such that the amplitudes of the lower frequency terms are greatest, hence the transform spectrum "energy" is concentrated at the lower frequencies. Fortunately, it is possible to truncate the coefficients by dropping higher frequency terms with minimal effect on picture quality. Also, when the coefficients are digitized, additional savings can be realized by amplitude quantizing the higher frequency terms to low precision.

The transform coefficients have a high degree of vertical (line-to-line) correlation and hence their differences are small (Figure 1-D). DPCM, which encodes differences, is a highly efficient method for transmitting the transform coefficients. In the present system, DPCM encodes the difference between the values of a particular transform coefficient of two vertically adjacent segments. Proper selection of DPCM parameters for each coefficient results in bandwidth saving.

For the system developed on the present program an average of one bit per PEL is adequate to produce performance comparable to 6 bit per PEL Pulse Code Modulation (PCM), the system usually used as a basis for comparing compression techniques.



COSINE TRANSFORM/DPCM ENCODING

Figure 1

A laboratory T.V. facility was constructed to simulate the entire system including the cosine transform/DPCM encoder and decoder and also a data link with error contamination. All system parameters such as frame rate, resolution, encoding precision, DPCM prediction coefficient, transform parameters and data link bit error rate could be and in fact were varied during the program. Simulator output was stored on video tape. Input video was generated from Air Force supplied film strips taken during flight over terrain containing typical targets.

Performance of the Cosine Transform/DPCM system was measured by having trained military flight officers "fly" simulated missions using the video tapes described in the previous paragraph as input material.

The final system parameters were selected by a three step process. In a first truncation effort single frames from the Air Force film strips were processed and recorded as photographic positives. Project staff personnel viewed these photos and selected those prints which retained the best target discrimination among the various combinations of parameters.

A second truncation further narrowed the possible parameter values. Laboratory personnel flew simulated missions using video tapes and also viewed static scenes to determine limits of error rate which could be tolerated.

The first two truncations produced a narrow range of parameters which were used in detailed, statistically meaningful simulated RPV flights by military flight officers. The subjects read a prepared Air Force statement, received a verbal briefing and then viewed a simulated mission on a TV monitor. The time interval between start of run and recognition of the target was recorded for each subject. Each run of a given set of parameters used 8 subjects and 12 different film strips, two of which were used to train the subjects.

Aeronutronic Ford developed an all-digital implementation of the overall system because such a system would require no adjustment, would be insensitive to environmental conditions, and would be easy to repair by plug-in replacement. An optional frame memory is included for presently available cameras which operate at a high frame rate. With large scale integration (LSI), two 5" x 10" boards and a miniature power supply would be required with a resultant volume of 150 cubic inches and 31 watts of power. The optional memory would add 90 cubic inches and 35 watts.

LSI development would be approximately \$600,000. Production costs per unit in 50 unit quantity would be \$1900 per airborne unit (no-memory) and \$19,000 per ground terminal.

Aeronutronic Ford is presently developing an implementation which would require only one 4" x 8" board, would consume less than 10 watts of power and is estimated to cost approximately \$1200 per unit in production.

TABLE OF CONTENTS

1.0	INTRODUCTION	1-1
2.0	REDUCTION/COMPRESSION ALGORITHM	2-1
2.1	Comparison of Compression Techniques	2-1
2.1.1	Adaptive Compression Techniques	2-1
2.1.2	Non-Adaptive Compression Techniques	2-1
2.1.3	Selection of the Candadate Compression Technique	2-2
2.2	Bandwidth Reduction	2-2
2.2.1	Frame Rate	2-2
2.2.2	Supplemental Bandwidth Reduction Techniques	2-3
2.3	Cosine Transfrom/DPCM Coding	2-5
2.3.1	Foundations	2-5
2.3.2	Implementation	2-7
2.3.2.1	Discrete Cosine Transform	2-7
2.3.2.2	DPCM Coding	2-11
3.0	TASK A - SIMULATION FACILITY	3-1
3.1	General Description	3-1
3.1.1	Input/Output Characteristics	3-1
3.2	Detailed Description	3-3
3.2.1	Input Circuitry	3-3
3.2.1.1	Camera and CCU	3-3
3.2.1.2	Video Input Circuits	3-3
3.2.1.3	Sample and Hold (Philco 9SK9278)	3-3
3.2.1.4	Analog-to-Digital (A/D) Converter (Philco 9SK9279)	3-5
3.2.1.5	Solid State Frame Memory	3-5
3.2.1.6	Input Line Buffer	3-5
3.2.2	Processor/Digital Tape Recorder	3-6
3.2.3	Output Circuitry	3-6
3.2.3.1	Output Line Buffer	3-6
3.2.3.2	Digital-to-Analog (D/A) Converter	3-6
3.2.3.3	Video Processing Circuits	3-7

TABLE OF CONTENTS (CONTINUED)

3.2.4	Video Disc Recorder and Video Tape Recorder	3-7
3.2.4.1	Video Disc Recorder	3-7
3.2.4.2	Video Tape Recorder (VTR)	3-7
3.2.5	System Timing	3-8
3.2.5.1	Line Select Logic	3-8
3.2.5.2	Capture Logic	3-8
3.2.5.3	Film Advance Logic	3-8
3.2.5.4	Video Disc and Video Tape Recorder Control . .	3-9
4.0	TASK B - EXPERIMENT DESCRIPTION	4-1
4.1	Purpose	4-1
4.2	Test Procedures	4-2
4.2.1	First Truncation Methodology	4-2
4.2.2	Second Truncation Methodology	4-5
4.2.3	Final Test Methodology	4-5
4.3	Test Subject Qualifications	4-5
4.4	Testing Methods	4-6
4.4.1	Test Orientation	4-6
4.4.2	Pre-Mission Briefing	4-6
4.5	Test Environment	4-8
5.0	TASK C - IMAGE QUALITY EVALUATION	5-1
5.1	Introduction	5-1
5.2	Truncation Results	5-1
5.2.1	Initial Conditions	5-1
5.2.2	Reduced Conditions	5-1
5.2.2.1	Frame Rate	5-2
5.2.2.2	Resolution	5-2
5.2.2.3	Coding Block Size	5-3
5.2.2.4	Bit Assignments	5-3
5.2.2.5	Determination of Prediction Coefficient	5-4
5.2.2.6	Summary of Reduced Conditions	5-4
5.2.3	Final Test Conditions	5-5
5.2.3.1	Frame Rates	5-5
5.2.3.3	Resolution	5-6
5.2.3.4	Coding Block Size	5-6
5.2.3.5	Bit Assignments	5-6
5.2.3.6	Prediction Coefficients	5-6
5.2.3.7	Summary of Final Test Conditions	5-8

TABLE OF CONTENTS (CONTINUED)

5.3	Final Test Results	5-9
5.3.1	Data Generation	5-9
5.3.1.1	Time to Detect	5-9
5.3.1.2	Time from Start to Ground Zero	5-9
5.3.1.3	Detect to Ground Zero	5-10
5.3.1.4	Slant Range	5-10
5.3.2	Data Presentation	5-10
5.3.2.1	Median Scores for Test Conditions	5-10
5.3.2.2	Slant Range at Target Detection	5-14
5.4	Analysis of the Final Test Results	5-15
5.4.1	Maximum Slant Range	5-15
5.4.2	Baseline Data	5-15
5.4.3	The 512 x 1 Simulations	5-16
5.4.4	The 256 x 2 Simulations	5-17
5.4.5	Interpolation	5-17
5.4.6	The 512 x 0.75 Simulations	5-18
5.5	Conclusions	5-18
5.6	Statistical Analysis	5-18
6.0	TASK D - IMPLEMENTATION STUDY	6-1
6.1	Introduction	6-1
6.2	RPV Video Compressor Implementation	6-4
6.2.1	Principles of Operation	6-4
6.2.1.1	Sensor and Video Preprocessing	6-5
6.2.1.1.1	Automatic Gain Control	6-5
6.2.1.1.2	Filtering	6-7
6.2.1.2	Analog to Digital Converter	6-7
6.2.1.3	Transmitter Frame Memory	6-8
6.2.1.4	Transform Coder	6-8
6.2.1.5	Digital DPCM Encoder	6-10
6.2.1.6	Sync Addition	6-12
6.2.1.7	Power Supply	6-12
6.2.2	Hardware	6-13
6.2.3	Alternate Approaches	6-16
6.3	Control Center Implementation	6-19
6.3.1	Principle of Operation	6-19

TABLE OF CONTENTS (CONTINUED)

6.3.1.1	Sync Decoder	6-19
6.3.1.2	DPCM Decoder	6-21
6.3.1.3	Transform Decoder	6-21
6.3.1.4	Dual Frame Memory	6-22
6.3.1.5	Digital-to-Analog Converter	6-22
6.3.1.6	T.V. Monitor	6-23
6.3.1.7	System Control and T.V. Sync Generator	6-23
6.3.2	Ground Based Control Station Hardware	6-23
6.3.3	Airborne Control Station Hardware	6-24
6.4	Airborne Relay Processing	6-25
6.5	Interface with Maverick and Stubby Hobo	6-25
6.6	Reliability and Maintainability Estimates	6-26
6.6.1	System Mean-Time-Between-Failure (MTBF)	6-26
6.6.2	Airborne RPV System MTBF	6-26
6.6.2.1	Frame Memory	6-29
6.6.3	Ground Display System MTBF	6-29
6.6.4	Equipment Failure Rate Estimates	6-32
6.6.5	Maintainability	6-33
6.6.5.1	RPV Equipment Maintainability	6-33
6.6.5.2	Ground Display System Maintainability	6-33
6.6.5.3	Off-Line Repair	6-34
6.7	Cost of Implementation	6-34
6.7.1	Basis of Cost Analysis	6-34
6.7.2	Non-Recurring Costs	6-36
6.7.3	Per-Unit Production Cost of RPV and Ground Equipment	6-36
6.8	Potential Hazards	6-39
6.9	Operational Constraints	6-40
7.0	CONCLUSIONS AND RECOMMENDATIONS	7-1
7.1	Coding Algorithm	7-1
7.2	Implementation	7-1
7.3	Sensor	7-1

TABLE OF CONTENTS (CONTINUED)

	Page
APPENDIX A Line and Frame Synchronization Analysis	A-1
APPENDIX B Supplemental Data for the RPV Image Bandwidth Reduction/Compression Study Program	B-1
APPENDIX C Video Compression Evaluation Orientation.	C-1
APPENDIX D Statistical Analysis of Test Data	D-1

LIST OF ILLUSTRATIONS

Figure		Page
1	Cosine Transform/DPCM Encoding.	2
2-1	Block Diagram of Hybrid Compression System.	2-7
3-1	Block Diagram - Video Compression Simulation Facility	3-2
3-2	Simulation Facility	3-4
4-1	Truncation Flow Chart	4-3
4-2	Final Test Flow Chart	4-4
4-3	Briefing Panel.	4-7
5-1	Selection of Final Encoding Bit Assignments	5-7
5-2	Slant Range at Target Detection	5-12
6-1	RPV Video System Block Diagram.	6-2
6-2	AGC Circuit	6-6
6-3	Transform Coder Block Diagram	6-9
6-4	Digital DPCM Encoder Block Diagram	6-11
6-5	Mechanical Configuration of Airborne Compression Equipment (Cover Removed)	6-14
6-6	Analog Cosine Transform/DPCM Coder.	6-18
6-7	Ground Control Station Block Diagram.	6-20
6-8	RPV Video System Reliability Math Model	6-27
6-9	Airborne RPV Compression System Reliability Math Model. . . .	6-28
6-10	Transmitter Frame Memory MTBF Math Model.	6-30
6-11	Ground Compression System Reliability Math Model.	6-31
B-1	Graphical Presentation of Mean and Deviation for All Simulations	B-14
B-2	Statistical Summary of Simulation Results	B-15
D-1	Plot of Means and Sample Standard Deviations.	D-14
D-2	Means and Estimates of Standard Deviation of Means.	D-16

LIST OF TABLES

Table		Page
2-1	Bit Distribution as a Function of Coefficient #	2-12
2-2	Quantitization Levels as a Function of Bit Precision.	2-14
4-1	Reduction/Compression Parameters.	4-1
5-1	Median Scores for Test Conditions	5-11
6-1	Transmitter Board Complement.	6-15
6-2	Range of Typical IC Quality & Resultant Cost.	6-35
6-3	Non-Recurring Development Costs	6-37
6-4	Fifty Quantity Production Costs	6-38
B-1	Data for Baseline Simulation.	B-2
B-2	Data for 512 x 1, BER = 0 Simulation.	B-3
B-3	Data for 512 x 1, BER = 10^{-4} Simulation	B-4
B-4	Data for 512 x 1, BER = 10^{-3} Simulation	B-5
B-5	Data for 512 x 1, BER = 10^{-2} Simulation	B-6
B-6	Data for 512 x 0.75, BER = 0 Simulation	B-7
B-7	Data for 512 x 0.75, BER = 10^{-3} Simulation.	B-8
B-8	Data for 256 x 2, BER = 0 Simulation.	B-9
B-9	Data for 256 x 2, BER = 10^{-3} Simulation	B-10
B-10	Data for 256 x 2, BER = 0, Interpolated Simulation.	B-11
B-11	Data for Each Simulation.	B-12
B-12	Tabulation of Mean and Deviation for all Simulations.	B-13
D-1	Slant Range at Detection for Baseline - Data from Table B-1 .	D-3
D-2	Slant Range at Detection for 512 x 1, BER = 0, Data from Table B-2	D-4
D-3	Slant Range at Detection for 512 x 1, BER = 10^{-4} - Data from Table B-3.	D-5
D-4	Slant Range at Detection for 512 x 1, BER = 10^{-3} - Data from Table B-4.	D-6

LIST OF TABLES (CONTINUED)

Table		Page
D-5	Slant Range at Detection for 512×1 , $BER = 10^{-2}$ - Data from Table B-5	D-7
D-6	Slant Range at Detection for 512×0.75 , $BER = 0$ - Data from Table B-6	D-8
D-7	Slant Range at Detection for 512×0.75 , $BER = 10^{-3}$ - Data from Table B-7.	D-9
D-8	Slant Range at Detection for 256×2 , $BER = 0$ - Data from Table B-8	D-10
D-9	Slant Range at Detection for 256×2 , $BER = 10^{-3}$ - Data from Table B-9.	D-11
D-10	Slant Range at Detection for 256×2 , $BER = 0$, Interpolation Data from Table B-10	D-12

1.0 INTRODUCTION

This report describes the Video Image Bandwidth Reduction/Compression Study (USAF Contract F33657-75-C-0353) as performed by the Communication Systems Division of Aeronutronic Ford. The results obtained are presented in detail.

The objective of this program is to develop a video bandwidth reduction and compression technique suitable for use in remotely piloted vehicle systems. The purpose of reducing the video system bandwidth is to make possible anti-jam protection on the RPV video data link. The performance of the reduction/compression technique is demonstrated and verified by computer simulation.

The Video Image Bandwidth Reduction/Compression Study consists of four tasks as outlined below and described in detail in subsequent sections of this report.

Task A - Preparation of the Simulation

This task includes the design and assembly of the simulation equipment used to demonstrate the bandwidth reduction/compression technique.

Task B - Experimental Design and Test Plan

Under this task a detailed experimental design plan was developed for collection and analysis of human subject responses to the simulator presentations.

Task C - Image Quality Analysis

The simulations of the reduction/compression technique generated with the equipment prepared in Task A were evaluated by gathering subjective responses according to the test plan developed in Task B.

Task D - Implementation Study

A practical implementation of the reduction/ compression technique was developed and a cost estimate prepared.

2.0 REDUCTION/COMPRESSION ALGORITHM

2.1 COMPARISON OF COMPRESSION TECHNIQUES

2.1.1 Adaptive Compression Techniques

Adaptive video compression techniques essentially adjust themselves to the statistics of the video signal being transmitted. As a result, the number of bits per picture element can vary considerably within a single frame, depending on picture content. If the frame rate is maintained constant, the data bit rate will therefore vary with picture content. Adaptive video compression techniques are potentially capable of providing considerably higher compression than non-adaptive compression techniques. However, the statistic dependent number of bits per picture element and the variable output data rate produce a serious drawback for the remotely piloted vehicle application. The disadvantage is that picture element rate, line rate, and possibly frame rate, are no longer cyclic. If the bit rate were constant, as in the non-adaptive system, vital timing parameters, such as end of line, end of frame, etc., can be anticipated in the ground display system once synchronization is established, even in the presence of jamming or loss of sync due to other causes. Conversely, the adaptive system cannot anticipate sync data and integrate a number of predictable sync codes.

Among the compression techniques which are adaptive by nature are Run Length and Bit Plane Run Length Encoding. Other techniques can be made adaptive at the cost of considerable increase in hardware complexity.

2.1.2 Non-Adaptive Compression Techniques

The non-adaptive compression techniques have a feature in common which is highly desirable in an RPV system; namely, the bit rate and the number of bits per picture element are constant. This feature is desirable in that the system, once synchronized, is highly tolerant to temporary loss of synchronization information due to any cause, including jamming.

If data clock integrity is maintained during jamming, the receiver video sync circuits can continue to count data clock pulses and stay correctly referenced to the transmitter video sync generator. To ensure this sync continuity a Loss of Spread Spectrum Sync signal, if available from the spread spectrum receiver, can force the video sync circuits to assume that they are locked. True, as in any system, video data will be lost during a loss of spread spectrum sync. However, correct video will very quickly be obtained as soon as spread spectrum receiver sync is restored. At worst, a minor line sync correction might be necessary. This is considerably better than requiring complete video resynchronization as would be the case with an adaptive compression system. This resync operation could take several one-second frame intervals.

The most common of the non-adaptive coding techniques are Differential Pulse Code Modulation (DPCM), Interpolation, Prediction, and the more recently developed category of Transform Coding.

2.1.3 Selection of the Candidate Compression Technique

For a given number of bits per picture element, adaptive and non-adaptive coding techniques provide approximately equivalent picture quality. Adaptive techniques can reduce the required bit rate when the picture statistics permit, while the non-adaptive technique requires the same bit rate as required for a more complex picture. However, this constant bit rate is considered desirable for the RPV application because of the degree of sync independence provided. Therefore, a non-adaptive compression technique was selected.

Aeronutronic Ford has, over the past 15 years, developed a comprehensive library of photographs of the results of a wide variety of compression techniques, whether simulated by computer or produced by actual hardware. To this were added photographs processed by transform coding algorithms, in particular the Cosine Transform/DPCM coding. This formed a data base from which to select the candidate compression technique. In addition, the literature on the subject was thoroughly reviewed.

The factors brought to bear in the selection of the candidate technique from this data base included efficiency (picture quality versus bits per picture element), complexity (amount of hardware required to implement the encoder), and susceptibility to channel errors. The result of this evaluation was the selection of the Cosine Transform/DPCM compression technique as the subject for the RPV Sensor Image Bandwidth Reduction/Compression Study.

2.2 BANDWIDTH REDUCTION

Bandwidth reduction for purposes of the study program was defined as any method which provides a reduction in the amount of data that must be transmitted other than that coding algorithm which operates directly on the video signal to remove the intraframe redundancy.

2.2.1 Frame Rate

Based on the reported results of other evaluations of observer performance as a function of frame rate, and verified by this study, it was determined that 30 motion frames per second are in excess of that required for the RPV application. It is essential that the physical display be refreshed at 30 frames per second to provide adequate luminance together with flicker-free performance; however, the displayed data can be updated less frequently and still support adequate observer performance.

Frame rates between 8 and 1/4 frames per second were initially considered as the range to be investigated as described in Section 5.

Note that reducing the frame rate is independent of target location, size, or contrast. Vehicle velocity is the only dependent feature. For a given altitude and flight profile, the required motion frame rate varies with vehicle velocity. The evaluations in this program were performed at simulated equivalent velocity of about 410 knots.

Frame rate reduction was found to be a viable method of bandwidth reduction.

In the study the 24 frame per second motion picture films were electronically processed and displayed to the subjects at reduced frame rates. The subjective performance achieved verifies that reduction of the transmitted and displayed frame rate is a satisfactory method of bandwidth reduction for briefed targets.

2.2.2 Supplemental Bandwidth Reduction Techniques

Other methods of bandwidth reduction were considered. They can be divided into two categories; those which affect the video signal, and those which require peripheral equipment and processes.

The bandwidth reduction techniques which operate directly on the video signal include (among others) variable resolution and reduced gray scale. Resolution in itself was one of the simulation parameters; that is, the image resolution was varied to determine performance, but was homogenous within a frame. It may be postulated that the resolution need not be kept homogenous within a frame, but could be reduced considerably at the edges. This technique is commonly known as foveal viewing. In fact, the higher resolution area of the field of view (foveal area) can be made positionable under control of the ground pilot.

Critical examination of the test film revealed two features which mediated against the recommendation of the foveal technique. First, the target often became initially identifiable at the edge of the film frame which in a foveal implementation would naturally be the lower resolution region and, therefore, identification would be delayed. This delay would be the same as if the entire field of view were displayed at the reduced resolution. Second, the erratic aircraft motion often caused the target to jump from one region of the display to another during the time when it was just beginning to be identifiable. The effect of the reduced resolution might again cause delays in the identification of the target to the same extent as reduced resolution over the entire field of view.

If the RPV flight path and stability can be planned and controlled to cause the target to appear in the foveal region, the lower resolution region might be useful for bandwidth reduction. However, that this is possible is not apparent from the film strips. If a better controlled flight path is possible, then the foveal concept can be implemented with most compression techniques, including cosine transform/DPCM coding.

When a foveal window which can be positioned by the operator is subject to the same analysis as above, there is an added problem in that if an erroneous initial target location is made and the window used to track it, the true target has a high probability of appearing in a low resolution area. Again, this concept is also implementable using cosine transform/DPCM coding.

Based on the above rationale, foveal viewing was not included in the simulations.

Zoom, the controlled change in the viewing angle, appears to have considerable merit. However, zooming requires an a priori knowledge of the target location and then, not only must the field of view be altered, but, it is likely that the direction of the optical axis must also be changed to center the narrower field of view around the target. The goal of this study is to compress the system base bandwidth without adversely affecting time to detect the target. But it is not until after this initial detection that zoom can be profitably employed. Now, if after the time has been spent in accomplishing zoom and redirecting the optical axis on becoming oriented to the narrow field of view, it is determined that an incorrect identification has been made, as verified by the zoom view, the time lost together with that required for reorientation to the full field of view can result in loss of the target. This conclusion was reached from examining the film strip. Furthermore, zoom is provided by switching to the Maverick or Hobo weapon sensors, if desired.

Based on the above rationale, zoom was not included as a study parameter, although simulations of the zoom function were made.

Grey scale ranges or step sizes can be varied to reduce the number of bits required to describe a picture element. In the cosine transform/DPCM coding simulations it was decided to vary the DPCM coding precision instead, which produces a related effect.

As far as cueing aids such as correlators or pattern recognition are concerned, the variety of the specific targets depicted in the film strips indicates that the sophistication of these devices, to be useful, is far beyond the scope of this program. Therefore, they were not considered for simulation.

On the other hand, although not simulated, Charge Coupled Device (CCD) cameras and stabilized gimballed mounts are expected to be highly desirable. The CCD cameras provide simple snapshot, and slow readout features. The stabilization removes the inherent jerkiness due to extraneous aircraft motion, while gimbaling permits following the target for additional verification.

2.3 COSINE TRANSFORM/DPCM CODING

2.3.1 Foundations

On the basis of fixed bit rate, encoding efficiency, ease of implementation, and natural noise immunity, the technique selected is a hybrid of two compression techniques, each complementing the other. The natural element-to-element correlation inherent in pictures is exploited by horizontal one dimensional cosine transform coding. Differential Pulse Code Modulation (DPCM) coding is then used to take advantage of line-to-line correlation of the transform coefficients. Immunity to channel errors is effected by the proper selection of the DPCM prediction coefficient. Recent advances in integrated circuit technology will make a low cost, minimal volume implementation of this technique practical.

Both DPCM and transform coding have been used with considerable success for coding pictorial data. Both systems have some attractive characteristics and some limitations. The transform techniques achieve superior coding performance at lower bit rates (moderate distortion levels). They show less sensitivity to data statistics (picture-to-picture variations) and distribute the coding degradation in a manner less objectionable to a human viewer, and so are less vulnerable to channel noise and jamming. On the other hand, DPCM systems, when designed to take advantage of spatial correlations of the data, achieve a better coding performance at a higher bit rate (low distortion levels). The equipment complexity and the delay due to coding operation is minimal, and the system does not require the memory needed in two dimensional transform coding systems. Perhaps the most desirable characteristics of this system are

the ease of design and the speed of the operation that has made the use of DPCM systems popular in real time coding of television signals. The limitations of this system are the sensitivity of the DPCM systems to picture statistics, and the propagation of the channel errors.

The selected candidate compression technique is a hybrid system consisting of a cascade of a unitary transformation, followed by a DPCM transformation to achieve the desired compressed bandwidth for the baseband RPV signal. The hybrid system combines the attractive features of both transform and DPCM coding, thus achieving good coding capabilities without many of the limitations of either system. This system exploits the correlation of the picture data in the horizontal direction by taking a one-dimensional transform of each picture line in segments. It then operates on each column of the transformed data using a DPCM system. The DPCM system quantizes the signal in the transform domain where it takes advantage of the vertical correlation of the transformed data to reduce the coding error. The unitary transformation involved is a one-dimensional transformation of individual lines of the pictorial data, thus the equipment complexity and the number of computational operations is considerably less than is involved in a two-dimensional transformation. Habibi⁽¹⁾ initially studied this system in considerable detail; he found, and the results of this study confirm, that the visual effect of small or moderate levels of channel error was negligible, and that the degradation in signal-to-noise ratio performance was also small. These advantages; simplicity, minimal hardware, excellent performance, make the hybrid system particularly suited for airborne (RPV) installation.

-
1. Habibi, A. "Hybrid Coding of Pictorial Data," Comm. Tech., COMM-22, pp. 614-624, May 1974.

2.3.2 Implementation

A block diagram of the hybrid approach is shown in Figure 2-1. The pictorial data is raster scanned to form N lines with appropriate vertical resolution, then each line is sampled at an appropriate rate.

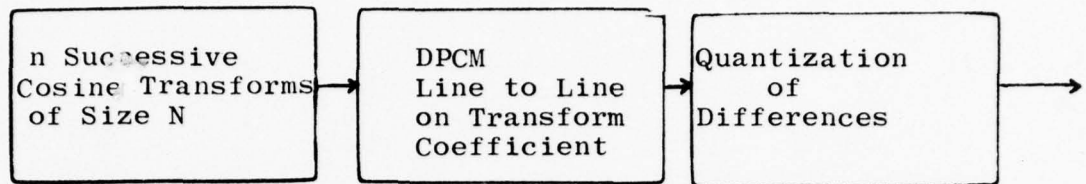


Figure 2-1 Block Diagram of Hybrid Compression System

When the video line is sampled at the rate of P pels per line, and N is chosen to be an integer such that these are $n (= P/N)$ segments in P . A cosine transform of size N is performed on each n th segment. From line to line the coefficients of corresponding segments are encoded in a DPCM quantizer and a code word generated for each differenced value. In the synthesizer the inverse functions are performed to reconstruct the video segment. The code words are converted to differences and accumulated in a bank of integrators. The integrator outputs become the input to the universe transform which generates a segment of the video line. Juxtaposition of the successive segments creates the composite video line.

2.3.2.1 Discrete Cosine Transform

Two different types of discrete cosine transform (DCT) are useful for reduced redundancy television image transmission. Both are obtained by extending the length N data block to have even symmetry, taking the discrete Fourier transform (DFT) of the extended data block, and saving N terms of the resulting DFT. Since the DFT of a real even sequence is a real even sequence, either DCT is its own inverse if a normalized DFT is used.

The "Odd DCT" (ODCT) extends the length N data block to length $2N-1$, with the middle point of the extended block as a center of even symmetry. The "Even DCT" (EDCT) extends the length N data block to length $2N$, with a center of even symmetry located between the two points nearest the middle. For example, the odd length extension of the sequence $A B C$ is $C B A B C$, and the even length is $C B A A B C$. In both cases, the symmetrization eliminates the jumps in the periodic extension of the data block which would occur if one edge of the data block

had a high value and the other edge had a low value; in effect it performs a sort of smoothing operation with no loss of information. It will be noted that the terms "odd" and "even" in ODC and EDCT refer only to the length of the extended data block - in both cases the extended data block has even symmetry.

Both types of DCT may be implemented using compact, high speed, serial access hardware, in structures similar to those which have been described for the Chirp-Z transform (CZT) implementation of the DFT.⁽²⁾

Let the data sequence be g_0, g_1, \dots, g_{N-1} . The ODC of g is defined as

$$G_k = \sum_{n=-(N-1)}^{N-1} g_n e^{\frac{-i2\pi nk}{2N-1}} \quad \text{for } k = 0, 1, \dots, N-1 \quad (1)$$

where

$$g_{-n} = g_n \quad \text{for } n = 0, 1, \dots, N-1$$

By straightforward substitution it may be shown that

$$G_k = 2 \operatorname{Re} \sum_{n=0}^{N-1} \tilde{g}_n e^{\frac{-i2\pi nk}{2N-1}} \quad (2)$$

where \tilde{g} is defined by

$$\tilde{g}_n = \begin{cases} 0.5 g_0, & n = 0 \\ g_n, & n = 1, \dots, N-1 \end{cases}$$

The EDCT of g is defined by equation (3), where the extended sequence is defined by equation (4).

$$G_k = e^{\frac{-i\pi k}{2N}} \sum_{n=-N}^{N-1} g_n e^{\frac{-i2\pi nk}{2N}} \quad \text{for } k = 0, 1, \dots, N-1 \quad (3)$$

-
2. N. J. Whitehouse, et al; "High Speed Serial Access Linear Transform Implementations" Digital Computer Symposium January 1973.

If the mutually complex conjugate terms in equation (3) are combined, then equation (5) results. Equation (5) may be viewed as an alternate way of defining the EDCT

$$G_k = 2 \operatorname{Re} \left\{ e^{\frac{-i\hat{u}_k}{2N}} \sum_{n=0}^{N-1} g_n e^{\frac{-i2\hat{u}_{nk}}{2N}} \right\} \quad (5)$$

$$= 2 \sum_{n=0}^{N-1} g_n \cos \frac{2\hat{u}(n + 0.5)k}{2N}$$

Ahmed⁽²⁾ has investigated the use of the EDCT as a substitute for the Karhunen-Loeve transform and finds that it is superior to the Fourier transform and is comparable to the Karhunen-Loeve (K-L) in rate-distortion performance while maintaining the computation simplicity of a transform which does not depend on the picture statistics. Habibi⁽¹⁾ has shown by simulation that the DCT is equivalent in a mean-square-error sense to the K-L transform under basis restriction.

The effective performance of the transform depends on the block size-N. Wintz⁽⁶⁾ concluded that, for a fixed coding strategy, mean square error improves with increasing N up to N = 16, but that beyond N = 16 there is no significant improvement. Alternatively, subjective quality is independent of N, for N ≥ 16. Therefore compression potential is increased by utilizing the longest possible block size. Conversely, since one or more bit errors in the block can cause the entire decoded block to be in error, the block size should be short to guard against jamming

-
3. Ahmed, N., Natrajan, T., and Rao, K. R., "Discrete Cosine Transform," IEEE Trans. on Computers, Vol. C-23, pp. 90-93, January 1974.

(1) Op. cited.

and system noise. The block size parameter N is selected as a compromise value between 16 and 512 (the minimum line size) to provide both a high degree of compression potential and protection against bit errors. In the current study the value of N = 32 was used for the transform block size in all simulations.

Though there are no restrictions on N, if N is highly composite (e.g. $n = 2^k$), then the Fast Fourier Transform may be used to compute the coefficients of the cosine transform.

In this particular implementation since N = 32, a modified odd extension of the data is employed to generate 64 data samples. With N = 64 a radix 4 ($64 = 4^3$) FFT algorithm is employed to generate the transform coefficients.

The transform coefficients are calculated according to the following equation:

$$G_K = 2 \sum_{n=0}^{31} \text{PEL}_{(n)} \cdot \cos \frac{2\pi n.k}{64} \quad (6)$$

$$n = 0, 1, \dots, 31$$

$$k = 0, 1, \dots, 31$$

This represents an even implementation of the Discrete Cosine transform. The computations are performed using an FFT algorithm, which significantly increases the processing speed and which, because of the symmetry property of the data and the Hermetian properties of the discrete transform operations, allows the simultaneous calculation of the transform coefficients for two segments of the video input.

The cosine terms are stored as 15 bit fractional numbers with a scale of 0.0000 to 0.5000. The magnitude of the transform coefficients is bounded by

$$2 \sum_{n=0}^{31} \text{PEL}_{(n)} / 2 \quad \text{or} \quad 11 \text{ bits if}$$

all PELs are equal to the maximum value of 6 bits, (PEL values are always positive). The maximum value of the coefficients is, therefore, less than 2048. The actual magnitudes observed were considerably less than this "bound", and decreased rapidly with increasing coefficient number. The distribution (variance) and relative range of the coefficients were assumed to have characteristics similar to those described by Habibi⁽¹⁾. This distribution is approximately an exponential decaying function as the coefficient number increases. The variance behaves in a similar manner.

Table 2-1

Bit Distribution as a Function of Coefficient #

Coeff. No.	<u>2 bit/PEL</u>	<u>1.0 bit/PEL</u>	<u>1.0 bit/PEL</u>	<u>0.75 bit/PEL</u>	<u>0.5 bit/PEL</u>
1	3	3	3	3	3
2	3	3	3	3	2
3	3	2	3	3	2
4	3	2	3	2	1
5	3	2	2	2	1
6	3	2	2	2	1
7	3	2	2	2	1
8	3	2	2	1	1
9	3	2	2	1	1
10	2	2	2	1	1
11	2	2	2	1	1
12	2	1	1	1	1
13	2	1	1	1	0
14	2	1	1	1	↓
15	2	1	1	0	
16	2	1	1	↓	
17	2	1	1		
18	2	1	0		
19	2	1	↓		
20	2	0			
21	2	↓			
22	2				
23	2				
24	1				
25	1				
26	1				
27	1				
28	1				
29	1				
30	1				
31	1				
32	1				

A line of video is divided into 8 segments of 32 samples. Each segment is then transformed via the DCT and the 32 coefficients are stored into memory. The DPCM computes a set of differences, $D(n)_k$, from the present coefficients, $G(n)_k$, and the predicted coefficients for the corresponding segment of the previous line, $\hat{G}(n)_{k-1}$. $D(n)_k$ is then quantitized to $\hat{D}(n)_k$ and added to the previously predicted value to produce a quantitized coefficient for the present line; i.e.,

$$\begin{aligned} D(n)_k &= G(n)_k - B \cdot \hat{G}(n)_{k-1} \\ \hat{G}(n)_k &= B \cdot \hat{G}(n)_{k-1} + \hat{D}(n)_k \end{aligned}$$

$B(n)$ is the binary representation of the quantitized difference $D(n)_k$.

If we think of the transformed video as k columns of coefficients $G_k(n)$, the DPCM operates on these columns to produce $\hat{G}(n)_k = G(n)_k - B \hat{G}(n)_{k-1}$, where B , the prediction coefficient, is a factor less than unity. The accumulator (integrators) in both the transmitter and receiver must have a decay associated with them to prevent errors from accumulating and degrading the picture. Errors occur during the transmission of the data so that the requirement for a decay factor is related to the receiver; i.e., if perfect error-free transmission were possible then B could be set to unity. Although some experimental work has been done which indicates that the optimum value of B is in the vicinity of .85 to .90, for this particular application of value of .93 appeared to give better results. One limitation on B is derived from considering the magnitude of the quantization levels. For example, in a uniform field with approximately equal values of $G(n)_k$ and $G(n)_{k-1}$, when $|G(n)_k - B G(n)_{k-1}|$ is greater than the minimum quantization level oscillations will occur in reconstructed image. Depending on the levels of the quantizer, the picture content, the frame rate, and the BER, this oscillation effect can be more objectionable than a slow decay of errors. Ideally, a unique value of B should be selected for each of quantizer values and for each coefficient. Some experimental work needs to be done to determine the improvement that could be obtained and to select the values of B .

The most critical portion of the DPCM is the design of the quantizer. For the coding of the coefficient differences all levels must be equally likely. Habibi⁽¹⁾ has shown that for a variety of pictures the differences between amplitudes of coefficients are exponentially distributed. The probability distribution for the differences is assumed to be

$$P[D(n)] = \alpha_n \cdot \exp^{-\alpha_n |D(n)|} \quad \text{where}$$

α_n is the variance of the nth coefficient. α_n is approximately equal for all n, although the average amplitude of the coefficients \bar{A}_n is also an exponentially decreasing function of n. The quantizer levels Q_n , must then be exponentially distributed over a range - $Q(n)$ max to $Q(n)$ max where $Q(n)$ max decreases for increasing n.

The quantizer values selected for the study system are shown in Table 2-2. In this system the levels are distributed logarithmically over the maximum range, but the range is changed as a function of the bit precision used to encode the differences. Since more bits are used to describe the lower order coefficients than the high order coefficients, the range is decreased as a function of coefficient number. The selection of the numbers (quantitative levels) was first attempted by approximating the function

$$D_{nq} = \frac{D_{\max} \ln \left(1 + \frac{d}{D_{\max}}\right)}{\ln (1 + G)}, \quad \text{where } D_{n \max}$$

was determined by examining the range of the coefficients and the range of differences for samples of video used in this study. As stated earlier, these levels were then optimized subjectively by evaluations of the reconstructed image. In general, the results of the subjective evaluation indicated that the minimum step size should be less than that which would be obtained from the equation above, however the higher levels were not altered. In fact, small changes in the higher levels made little or no difference in picture quality. In fact the size of the max difference has more effect than the spacing of the levels.

In the receiver an inverse process takes place as shown below.

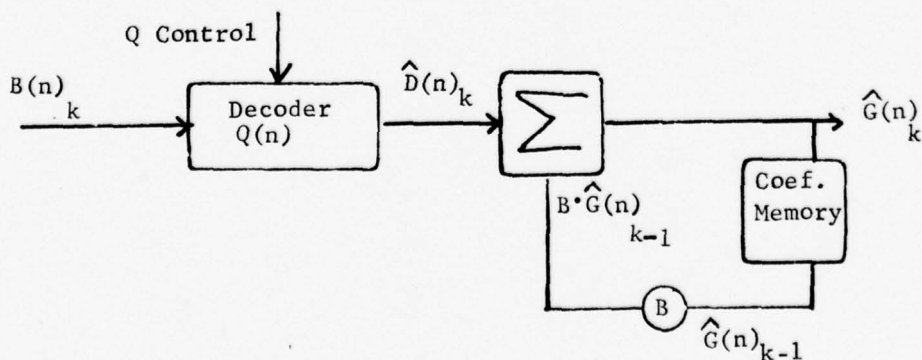


Table 2-2

Quantitization Levels as a Function of Bit Precision

<u>Comparison Level</u>	<u>Quantitization Level</u>	
700.	500.	3 bit
350.	225.	
100.	50.	
25.	10.	
0.0	-10.	
-25.	-50.	
-100.	-225.	
-350.	-500.	
-700.		
300.	100.	2 bit
50.	10.	
0	-10.	
-50.	-100.	
-300.		
		1 bit
0	+50.	
	-50.	

The bit stream is converted into quantitized differences, D_n , which are then accumulated with the previous corresponding coefficient to produce a replica (approximately) of the original input sample. The quantization table used in the receiver is identical to that used in the transmitter. Control of the quantizer is a function of the coefficient number. The decay factor B is identical to that used in the transmitter.

3.0 TASK A - SIMULATION FACILITY

3.1 General Description

The purpose of the Simulation Facility is to permit computer simulation of imagery compression techniques. Input material is imagery on 35 mm film strips. The result of the simulation is reproduced as television signals on video tape or as photographic hard copy.

A block diagram of the simulation system is shown in Figure 3-1. A transparent film strip (motion pictures) is inserted in the film strip projector. The TV camera converts the first frame to a video signal which is stored in a digital frame memory. One picture line at a time is transferred from the frame memory to the line buffer at TV rates for subsequent transfer to the CSP-30 processor at I/O rates until the frame memory has been emptied. The next film frame is pulled into place in the filmstrip projector and the process repeats. The CSP-30 can store the digitized video data on digital tape for subsequent processing or can process input data directly.

Various programs have been written for the CSP-30 which simulate one dimensional cosine transform/differential PCM encoding, error contamination, and cosine transform/differential PCM decoding. Another program can reduce resolution with or without horizontal and vertical interpolation.

The processed data is outputted through a line buffer at I/O rates and converted to analog form for precise entry onto a video disc where a new frame, and eventually the film strip, is built up. The video signals are then transferred to video tape for viewing.

3.1.1 Input/Output Characteristics

A wide variety of input formats can be handled by the scanning device, depending on the type of lens used on the T.V camera. For the present program a lens was chosen which matches the T.V. camera scanning raster size to the single-frame motion picture film format of 0.98 inch width by 0.735 inch height (SMPTE-PH22.59, Style C). The film is advanced one frame at a time on command of the system control electronics. Each frame is precisely registered with respect to the previous frame to prevent image jitter on the output display. Registration is by frame perforations rather than by matching of the location of objects in the depicted scene so that jitter due to aircraft motion when the ground scene was photographed is not eliminated.

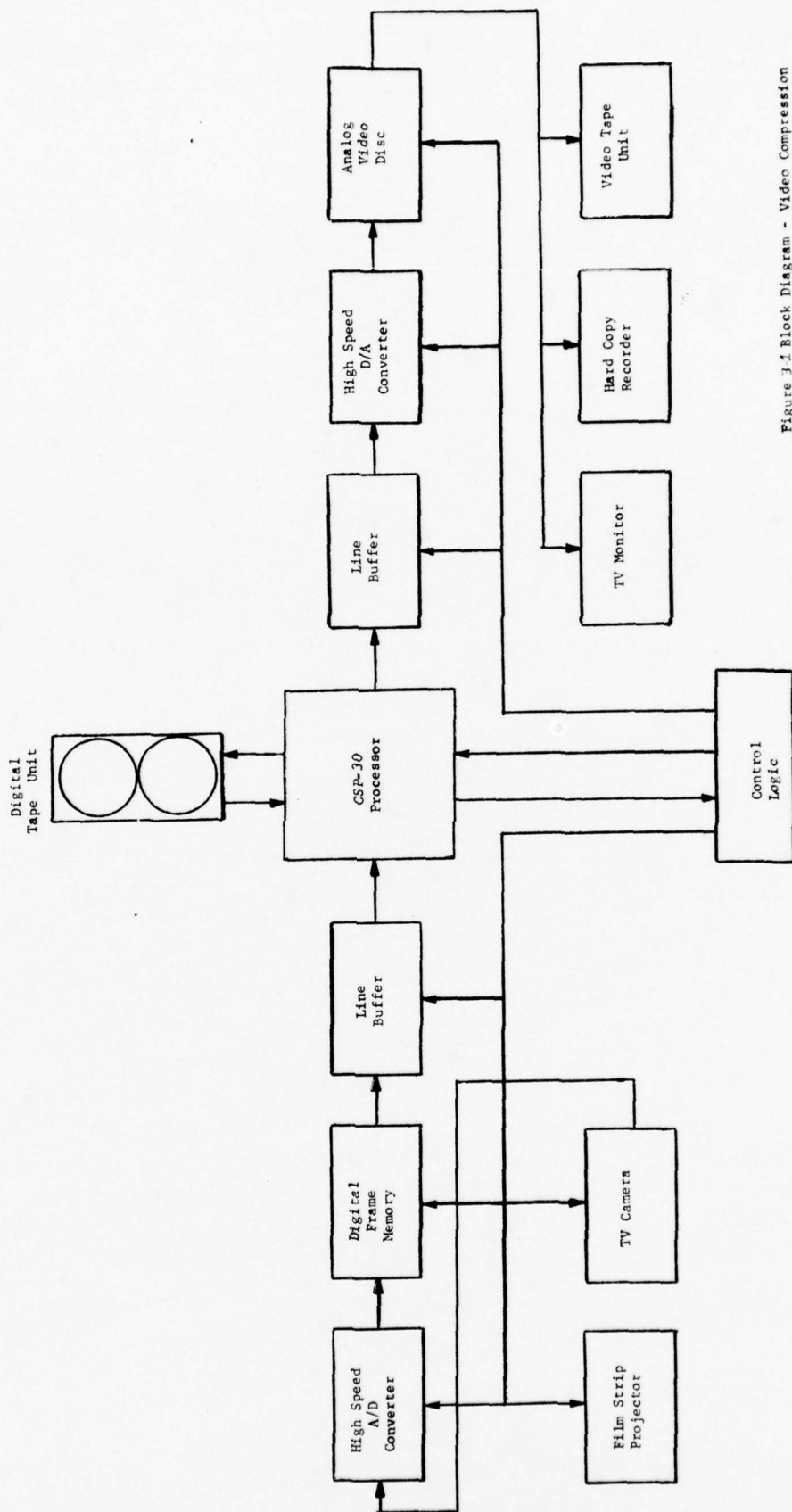


Figure 3-1 Block Diagram - Video Compression Simulation Facility

Output images are recorded on a wideband International Video Corporation Model IVC870 Video Tape Recorder (VTR) using 525 line, 2:1 interlaced RS-170 standards. Display field and frame rates are 60 and 30 respectively, regardless of processing frame rates. Low processing frame rates are displayed by repeating fields in the proper proportions. A flicker-free display is thus produced, even at low information rates.

3.2 Detailed Description

3.2.1 Input Circuitry

A detailed diagram of the simulation facility is shown in Figure 3-2.

3.2.1.1 Camera and CCU

A high resolution COHU 6150 camera head with a series 6900 Camera Control Unit (CCU) has been chosen as the system input device. An 8541A separate mesh vidicon is used for good corner and center resolution and also uniform video output in all parts of the field of view. In addition, electronic shading correction is included in the CCU to assure constant video amplitude throughout the frame.

3.2.1.2 Video Input Circuits

A cable-terminating amplifier (Philco 9SK9277) is used at the input, followed by a clamped driver (Philco 9SK9285A) which restores video D.C. level by clamping the video back porch to a reference voltage at the beginning of each scan line. This is necessary to insure that video always falls within the A/D converter range. Video voltage is boosted to the level required by the A/D converter.

3.2.1.3 Sample and Hold (Philco 9SK9278)

A sample and hold circuit, running at the same clock rate as the Analog-to-Digital (A/D) converter which follows, measures the video level at a given point and holds that value until the next sample is taken. This operation is necessary because the A/D converter uses six serial-processes, each requiring the same input voltage, to perform its conversion.

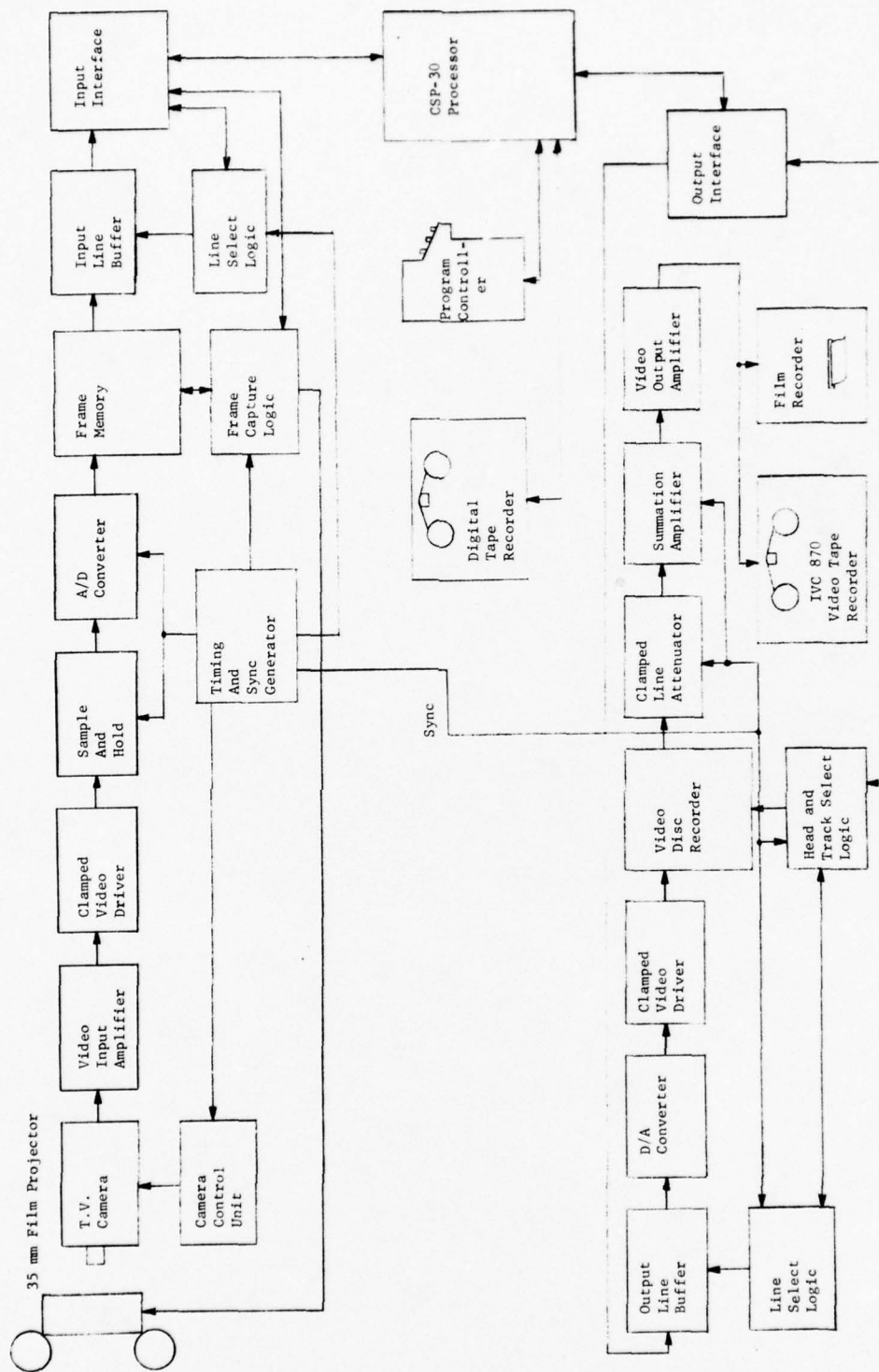


Figure 3-2 Simulation Facility

3.2.1.4 Analog-to-Digital (A/D) Converter (Philco 9SK9279)

Functionally, the converter is of the serial type, with six comparators or decision-making elements connected in cascade. The sampled and held video is applied to the first comparator which determines whether video is above or below mid range (most significant bit). The results of the first decision are subtracted from the original analog signal and the amplified difference is applied to the second comparator. The results of the second decision are subtracted from the input video to the second comparator and the amplified difference is applied to the next comparator. This process of successive approximations continues until the least significant bit is decided within the sixth stage.

3.2.1.5 Solid State Frame Memory

Because the CSP30 Digital Processor cannot operate at realtime T.V. data rates (approximately 10 MHz in this system), a rate conversion must be performed. The method chosen stores an entire frame of video in a digital frame memory. This permits the T.V. camera and ancillary equipment to operate in a normal manner and provides storage for an indefinite period with zero degradation due to the storage medium. Once "captured", a frame is read out at any desired rate on command of the processor. Also, once a frame is captured a new film frame can be pulled into the field of view and the camera video output level allowed to stabilize.

In the present system a dynamic shift register memory is used. This memory has capacity for 6 bits per Picture Element (PEL), 640 PELs per line and 480 active scan lines per frame. Since the memory is dynamic, it must be continually clocked, in this case at the A/D sampling rate. Data is accessed from the memory a line at a time as it becomes available at the memory output. The data is stored with zero degradation because the binary bits are constantly reclocked and requantized. The frame memory consists of 8 Intel IN60 boards interfaced with Philco designed mux and demux circuit cards.

3.2.1.6 Input Line Buffer

Data stored in the frame memory is fed to a static Random Access buffer one line at a time as the data becomes available at the frame memory output. At the beginning of a frame-processing cycle the data corresponding to the first active T.V. line is transferred to the line buffer at a 10 MHz rate as it becomes available at the frame memory output. The data is read out of the static line buffer on demand under CSP30 processor clock control. When the last PEL is read from the line buffer a new load cycle is initiated and the second scan line is fed into the line buffer as it becomes available at the frame memory output. During this load cycle a ready signal is removed from the CSP30, causing it to mark time.

3.2.2 Processor/Digital Tape Recorder

Simulation of compression/decompression and error corruption are performed by a Computer Signal Processors Incorporated CSP30 processor. Data input and output is via one of the fast data channels of the machine. Input image data can be stored on an MDS Bucode 4025 digital tape transport. Data thus stored can subsequently be fed directly back to the processor for further processing. Any other pertinent data can also be stored on the digital tape transport.

3.2.3 Output Circuitry

Processed data is recovered a line at a time from the CSP30 at its operating rate, temporarily stored in a line buffer and then assembled a line at a time on a track of the disc recorder whose speed is synchronized to the T.V. camera sync generator. When a full frame of data is accumulated on the disc, its heads are stepped to adjacent tracks and the process repeats. When 300 frames of data have been accumulated on the disc, they are transferred in real T.V. time to the Video Tape Recorder (VTR) for permanent storage. If a run consists of more than 300 frames, a second sequence of frames is assembled on the disc and electronically "spliced" to the end of the preceding 300 frames.

3.2.3.1 Output Line Buffer

Picture element data from the CSP30 processor is loaded into a line buffer (identical to the Input Line Buffer) under command of the CSP30 clock. When the line buffer is filled, the Buffer Available signal is removed from the processor and the buffer data is transferred to the disc recorder at a 10 MHz rate via the Digital-to-Analog (D/A) converter. Transfer occurs when the particular slot on the disc corresponding to the stored line is moving beneath the video heads. When the buffer is empty, it reverts to the load condition and accepts the next line of data from the CSP-30 processor.

3.2.3.2 Digital-to-Analog (D/A) Converter

A Datel Systems DAC-HI8B D/A converter with an extremely short settling time transforms the 6 bit binary data to analog video at the 10 MHz clock rate.

3.2.3.3 Video Processing Circuits

The D/A output feeds a clamped video driver (Philco 9SK9285A) which raises the signal to the + 1.0, -0.4 volt levels required by the disc recorder input circuits. This amplifier drives a 75 ohm coaxial cable needed to connect the output electronics with the video disc recorder in an adjacent cabinet.

Video out of the disc is processed by a clamped line attenuator (Philco 9SK2901-10) which removes a switching transient in the horizontal blanking interval caused by recording video a line at a time. Composite sync needed for monitor and VTR synchronization is added by a summation amplifier (Philco 9SK9280) and the resulting composite video is fed to an output amplifier (Philco 398-11239-1) which is capable of driving a terminated 75 ohm video output cable.

3.2.4 Video Disc Recorder and Video Tape Recorder

3.2.4.1 Video Disc Recorder

A Data Disc Model 3302V Video Disc Recorder is used to assemble frames of video from the CSP30 processor and to provide temporary storage of 300 T.V. frames. The disc rotates at 3600 RPM to produce the greatest possible bandwidth. At this speed, one revolution corresponds to one T.V. field; thus 2 tracks are required for a complete 2:1 interlaced frame. Two movable heads are provided; one on each side of the disc. Odd numbered fields are recorded on one side of the disc, even numbered fields on the other. While one head is reading or writing the other head can be moved to the next track (next field). The same modulator/demodulator combination is shared by the heads on an alternating basis so that video quality will be consistent for alternate fields.

3.2.4.2 Video Tape Recorder (VTR)

An International Video Corporation (IVC) model IVC-870 video tape recorder is used to accumulate output imagery. This machine was chosen because it produces wideband, low noise recordings and initiates assembly edit during the vertical blanking interval to produce display continuity at the point of electronic "splicing". This feature is necessary to assemble video sequences longer than 300 frames.

3.2.5 System Timing

At the heart of the system is a Philco-constructed television synchronizing generator. This generator uses a stable 14 MHz clock to generate drive, blanking and sync signals for the camera, VTR and all display monitors. These signals meet EIA RS170 specifications for studio equipment. Also, signals are brought out of the sync generator to control the disc drive servo and to select lines for processing.

3.2.5.1 Line Select Logic

The input line buffer is loaded one line-at-a-time and the output line buffer is unloaded a line-at-a-time on command of the line select logic. A static counter, which stores the number of the line which is to be loaded or unloaded, is continually compared with the sync generator counter so that a correlation is produced during the precise 63 usec interval when the desired line information actually occurs. A 63 usec "gate" is thus produced which enables the high speed (real-time) clock to load video data into the input line buffer or unload video data bits from the output line buffer.

3.2.5.2 Capture Logic

Capture circuits are enabled when a new frame of video data is to be read into the Solid State Frame Memory. This command is initially triggered by a start button and subsequently triggered by an End of Frame command from the CSP30 processor. "Capture" breaks the recirculation loop of the Frame Memory for one frame duration and admits new data from the A/D converter. At the end of a load cycle the Frame Memory is restored to the recirculate condition and data transfer to the Processor is activated.

3.2.5.3 Film Advance Logic

As soon as a frame is captured by the Solid State Frame Memory, a pulse is sent to the Film Projector to initiate a film frame advance cycle. Approximately 8 seconds are available for the film to advance and the T.V. camera gain control circuits to stabilize video output. This is sufficient time for the film projector and T.V. camera being used.

3.2.5.4. Video Disc and Video Tape Recorder Control

The line select logic provides video to the write circuits of the disc recorder when the precise segment of the disc corresponding to the line to be written passes under the recording head.

Head select logic connects the disc modulator and demodulator either to the top or bottom head, depending upon which field the line belongs. (Odd numbered lines are recorded on one side of the disc, even lines on the other).

In the write mode the logic enables the erase function during the next field interval after a head is stepped. Vertical blanking is written and then line-by-line writing begins.

Track select logic controls the motion of the two heads depending upon what sequence is being recorded or played back. The most elementary control is to step one head while the other head is reading or writing and then stepping the second head while the first head is reading or writing. This produces a sequence of 60 fields per second, 30 frames per second, 2:1 interlaced as in standard T.V. display. More complex sequences can be produced to simulate low frame rates. For example, if every frame is recorded and then every other frame is displayed twice, motion frame rate is halved while 60 field per second refresh rate is maintained. The amount of reduction which can be thus obtained is limited by the number of tracks which the heads can be stepped in 1/60th second. Reductions other than 2:1 and 4:1 are possible (such as 24 motion frames per second with a 60 field per second refresh rate) by displaying fields an unequal number of times. Frame rates which were simulated were 24 frames per second (baseline) and 4, 2, and 1 frames per second (compression runs).

For film strips where more than 300 frames are processed, several transfers from disc to VTR are necessary to generate a complete tape. This is accomplished by recording a pulse on a VTR audio track near the end of the first 300 tracks. When the next group of tracks is recorded, this pulse is recovered and used to trigger the write cycle at the 301st frame.

4. TASK B - EXPERIMENT DESCRIPTION

4.1 Purpose

The purpose of this section is to describe the methodology and content of the simulation studies of the Video Image Bandwidth Reduction/Compression Study. The objective of the simulation studies was to determine the effects on target acquisition time which result from a range of video processing variables applied in a number of different combinations. The large number of test conditions which can be permuted from Table 4-1 indicates that a considerable amount of pre-selection was required. The range of parameters shown in the table was truncated in order to determine the optimal technique for the final nine (9) test conditions (plus baseline).

Table 4-1 Reduction/Compression Parameters

<u>Parameter</u>	<u>Range of Variation</u>
Frame Rate	8, 4, 2, 1, $\frac{1}{2}$, $\frac{1}{4}$ frames/second
Resolution	512 x 480, 256 x 240 picture elements
Number of Coefficients	64, 32, 16 and 8 coefficients per linear segment
Bits per Pixel	2, 1.5, 1, 0.75, 0.5 average bits per picture element assigned to the DPCM description of the transform coefficients in an optimum manner
Bit Error Rates	10^{-5} , 10^{-4} , 10^{-3} and 10^{-2}
Error Effect Reduction	Two values of prediction coefficients.

NOTE: This table represents the range of parameters considered in the selection of the final technique as described in the text. Only some of the many possible combinations were used.

4.2 Test Procedures

The test procedures that were used permitted the gradual narrowing of the parameters in Table 4.1 in order to identify those reduction/compression system parameters which provide best performance within a base bandwidth of 450 kHz. The resulting combination of variables was used for final system testing. To this end Aeronutronic Ford examined the effect of each system parameter on overall performance by the sequence shown in the accompanying flow charts. (Figures 4-1 & 4-2). This process involved engineering and human factors evaluation for initial selections, and the use of test subjects on these selected preliminary test conditions. Once the optimum parameters were selected, final testing was performed using 8 subjects and 10* film strips for each of the final experimental conditions.

4.2.1 First Truncation Methodology

Single frames were selected from the film strips for simulation processing utilizing various combinations of parameters including resolution, coefficient number and DPCM bit assignment. The processed images were displayed on a TV monitor and photographed as film negatives. These negatives were printed as 8" x 10" positives for image quality evaluation. The preparation of hard copy prints allowed simultaneous comparison of the processed imagery. Since these prints were made from a cathode ray tube, the inherent effects of normal video presentation due to scan-lines, gray-scale translation, etc., were acting upon the image quality. The selection task involved viewing the prints at a fixed distance under controlled illumination. Project staff personnel selected those prints which retained the best target discriminability among the various combinations of parameters. Ultimately, prints representing the best simulation processing techniques were identified. The sets of parameter values represented by these prints were then used for the second truncation.

* Two additional film strips were used for subject training.

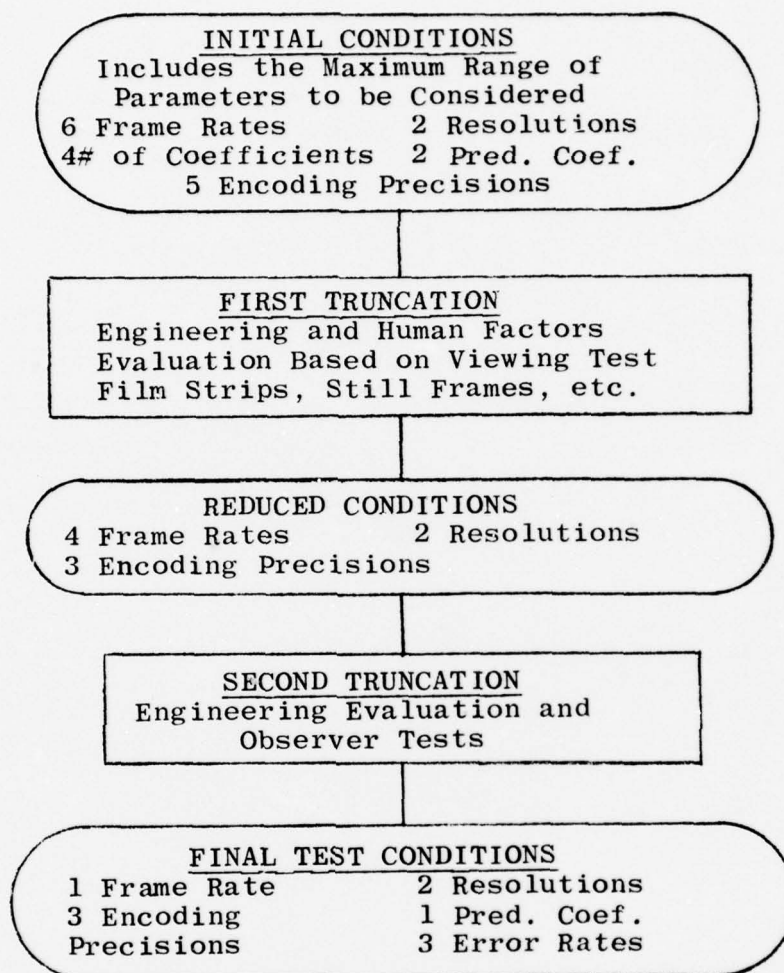


Figure 4-1 Truncation Flow Chart

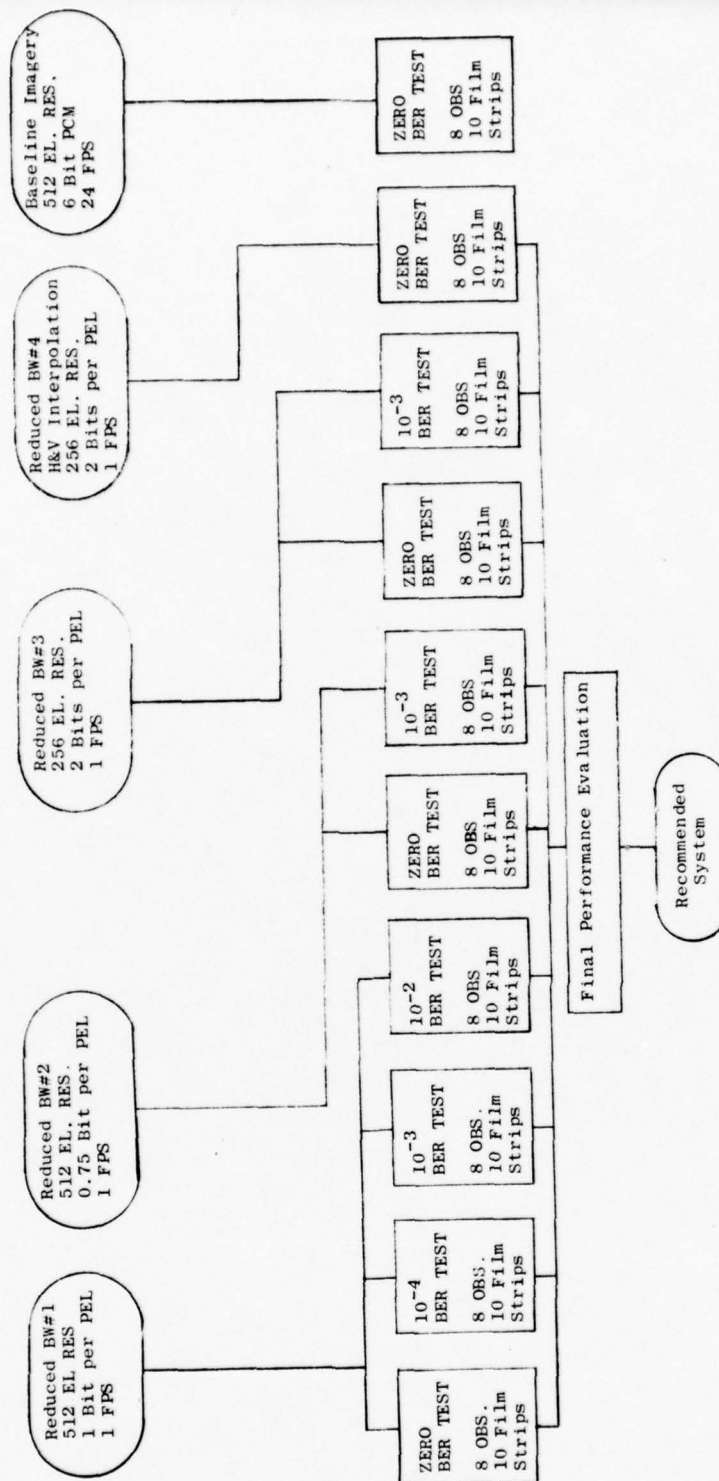


Figure 4-2 Final Test Flow Chart

4.2.2 Second Truncation Methodology

The number of parameters to be evaluated in the final test phase was further narrowed by a Second Truncation Effort. Observer tests and engineering evaluation were used to determine the limits of compression which could be tolerated before object recognition was seriously impaired. The truncation of frame rates was accomplished by measuring target acquisition time on full-length runs of processed imagery utilizing the same equipment which was used for final testing. Also, static tests were performed to determine a limit of error rate beyond which object recognition was seriously impaired. Figure 4-1 shows the number of parameters selected for use in the final test. The rationale for selecting these parameters is given in Section 5.2.2 of this report.

4.2.3 Final Test Methodology

The baseline imagery test was run first to establish an "ideal video" reference for comparison of compression test results. (See Figure 4-2). The highest quality reduced bandwidth system chosen during Second Truncation (Reduced Bandwidth #1 test in Figure 4-1) was tested next to obtain the first measure of possible performance degradation due to bandwidth compression. This system was also tested at three transmission error rates (10^{-4} , 10^{-3} , and 10^{-2} errors per bit).

The results of the Reduced Bandwidth #1 test were so favorable that it was decided to increase compression by reducing the number of DPCM bits to 0.75 per PEL at 512 element resolution and subsequently by reducing original resolution to 256 elements per picture dimension. These latter systems were also tested at a 10^{-3} error rate.

The results of the above tests and their interpretation are presented in Sections 5.3 and 5.4 of this report.

4.3 Test Subject Qualifications

Reserve officers (pilots and navigators) supplied by the training office at the Willow Grove, Pa. Naval Air Station were used to perform the final tests. Flight officers rather than laymen were used because they are trained to identify objects from the air and are also trained in reading maps similar to those supplied for the tests. One might expect the flight officers to find the desired object faster than laymen, and in fact they did locate the objects sooner but delayed reporting this fact, obviously taking time to be certain their detection was correct. This is the result of years of training; that is, to be certain of the target before taking any aggressive action.

It was noted that the officers relied more heavily on the maps than did laymen. This is significant because the maps can show features which might be obscured in the two reference photos. The maps would probably have been even more useful had they been in color because elevation contour data was not readily apparent.

The types of aircraft on which the flight officers collectively had experience are:

A-6, 7
C-118, 121
F-3, 4, 8, 9
H-2, 3, 46, 53
P-2, 3, 5
S-2

4.4 Testing Methods

4.4.1 Test Orientation

Each subject participating in the tests was oriented by a member of the Aeronutronic Ford project team. The subjects were first required to read the set of instructions supplied by the Air Force and included in this report as Appendix C. Next, they were given a description of the purposes of the study, a familiarization with the testing setup, and an explanation of the tasks which they would be performing.

4.4.2 Pre-Mission Briefing

Each map and the reconnaissance photographs relevant to a specific film strip were mounted together on a single sheet of heavy cardboard. See Figure 4-3. During the pre-mission briefing the appropriate panel (map and photographs) was placed on an easel next to the T.V. monitor for viewing by the subject. The subject was permitted to study the briefing material without interruptions. This interval never exceeded three minutes. Other information which was given to the subject was to show him the target as it appears on the one mile and three mile photographs. In several cases where aircraft approach is significantly different from that used to generate the reference photos, the actual heading was indicated to the subject.

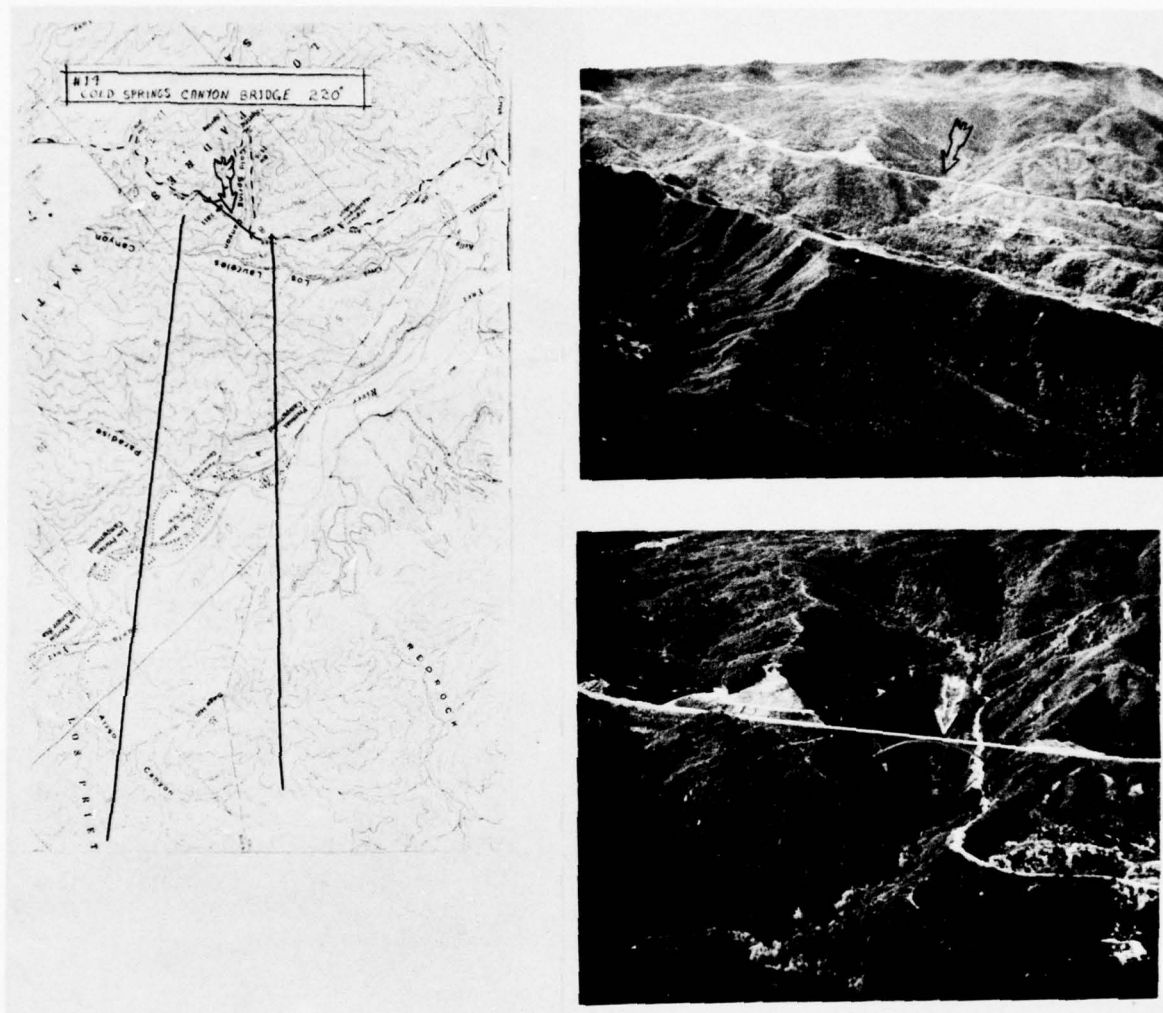


FIGURE 4-3 BRIEFING PANEL

The test subjects were instructed during the pre-test briefing to sit at a distance from the monitor where the entire screen could be easily scanned. The subject was told to point to the target as soon as he could detect it as per the printed Air Force instructions. The time between beginning of a run and detection was measured with a stop-watch by a member of the testing team. If the subject failed to find the target before it went out of the camera field of view, a no detect (N.D.) was recorded.

4.5 Test Environment

Figure 4-4 shows the setup used in the tests and the relative location of the various components. In order to assure the validity of the collected test data, close control over all significant elements of the test environment was exercised. In terms of physical configuration of the equipment, the only change permitted was individualized adjustment of the subject's chair to assure a comfortable operating position. Illumination was controlled both in terms of level of ambient illumination and prevention of specular reflection and glare on the CRT surface. Acoustic noise was minimized and distractions or interruptions by non-essential personnel was prohibited.

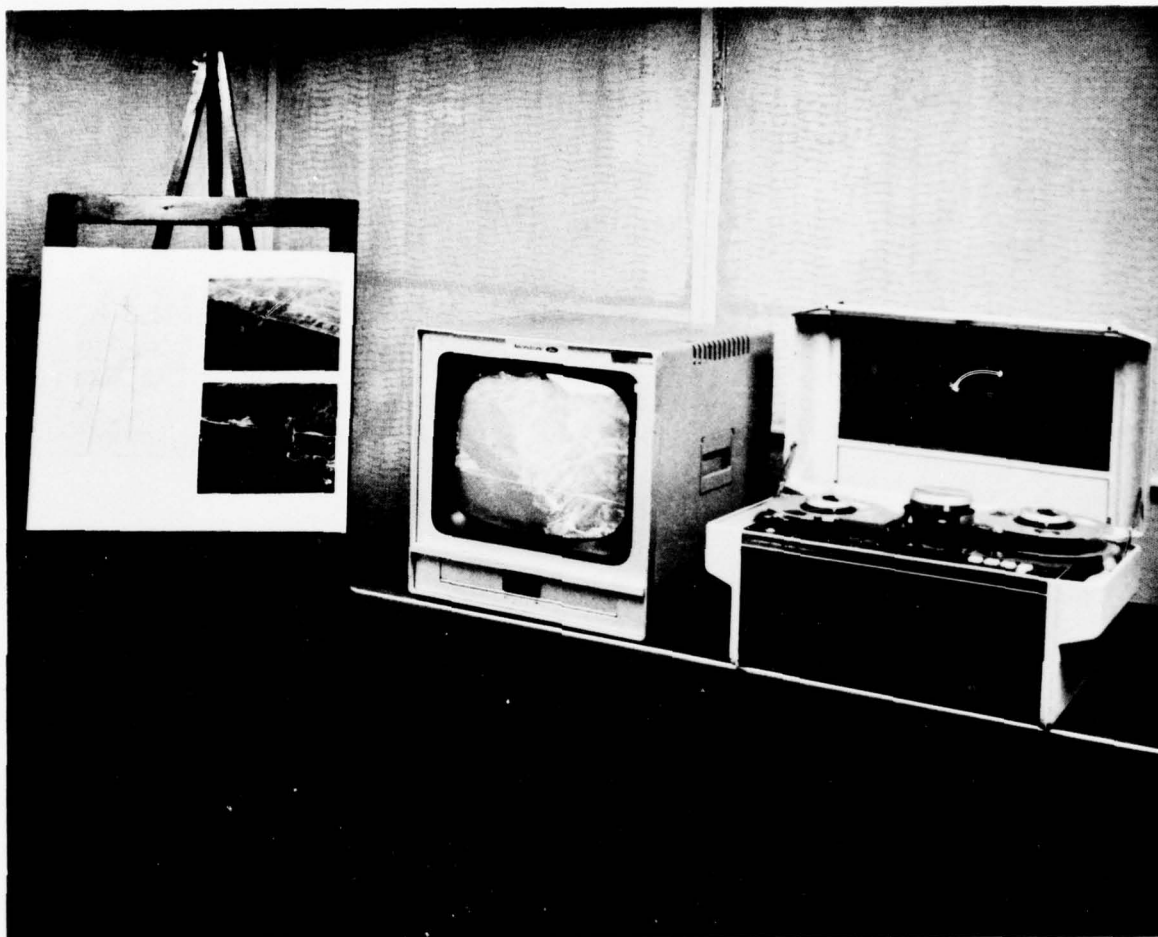


FIGURE 4-4 EXPERIMENTAL TEST SETUP

5. TASK C; Image Quality Evaluation

5.1 Introduction

The purpose of this section is to describe first, the rationale employed in arriving at the simulation parameters used in the final tests and, second, the selection of the optimum final system parameters as verified by subjective testing.

The procedure adopted in selecting the parameters for final simulations consisted of initially generating a list of all of the major parameters which might be varied as well as the logical ranges of these variations. The effect of these parameters on system bandwidth was then analyzed and the upper frame rate vs bit per pixel contour established. The range of parameters thus developed was subjected to a successive truncation process designed to isolate the parameters which will provide adequate performance with minimum bandwidth requirements.

5.2 Truncation Results

5.2.1 Initial Conditions

Among the parameters included in this tabulation and their ranges are the following:

Frame rate:	8 to $\frac{1}{4}$ frames per second
Resolution:	512 x 480 to 256 x 240 pixels
Coding Block Size:	64 to 8 elements
No. of Coefficients:	64 to 8 coefficients
Bits Assignment:	2 to 0.5 bits per pixel
Prediction Coefficient:	1.0 to 0.8

5.2.2 Reduced Conditions

The films provided as simulation input material are assumed to be typical of the range of scenarios to be considered and therefore were thoroughly analyzed by engineering and human factors personnel to determine the upper and lower limits of the parameter ranges.

5.2.2.1 Frame Rate

The aircraft velocity and altitude determine the length of time that a target is visible in the display of the film. In addition, in some cases aircraft motion perturbations, such as roll, pitch, yaw, sudden heading changes, etc., caused rather radical displacement of the target within the display area. Based on these two considerations $\frac{1}{4}$ and $\frac{1}{2}$ frames per second were discarded because the target may be visible in only one or two frames and then possibly in highly diverse locations. Thus, reliable performance at $\frac{1}{2}$ frame per second or lower cannot be anticipated. As a result, one frame per second was established as a lower limit. Eight frames per second was selected as an upper limit for several reasons. Previous reports indicate that eight frames per second is entirely adequate for target location.

Furthermore, eight frames per second is the highest frame rate that will support even as little as 256 x 240 element resolutions within the confines established by the system bandwidth. On this basis, obviously one frame per second would be the logical choice since minimum bandwidth is the goal. It remains to be proven, however, that one frame per second provides performance equivalent to eight frames per second.

5.2.2.2 Resolution

The problem of resolution was attacked with the following philosophy: the unprocessed television image should provide a discernable target to the observer in any target run at about the same elapsed time as the actual film strip under similar viewing conditions. This was found to be generally true when the television system had 512 by 480 element resolution, as determined from still frames. Consequently, it was deemed unnecessary to use higher resolution such as 1000 x 1000, which would have forced unrealistic requirements on the compression algorithm to achieve the 450 kHz bandwidth specified. The selection of 512 by 480 at 1 frame per second permits using up to 2 bits per PEL which appeared to be a quite easily achievable compression.

While it was felt that the 512 by 480 resolution would produce satisfactory results, it was not clear what results 256 by 240 resolution would produce. From the still photographs it appeared that the target could be discerned very shortly after it was discernable in the 512 x 480 photographs. However, the 256 x 240 photographs were esthetically poor in comparison. This was eventually verified in the final tests by just a slight increase in target detection time, but a large increase in the number of missed detections. At this time, however, there was no firm reason to delete 256 by 240 from the viable system parameters.

Considerable thought was given to the concept of using zones of graded resolution within the viewing area, such as the foveal-peripheral field of view. Examination of the target location at the point of entry into the realm of detectability indicated that the target had often been at the extreme edge of the viewing area at that time and its detection might well have been delayed had the system resolving power been lower in that area. The effect would be quite similar with a dynamically movable high resolution area. In fact, since several targets are visible for just a few seconds, it is questioned whether an operator could scan the field of view with the higher resolution area to any advantage.

Therefore, it was decided that 512 by 480 should be selected as the principal system resolution and a dynamic test be made to ascertain the usefulness of 256 x 240 resolution. Finally, it was decided not to simulate a variable resolution field of view for the reasons given above and because the proposed compression system would perform as well as any other system with a variable resolution field.

5.2.2.3 Coding Block Size

The coding block is the serial picture element segment whose cosine transform is calculated as the first step of the coding process. The optimum length of this segment was selected as 32 pixels. Sixty-four pixel blocks require excessive time to process digitally and present considerably more difficulties in analog processing as compared to 32 pixel blocks with essentially no improvement in compression. Eight element blocks, on the other hand, are easy to process, but do not permit aggressive compression for equivalent picture quality. The 32 pixel block size was finally selected as the best trade-off between picture quality, achievable compression, and processing complexity.

5.2.2.4 Bit Assignments

The problem of bit assignments is somewhat complex, since it involves an interrelationship between the number of coefficients utilized per coding block and the number of bits assigned to the DPCM word assigned to each coefficient location. Thirty-two transform coefficients can be calculated per 32 pixel coding block. If adequate precision (bits per coefficient) is retained, the inverse transform will identically reproduce the original picture.

During the time that the Aeronutronic Ford simulation facility was being fabricated, an analysis of several typical film frames was undertaken under subcontract by Dr. Paul Wintz to determine the optimum bit distribution on an rms error basis. The results of this analysis formed the basis for generating several series of still photographs from which subsequent decisions could be made. For example, it appeared that using 19 coefficients at an average of 1-bit per pixel (i.e. 32-bits spread over 19 coefficients) was adequate for target location at 512 by 480 resolution. The distribution selected was later modified as described below. At 256 by 240 resolution the same series of photographs indicated that for the same field of view, 2-bits per pixel (64 bits) spread over 32 coefficients would be required. The two bit assignments described were retained for further evaluation.

5.2.2.5 Determination of Prediction Coefficient

Minimizing error effects is achieved by use of a prediction coefficient in the DPCM encoding algorithm. Still photographs were made of typical scenes with about 20 errors per picture. Various prediction coefficients were simulated. The results were difficult to evaluate because the effect of errors in an actual scene is rather subdued. The same simulations were then performed on an electronically generated frame consisting of a left to right ramp signal. Here the errors were obvious and were caused to occur at all levels of the video dynamic range. Values of 0.96 and 0.91 were selected for the prediction coefficient for further evaluation as the best compromise between short propagation of errors and generation of DPCM oscillation patterns and reduction of dynamic range.

5.2.2.6 Summary of Reduced Conditions

The following tabulation shows the ranges to which the various video compression system parameters have been reduced, through the use of engineering and human factors analysis of the original film strips and of still photographs of various computer simulations.

Frame Rate: 8 to 1
Resolution: 512 x 480 and 256 x 240 pixels
Coding Block Size: 32 pixels in a linear segment
Number of Coefficients: 19 at 512 x 480, 1-bit/pixel
32 at 256 x 240, 2-bit/pixel

(During the subjective tests it was decided to investigate 14 coefficients at 512 x 480, 0.75-bits/pixel also)

Bit Assignment: 1-bit/pixel at 512 x 480
2-bit/pixel at 256 x 240
(0.75-bit/pixel at 512 x 480 as described above).

Prediction Coefficient: 0.96 and 0.91

5.2.3 Final Test Conditions

The previous truncation process utilized engineering and human factors evaluation of the original film strips and hard copy of single frame simulations of selected film frames to produce a set of reduced parameter ranges. The next step was to evaluate the reduced conditions with groups of observers viewing simulated film strips or filmstrip segments. The goal is to select, ideally, the parameters for the nine final test runs. A slightly different approach was taken; namely, two sets of parameters were selected, which, with two additional error rates each, constituted 6 runs. The remaining set of parameters was tentatively selected but left open for possible redirection based on the results of the first six runs.

5.2.3.1 Frame Rates

The initial truncation could reduce the range of frame rates only to 8, 4, 2 and 1 frame per second. Simulations of several film strips were generated at 8, 4, 2, and 1 frames per second using PCM. Laboratory personnel served as test subjects so that target location performance at the four frame rates was evaluated. Slightly better results were obtained at 8 and 1 frames per second; therefore additional runs were made at 8 and 1 frames per second, again with in-house personnel. The results indicated that performance at 1 frame per second was no worse than at 8 frames per second. One frame per second was selected as the frame rate for the final tests.

5.2.3.3 Resolution

Short runs of 512 x 480 and 256 x 240 simulations were made. Lab personnel again served as test subjects to evaluate the effects of resolution on target location. The results at 512 x 480 were comparatively consistent. At 256 x 240, however, the results were somewhat erratic; many performances were as good as 512 x 480, but a larger number of no detects also occurred. The conclusion was that 512 x 480 was the better selection for system resolution and should serve as the starting point for the final test. However, the many cases of excellent results at 256 x 240 indicated that it should also be subjected to one set of first tests.

5.2.3.4 Coding Block Size

The initial coding block size of 32 sequential pixels was simulated and found to provide excellent performance. Therefore, it was retained for the final tests.

5.2.3.5 Bit Assignments

The bit assignments previously selected were simulated and evaluated. Slight modifications were made to the bit assignments based on artifacts which, although negligible in still frames, became quite objectionable in motion simulations. These artifacts are the breakup of the highway in the lower right corner of Figure 5-1A. In this figure 19 coefficients were encoded with a total of 32 bits. In Figure 5-1B, only 17 coefficients were encoded with a total of 32 bits. The redistribution of bits, to favor the low frequency coefficients eliminated the artifacts while having negligible effect on high detail rendition. The versatility of the now completed simulation system permitted reevaluation of previously discarded bit assignments and verified those selected. Thus 1-bit per pixel at 512 x 480 was the principal selection for final test while 256 x 240 with 2-bits per pixel appeared worthy of further tests.

5.2.3.6 Prediction Coefficients

The prediction coefficient values selected by means of the still frame simulations (0.96 and 0.91) were reviewed with motion simulations and a value of approximately 0.93 was selected as the optimum compromise.



A. Nineteen Coefficients Encoded With a Total of Thirty-Two Bits



B. Seventeen Coefficients Encoded With a Total of Thirty-Two Bits - Low Order Coefficients Favored.

Figure 5-1 Selection of Final Encoding Bit Assignments

5.2.3.7 Summary of Final Test Conditions

A Baseline test was run first to serve as a calibration for the reduced/compressed tests which followed. The Baseline run is a minimum-degradation case representing the best that could be achieved with the Aeronutronic Ford simulation system. The parameters of the baseline system are 512 samples per scan line, 480 active scan lines per frame, 24 motion frames per second, 6 bit (64 levels) quantizing precision and zero error rate. In the following tabulation of the parameters for the final compressed video tests, runs 1 through 6 represent the initial selections. In this report "run" means "test condition", not target.

Run Parameter	1	2	3	4	5	6	7	8	9
Frame Rate	1	1	1	1	1	1	1	1	1
Resolution	512	512	512	512	256	256	256	512	512
Coefficients	17	17	17	17	32	32	32	12	12
Bits/PEL	1	1	1	1	2	2	2	0.75	0.75
Prediction Coefficient	0.93	0.93	0.93	0.93	0.93	0.93	0.93	0.93	0.93
Bit Error Rate	0	10^{-4}	10^{-3}	10^{-2}	0	10^{-3}	0	0	10^{-3}
Other Features							<div style="text-align: center;"> \uparrow 0 H & V Interpolation </div>		

Runs 7, 8, and 9 evolved from results of the first six runs. Although the performance at 256 did not represent a drastic increase in SLANT RANGE AT DETECTION the number of NO DETECTS seriously increased. It was considered possible that this could be due in part to the repeat field presentation of the display to the observer. Because of the 2:1 reduction in bit rate realizable at 256 x 2 over 512 x 1, run 7 was allocated to 256 x 2 with both horizontal and vertical interpolation which produced a marked improvement in the appearance of the display. The SLANT RANGE AT DETECTION results did not improve significantly, so no further runs were allocated to this approach.

In work described in Sections 5.2.2.4 and 5.2.3.5, the 512 x 0.5 bit per PEL still results were considerably poorer than the equivalent bit rate 256 x 2. Therefore it was never considered as a viable candidate. The requirement to further reduce the bit rate below that produced by the initial selection (512 x 1) led to a reevaluation of 512 x 0.75 and 256 x 1. Still frame results found the 512 x 0.75 to be far superior to those of the 256 x 1 simulation. Therefore, runs 8 and 9 were allocated to 512 x 0.75.

5.3 Final Test Results

5.3.1 Data Generation

The data to be described in this section includes the data gathered during the subjective tests, measurements from the original film strip, and calculations based on the given aircraft flight characteristics.

5.3.1.1 Time to Detect

The principal data gathered during the subjective tests is the elapsed time from the beginning of the simulation run up to the time the subject indicates that he has located and correctly identified the target. Since 8 observers are used to evaluate each test run, a conversion to a single number is required, the median of the 8 observer scores was selected. This interval, the median of the eight observer scores, has been designated TIME TO DETECT. A variation of this data item which occurred during the subjective test is the case where the subject fails to locate and correctly identify the target. In this case no specific TIME TO DETECT can be assigned. Instead, the run is defined as a NO DETECT and carries a special weight.

5.3.1.2 Time from Start to Ground Zero

These measurements from the original film are required to determine the time from the start of the run to the time the aircraft is directly over the target; i.e., SLANT RANGE equals altitude at a ground range equal to zero. This time was determined by measuring the time from the beginning of the film to the point where the camera was stopped. There were several films where this was obviously inaccurate. In these cases the time from start of film to the time at which the target passed the lower edge of the film frame was determined. Six seconds were added to this interval to give the TIME FROM START TO GROUND ZERO.

5.3.1.3 Detect to Ground Zero

The difference between the two previous intervals specifies a time interval from which slant range may be determined. It is defined as DETECT TO GROUND ZERO.

$$(\text{DETECT TO GROUND ZERO}) = (\text{TIME FROM START TO GROUND ZERO}) - (\text{TIME TO DETECT})$$

NO DETECTS are weighted so that TIME TO DETECT equals TIME FROM START TO GROUND ZERO, therefore for a no detect condition the DETECT TO GROUND ZERO = 0.

5.3.1.4 Slant Range

Slant range can then be readily determined from the DETECT TO GROUND ZERO data by the following equation.

$$\text{SLANT RANGE} = \sqrt{690 \times (\text{DETECT TO GROUND})^2 + 1500^2}$$

The following factors are incorporated in the above equation. Aircraft velocity is 690 feet per second (~ 410 KNOTS). Aircraft altitude is 1500 feet.

5.3.2 Data Presentation

The data generated from the final observer tests is presented in two forms; a) tabular form, Table 5-1, Median Scores for Test Conditions, and b) graphic form, Figure 5-2, Slant Range at Target Detection. Additional data are included in Appendix A.

5.3.2.1 Median Scores for Test Conditions

Table 5-1 is a compendium of all the data gathered arranged in a single table to facilitate data analysis. In addition to the essentially raw data and the performance summary for all targets, three other sets of data have been computed and tabulated. This is the performance data of groups of targets occurring at similar ranges; long, medium, and short.

The test film strip numbers are tabulated in the left-most column of the chart and apply across the entire corresponding row. The ten test strips as well as the two practice strips are included. The data from the latter have not been included in any of the calculations.

Table 5-1 Median Scores for Test Conditions

Film Strip No.	Time From Start To Ground Zero	512 With 1 Bit Per PPI									
		Baseline (13 Subjects)					HER = 0				
		Time to Detect	Start Range At Detection	Ground Zero	Start Range At Detection	No Detects	Time to Detect	Start Range At Detection	Ground Zero	No Detects	Time to Detect
10	30	21	31.5	18.5	11	1	39	11	13.3	1	39.5
4	24	16	15	14	15.7	1	15.7	13.3	8.0	3	20
14	36	11	12	24	12	1	12	24	23.0	1	12.5
17	31	14	15	16	16.5	1	16.5	14.5	13.5	1	17.5
7	39	24	26	13	26	1	26	13	10.0	1	10.0
12	45	26	29	16	30	1	30	15	12.5	1	12.5
2	44	34	33	11	35	1	35	9	9.0	1	9.0
11	38	13	17.5	20.5	19	1	19	16.5	8.0	1	8.0
13	44	23	24.5	19.5	27.5	1	27.5	16.5	14.5	1	14.5
3	50	28	37	13	36	1	36	14	12.0	1	12.0
5	36	42	41	15	42	1	42	14	15.5	1	15.5
16	41	6	14.5	26.5	20	1	20	21	18.5	1	18.5
Sum	221	201	240.5	174.5	160	1	160	111.5	10.7	1	10.7
Average	22.1	20.1	24.05	17.45	16.0	1	16.0	11.15	10.7	1	10.7
Average, LR	10.0	28.3	14.08	25.5	24.4	2	24.4	14.08	13.7	4	13.7
Average, SR	22.8	19.8	13.74	16.1	27.5	0	27.5	10.458	13.4	0	13.4
Average, SR	33.3	13.0	9.095	13.0	34.3	1	34.3	8.415	10.7	1	10.7
HER = 10 ⁻²											
Time to Detect	39	11.0					39	11.0			
Start Range At Detection	20	9.0					20	9.0			
Ground Zero	19	17.0					19	17.0			
No Detects	3						3				
HER = 10 ⁻³											
Time to Detect	40.5	9.5					40.5	9.5			
Start Range At Detection	21	8.0					21	8.0			
Ground Zero	12.5	23.5					12.5	23.5			
No Detects	3						3				
HER = 10 ⁻⁴											
Time to Detect	39.5	10.5					39.5	10.5			
Start Range At Detection	21	8.0					21	8.0			
Ground Zero	13	23.0					13	23.0			
No Detects	1						1				
HER = 10 ⁻⁵											
Time to Detect	27	12.0					27	12.0			
Start Range At Detection	31.5	13.5					31.5	13.5			
Ground Zero	36	8.0					36	8.0			
No Detects	1						1				
HER = 10 ⁻⁶											
Time to Detect	20	18					20	18			
Start Range At Detection	36	8.0					36	8.0			
Ground Zero	21	17.0					21	17.0			
No Detects	1						1				
HER = 10 ⁻⁷											
Time to Detect	27.5	16.5					27.5	16.5			
Start Range At Detection	36	8.0					36	8.0			
Ground Zero	20	14.5					20	14.5			
No Detects	1						1				
HER = 10 ⁻⁸											
Time to Detect	44	12.0					44	12.0			
Start Range At Detection	22.5	18.5					22.5	18.5			
Ground Zero	26	15.0					26	15.0			
No Detects	1						1				
HER = 10 ⁻⁹											
Time to Detect	27.5	13.5					27.5	13.5			
Start Range At Detection	36	8.0					36	8.0			
Ground Zero	20	14.5					20	14.5			
No Detects	1						1				
HER = 10 ⁻¹⁰											
Time to Detect	44	12.0					44	12.0			
Start Range At Detection	22.5	18.5					22.5	18.5			
Ground Zero	26	15.0					26	15.0			
No Detects	1						1				

Film Strip No.	Time From Start To Ground Zero	512 With 0.75 Bit Per PPI									
		HER = 0					HER = 10 ⁻³				
		Time to Detect	Start Range At Detection	Ground Zero	Time to Detect	No Detects	Time to Detect	Start Range At Detection	Ground Zero	No Detects	Time to Detect
10	50	34.5	15.5	11.5	40	10.0	42	8.0	1	36	14.0
4	24	17.5	11.5	10.0	19	10.0	17	12.0	1	19	10.0
14	36	12	24.0	13.5	13.5	22.5	15	21.0	1	13	23.0
17	31	18	13.0	18.5	12.5	12	19.0	12	13.0	1	16.5
7	39	25.5	13.5	26.5	12.5	26.5	26.5	12.5	2	29	10.0
12	45	32	13.0	33	12.0	33	34	11.0	2	45	0
2	44	36	8.0	36	8.0	36	35.5	8.5	2	36	8.0
11	38	14.5	23.5	20	18.0	1	23.5	14.5	2	20	18.0
13	44	27	17.0	27.5	16.5	1	27	17.0	29	15.0	28.5
3	50	33	17.0	37	13.0	40.5	40.5	9.5	40	10.0	38.5
5	56	41.5	14.5	43	13.0	45.5	45.5	10.5	46	10.0	42
16	41	20	21.0	27	14.0	1	25	16.0	19	22.0	25.5
Sum	259.5	164.5	114.5	282	14.2	3	284.5	139.5	295	129	288
Average	25.95	16.45	11.45	28.2	1.42	0.3	28.45	13.95	29.5	12.9	28.8
Average, LR	10.0	28.3	14.08	25.5	24.4	2	24.4	14.08	13.7	4	13.7
Average, SR	22.8	19.8	13.74	16.1	27.5	0	27.5	10.458	13.4	0	13.4
Average, SR	33.3	13.0	9.095	13.0	34.3	1	34.3	8.415	10.7	1	10.7
HER = 10 ⁻²											
Time to Detect	40	10					40	10			
Start Range At Detection	20	9.0					20	9.0			
Ground Zero	19	17.0					19	17.0			
No Detects	3						3				
HER = 10 ⁻³											
Time to Detect	40.5	9.5					40.5	9.5			
Start Range At Detection	21	8.0					21	8.0			
Ground Zero	12.5	23.5					12.5	23.5			
No Detects	3						3				
HER = 10 ⁻⁴											
Time to Detect	39.5	10.5					39.5	10.5			
Start Range At Detection	21	8.0					21	8.0			
Ground Zero	13	23.0					13	23.0			
No Detects	1						1				
HER = 10 ⁻⁵											
Time to Detect	27	12.0					27	12.0			
Start Range At Detection	31.5	13.5					31.5	13.5			
Ground Zero	36	8.0					36	8.0			
No Detects	1						1				
HER = 10 ⁻⁶											
Time to Detect	20	18					20	18			
Start Range At Detection	36	8.0					36	8.0			
Ground Zero	21	17.0					21	17.0			
No Detects	1						1				
HER = 10 ⁻⁷											
Time to Detect	27.5	16.5					27.5	16.5			
Start Range At Detection	36	8.0					36	8.0			
Ground Zero	20	14.5					20	14.5			
No Detects	1						1				
HER = 10 ⁻⁸											
Time to Detect	44	12.0					44	12.0			
Start Range At Detection	22.5	18.5					22.5	18.5			
Ground Zero	26	15.0					26	15.0			
No Detects	1						1				
HER = 10 ⁻⁹											
Time to Detect	27.5	13.5					27.5	13.5			
Start Range At Detection	36	8.0					36	8.0			
Ground Zero	20	14.5					20	14.5			
No Detects	1						1				
HER = 10 ⁻¹⁰											
Time to Detect	44	12.0					44	12.0			
Start Range At Detection	22.5	18.5					22.5	18.5			
Ground Zero	26	15.0					26	15.0			
No Detects	1						1				

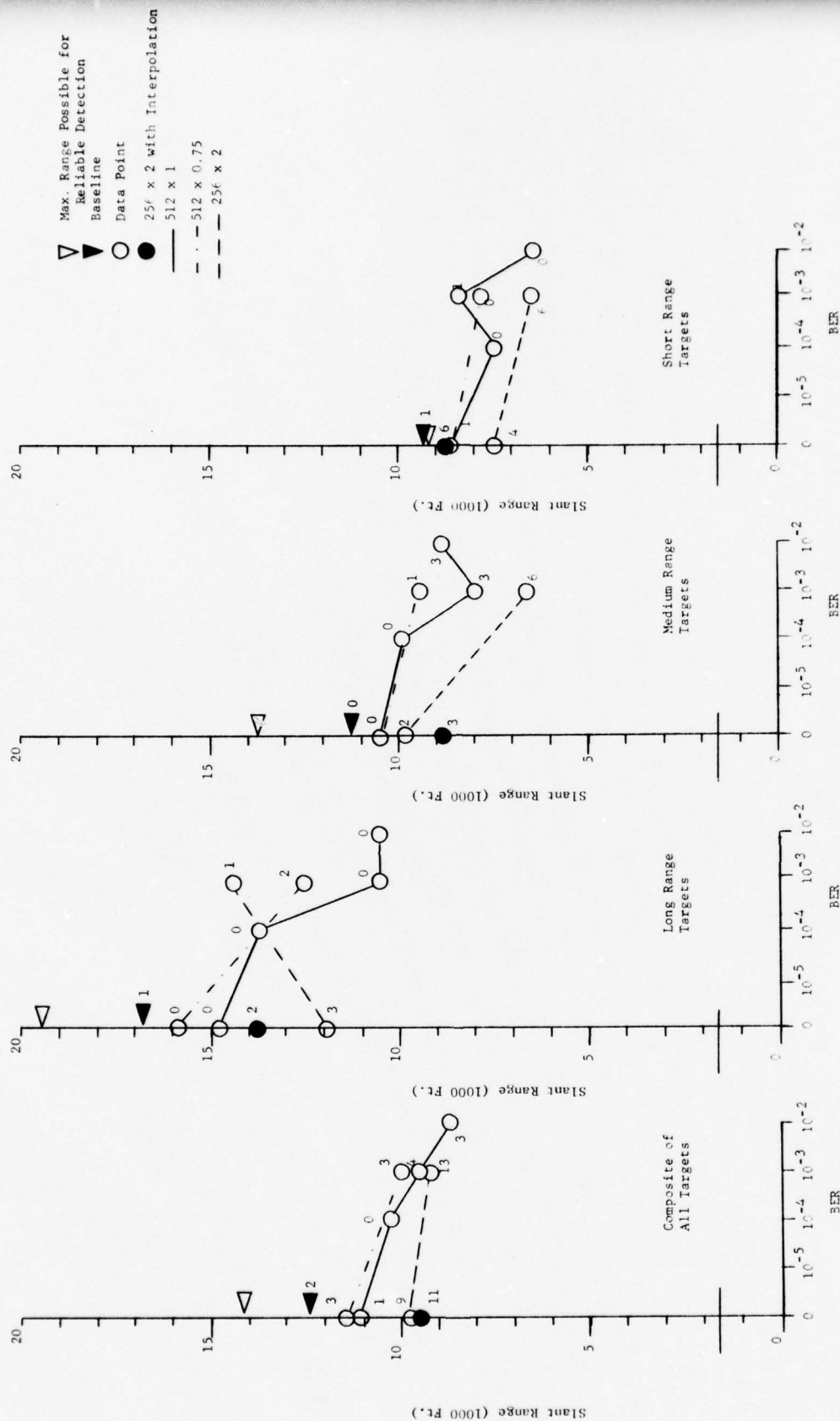


Figure 5-2 Slant Range at Target Detection

The second column is a tabulation of the TIME FROM START TO GROUND ZERO for each film strip as defined in Section 5.3.1.

The third major column is entitled MAXIMUM RANGE. The subcolumn TIME TO DETECT is similar to the definition for that parameter as defined in Section 5.3.1 except that it was determined by personnel who were thoroughly familiar with the film strips. They were given the opportunity to run each strip as often as desired to determine the earliest time at which they could reliably locate the target. The viewing conditions were similar to those for the subjective tests. Although subjective, this time represents approximately the earliest that the target could be located and therefore the maximum SLANT RANGE AT DETECT.

Both subcolumns, TIME TO DETECT and DETECT TO GROUND ZERO, represent medians of the 8 observer results. The results of the 10 runs are summed vertically and the sum listed in the sum row. The average of this sum over the 10 test runs is listed. The SLANT RANGE AT DETECTION for all 10 runs is tabulated in this third subcolumn.

Strips 14, 16, and 11, the long range test strips, LR were used to compute average LR by averaging the medians for those test strips. A corresponding SLANT RANGE AT DETECTION was calculated. This data is tabulated in the average, LR row under the appropriate column headings.

Similarly, strips 13, 3, 12 and 17 provided the initial data for the medium range computations tabulated under average MR and strips 7, 2, 5 for the short range data tabulated under average, SR.

The same data structure appears under the major columns representing the baselines and each of the 9 simulation runs across the chart with the addition of a fourth subcolumn tabulating NO DETECTS.

The most pertinent of this data, namely SLANT RANGE AT DETECTION and NO DETECTS, has been plotted in graphical form in Figure 5-2.

5.3.2.2 Slant Range at Target Detection

Figure 5-2 is a graphical presentation of the results of the 10 final subjective tests. It represents the major data from Table 5-1, SLANT RANGE AT DETECTION and NO DETECTS, plotted against BER. In addition, the MAXIMUM RANGE indicator is plotted as a reference mark (see Section 5.3.2).

The left graph indicates the performance on all ten test strips for all ten test runs. The 512 by 1 bit per PEL data is plotted as a solid line for four BER; namely, 0, 10^{-4} , 10^{-3} and 10^{-2} . The 512 by 0.75 bit per PEL data is plotted as a dash-dot line for BER equal to 0 and 10^{-3} . The 256 by 2 bit per PEL data is plotted as a broken line also for BER equal to 0 and 10^{-3} . The solid data point locates the performance of the 256 by 2-bit per PEL with interpolation at BER equal to 0. The numerals inside or next to the data point circles indicate the total number of NO DETECTS at that point for all test strips using the given compression parameters and BER. Baseline data is presented as a solid triangle, while the MAXIMUM RANGE data is a white triangle.

The next three graphs are plots of the slant range data from Table 5-1 for the long range, medium range, and short range test strips. Baseline and MAXIMUM RANGE points are also included.

5.4 Analysis of the Final Test Results

5.4.1 Maximum Slant Range

The initial data generated in the analysis portion of the program was a determination of the maximum slant range at which the targets could be dependably detected. This data was generated by personnel who were familiar with the film strips. They examined each of the film strips to determine the time from the start of the film to the point at which they could undoubtedly identify a unique artifact which in subsequent film frames proved to be the target. Landmarks which specified the location of the target were not accepted either here or in subsequent tests as valid identifications. From the data gathered the TIME TO DETECT and TIME TO GROUND ZERO were determined from which the MAXIMUM SLANT RANGE was calculated for the composite of the 10 film strips as tabulated in Table 5-1. These points are also plotted in Figure 5-2 as white triangles. These data points were used to determine the validity of subsequent data.

5.4.2 Baseline Data

The baseline data was generated next and was found to agree rather well with the MAXIMUM SLANT RANGE results. In the overall results for all 10 film strips, the TIME TO DETECT increased 2.9 seconds (15%) while the slant range decreased 1919 feet (14%). It is interesting to look at this data for the three different target ranges. The analysis indicates the results are considerably closer than it would at first appear. For example, in the case of the long range targets the best TIME TO DETECT averaged 10 seconds; that is, the target could be found very shortly after the start of the run by experienced persons. The test observers who had not seen these films before, and therefore needed time for orientation required only 14.7 seconds for the baseline average TIME TO DETECT. This is an increase of 4.7 seconds. The equivalent medium range comparison is 22.8 to 26.4 seconds or a change of 3.6 seconds. Since the targets appear later in the film, the orientation time perhaps does not weight the baseline average TIME TO DETECT as heavily. In the short range target film strips, the TIME TO DETECT is essentially identical for the Baseline and MAXIMUM SLANT RANGE data.

5.4.3 The 512 x 1 Simulations

The next test run made was at 512 x 480 resolution, 1-bit per picture element (512 by 1) and the BER=0. The overall TIME TO DETECT increased only 1.4 seconds (6%) from the Baseline. The SLANT RANGE decreased 1027 feet (8%). In general, the change in performance was less than expected considering the Baseline simulations were 6-bit PCM while this run allowed only 1-bit per picture element. The TIME TO DETECT increased 2.3 seconds for the long range targets, but only 1 second for the medium and short range target: SLANT RANGE decrease percentage was roughly the same for each range of targets as it was overall.

The 512 by 1 simulation was next subjected to a BER = 10^{-4} . The results, as would be expected, showed an increase in TIME TO DETECT and a decrease in SLANT RANGE. TIME TO DETECT increased 1.2 seconds (4.5%) and SLANT RANGE decreased 751 feet (6.7%). The increase, again, appears surprisingly low. At BER = 10^{-3} the TIME TO DETECT increased on additional 1.1 seconds (4.2%) and the SLANT RANGE decreased 819 feet (7.4%). Raising the BER to 10^{-2} produced only an additional increase of 1.2 seconds (4.5%) in the TIME TO DETECT and 817 feet (7.3%) in SLANT RANGE. The latter condition essentially simulates a jamming situation. As can be seen in Figure 5-1, the plot of these data points is a line whose base lies close to the Baseline data point indicating good error free performance, the line slopes gently downward with increasing BER, indicating good performance in a hostile environment.

A second set of data compiled is the number of NO DETECTS occurring in each run. A certain number are to be expected due to the nature of the test. This is verified by the occurrence of two NO DETECTS during the Baseline run. Only one NO DETECT occurred in the 512 x 1, BER = 0 run and none in the 512 x 1, BER = 10^{-4} run. On this basis, the 512 x 1 simulation was more than adequate. At 10^{-3} and 10^{-2} a sum of only 7 NO DETECTS occurred, which was surprising considering the extremely high error density. Again, this should be considered excellent performance.

The performance of the 512 x 1 simulation was, therefore, judged to be adequate.

5.4.4 The 256 x 2 Simulations

The next process was to determine if a lower bit per picture element rate would provide adequate performance. A set of simulations were prepared in which the resolution was reduced to 256 by 240 elements and the video encoded to 2-bits per picture element. The 256 x 2 simulations represents a 2:1 reduction in the number bits per frame over that required for the 512 x 1 simulation.

The 256 x 2 simulation with BER = 0 produced a 3.5 second (14%) increase in TIME TO DETECT over the Baseline results and 2.1 second/increase over the 512 x 1 results. The SLANT RANGE decreased by 2392 (19.7%) feet from the Baseline and 1365 (12.3%) feet from the 512 x 1 results. These results were also rather good considering the reduction in bit rate achievable. However, the NO DETECT rate increased significantly. The NO DETECTS for the 4 ~ 512 x 1 data points were 1, 0, 4, and 3 for an average of 2 per data point (same as the Baseline). For the 256 x 2 simulation the NO DETECTS for the 2 data points were 9 and 13 for an average of 11 per data point or 11 NO DETECTS for 10 film strips shown to each of 8 observers: that is, 11 out of 80 possible occurrences. The 256 x 2 data was consistent throughout the three ranges of targets except for one data point; namely, that for the long range targets with BER = 10^{-3} . The only explanation available is that the observers for that run were exceptionally capable. Based primarily on the NO DETECT performance, the 256 x 2 simulations were considered inadequate.

5.4.5 Interpolation

It was concluded that possibly the repeat field effect of the 256 x 2 simulations could have affected the observer performance. Therefore, a 256 x 2 simulation was produced with the scan lines of field B being produced as an interpolation between the scan lines of field A. The results were quite similar to the 256 x 2 without vertical interpolation and BER = 0. NO DETECTS remained at an average of 11 per data point, SLANT RANGE decreased from 9776 to 9435, while TIME TO DETECT increased from 28.5 to 28.9 seconds. As a result of the lack of improvement, no further simulations were conducted in this direction.

5.4.6 The 512 x 0.75 Simulations

It was decided to simulate a compression rate midway between 512 x 1 and 256 x 2. The selection was 512 x 0.75. The results achieved were remarkably good, as is immediately evident in Figure 5-2. The TIME TO DETECT and SLANT RANGE are on a par with the 512 x 1 results. The NO DETECT results are just slightly poorer, 3 NO DETECTS per data point rather than 2.

5.5 Conclusions

The data gathered for the 512 x 1 and the 512 x 0.75 simulations are essentially equivalent. At 512 x 0.75 the SLANT RANGE is slightly better than at 512 x 1, but the number of NO DETECTS is somewhat higher. One would conclude probably that the 512 x 0.75 is the natural choice, since minimum overall bit rate is the program goal. Two factors were considered at this point; data accuracy and display picture esthetics. It is typical of cosine transform coded pictures to degrade gracefully up to some threshold of bits per picture element after which degradation is rapid. Therefore, this threshold appears to be below 0.75 bits per picture element. None-the-less, the 512 x 0.75 performance should be somewhat poorer than that at 512 x 1. Because of the limited number of observers, it is possible that either the 512 x 1 results appear somewhat poorer than they actually are, or the 512 x 0.75 result appear somewhat better than they actually are. The reverse is illogical. Therefore, the conclusion reached is that 512 x 1 performance is better than 512 x 0.75. Second, the displayed pictures at 512 x 0.75 appear esthetically poorer in quality than those at 512 x 1. If the target and flight path are not as well documented as they were for the subjective tests, the additional quality of the 512 x 1 technique may well provide the added margin to assure success of the mission.

Therefore 512 x 1 is conservatively selected as the candidate compression technique, and the recommended frame rate is one frame per second.

5.6 Statistical Analysis

An alternate approach to analyzing and presenting the test data is described in Appendix D. This approach differs from that of Section 5.4 in that (1) no detects are included as valid data points with a slant range of zero feet, (2) detection ranges for different targets are normalized to mean baseline ranges so that all targets are given equal weight, and (3) average (mean) ranges are calculated rather than median ranges. The results support the conclusions of Section 5.5.

6.0 TASK D - IMPLEMENTATION STUDY

6.1 Introduction

Section 5.0 of this report selected compression system parameters on a very conservative basis which satisfy the scenario described in the statement of work. Aeronutronic Ford is aware that in reality there is no single RPV requirement, but that many different mission profiles and RPV configurations are being developed. For this reason, the Compression System Implementation should have sufficient flexibility to be readily adaptable to a large number of RPV systems and missions. The parameters in Section 5.0 thus form a basic system about which changes can be made for specific missions or parts of missions. Three principal classes of missions include Reconnaissance, ECM and Strike. Navigation may be a common requirement of all three; the first and third, however, may have special video requirements, such as high resolution low frame rate sensor data for reconnaissance and high frame rate and comparatively low resolution sensor data for target tracking. The basic system parameters developed in Section 5.0 of this report were optimized for target detection at a particular aircraft velocity (approximately 400 knots). The compressor selected can also handle high resolution low frame rate video from a reconnaissance camera or selected frames from a real time tracking camera in a strike vehicle. The mechanism for the latter is an optional solid state frame memory which "snatches" a fast frame from a real-time camera and outputs the video at a slow rate consistent with the RF channel bandwidth and therefore also the video compressor processing rate.

The basic compression system uses a cosine transform encoder whose output coefficients are compressed by a differential PCM encoder. The basic system has 512 horizontal by 480 vertical picture elements, output coding precision of 1 bit per picture element and a frame rate of 1 frame per second. Output data rate is approximately 250 K Bits Per Second.

The basic Video Compression system is shown in Figure 6-1. The optional frame memory in the airborne portion of the system is required with existing real time (30 frames/sec) cameras to act as a speed buffer between the high data rate camera and the compression electronics. This frame memory would not be necessary with a slow-scan camera which outputs data at the processing rate. For this study the memory is considered not as an integral part of the compressor, but as a separate subunit which can be added if required.

Airborne RPV System

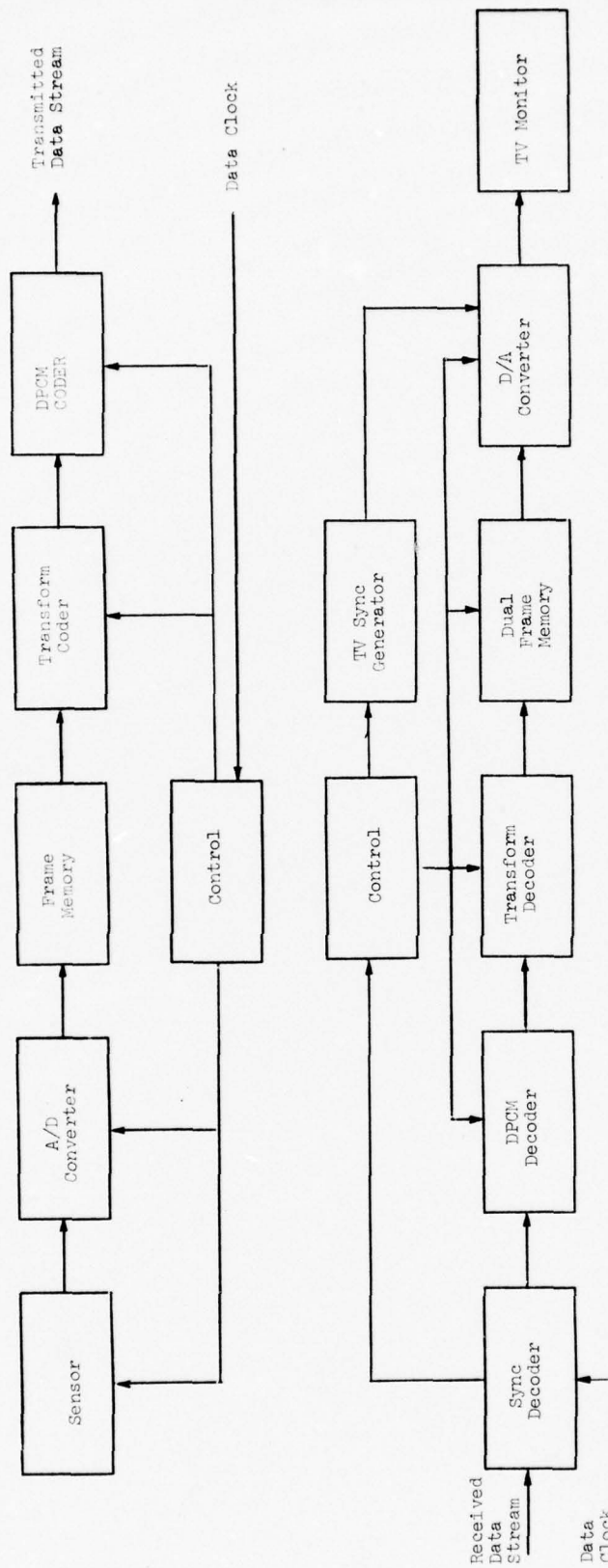


Figure 6-1 RPV Video System Block Diagram

The Aeronutronic Ford implementation is totally compatible with video from vidicon cameras, FLIR sensors, and anticipated solid state sensors such as CCD, CID, etc. The gamut of T.V. sensors presently in use or anticipated for use includes:

- 1) Existing 30 frame per second vidicon cameras which are readily available at low cost and have reached a highly developed state. These are used on RPV's presently being evaluated. A frame memory would be required with these cameras to slow down high rate video to the compression circuit operating rates.
- 2) High frame rate weapon cameras necessary to track targets. Regardless of the type of sensor used for this application, frame rate will be high and will cause the video data rate to be high. Transmitting low frame rate data from the weapon sensor to ground in accordance with the mission profile required by the present program will also necessitate the use of a frame memory.
- 3) Surveillance and reconnaissance missions where low frame-rates are permissible require long term storage (one second in the present program). Items 2) and 3) above considered an electronic frame memory. Another approach would be to use a storage target vidicon which could output video at the rate required by the video compressor. Electronically exposed vidicons are available but are rather complex. Alternatively, the vidicon would be flash exposed by a shutter to prevent image smear due to vehicle motion. A simple reliable pair of counter rotating discs with slits in the lens plane can be driven by a stepper motor synchronized to the processing frame rate.
- 4) Anticipated sensors - A variety of solid state sensors are being developed which will be ideally suited to RPV use due to their small size, low power consumption, ruggedness and low cost. Available devices have insufficient resolution for the present program. Noteworthy are the RCA SID with 256 lines x 320 elements/line and the GE CID with 244 x 188 elements. Although these resolutions are too low for the present program, both of these companies, as well as others, expect to develop larger arrays. An indication is the development of a 496 line x 475 element sensor by Bell Telephone Laboratories. Even with the smaller arrays the possibility exists of simply optically multiplexing

several smaller arrays. This approach is much more feasible with solid state sensors than with vidicons because the sensors are small and have image areas whose dimensions are essentially perfect. Vidicons have electrically generated "raster" areas which can drift in size and location and can have shape distortions caused by deflection components.

Another advantage of the solid state sensor devices under development is storage capability for low frame-rate applications. The RCA SID has a separate storage area and the GE CID can store on the primary image area. Both devices are capable of electronic "flash exposure" by enabling certain electrodes. This eliminates the need for a mechanical shutter.

6.2 RPV Video Compressor Implementation

6.2.1 Principles of Operation

The transmitter portion of the video system which is located in the RPV is shown in the top half of Figure 6-1. One sensor is shown in the figure but several sensors could be used, for example one sensor in the RPV and others in weapons carried by the RPV. A remote switch would permit the ground located pilot to select any one of the airborne sensors. An optional Frame Memory is shown in 6-1 for the case where the sensor generates high frame rate video.

Aeronutronic Ford has selected a digital approach to implementing the RPV video compression equipment. Advantages of the digital approach are insensitivity to temperature, component aging, and power supply voltage variations, no adjustments required and greater reliability. Maintenance, should it be required, is simpler and faster with the digital approach because no adjustments are required after a board (or module) is replaced. No special measuring equipment is needed and very little service training is necessary at the operational level because "trial and error" board substitution can be used.

The system which is described in this report can readily be structured so that system parameters could be changed by the ground-located mission operator. Such factors as resolution, frame rate and bit precision could be changed to match mission requirements through a control link.

6.2.1.1 Sensor and Video Preprocessing

The extremes of the range of sensors directly considered in this study are 30 frames per second, 525 line standard vidicon cameras and slow scan flash-exposed cameras. The Picture Element (PEL) rate for the fast camera (assuming 512 PELS per line) is approximately 10 MHz. The PEL rate for the slow scan camera based on 512 Pels Per Line, 480 Lines Per Frame, 1 Frame Per Second, 1/60 Sec Exposure Time, 7 uSec Horizontal Blanking Time is approximately 250 kHz.

6.2.1.1.1 Automatic Gain Control

The camera should have an AGC (Electrical and/or optical attenuator) to maintain constant video output level. This is important because any video compressor, of necessity, has a limited dynamic range determined by maximum input level (saturation) relative to minimum level (quantization threshold). The AGC should clip very bright reflections caused by specular reflecting objects, bodies of water, and most detrimental, the sky. The AGC should ignore these bright areas while attempting to fill the system dynamic range with useful information.

Simulation studies on the present program dramatically illustrated two extremes in scene brightness and contrast, namely low contrast desert scenes (low contrast of high average brightness) and forest area (low contrast at low average brightness). The AGC should expand the range of the desired video modulation around the average signal level. Sky light presents a common but serious problem because it represents both high intensity and large area. Furthermore, the size and relative location of sky area in the camera field of view changes if sensor attitude changes during RPV maneuvers.

Figure 6-2 shows a concept for performing the required AGC function. Video from the sensor is fed into a black-level negative peak clamp which is enabled during the active video time. This clamp causes video level to shift down to a reference voltage level. A true peak detector would clamp on very thin black video spikes, therefore a small amount of averaging is provided to insure that a large amount of dark video is near the black reference. The clamp is disabled during blanking.

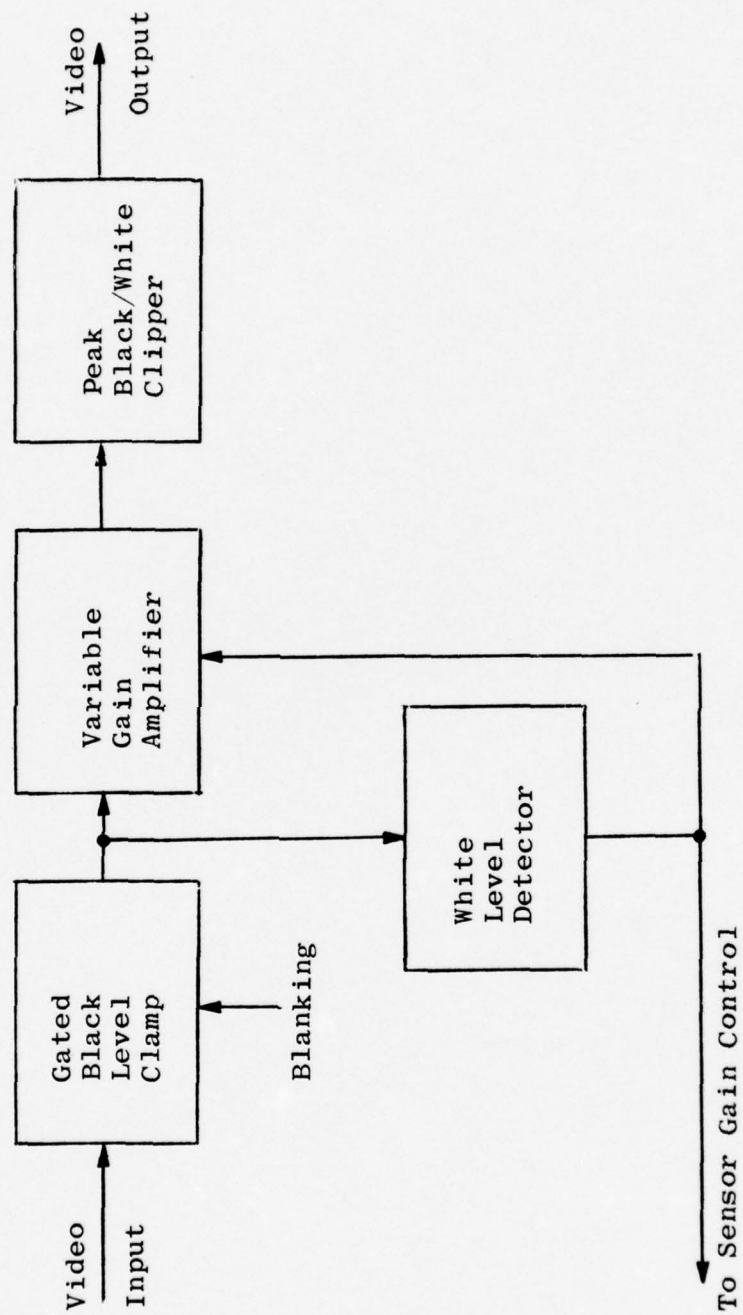


Figure 6-2 AGC Circuit

The output of the black level clamp is fed to a white peak detector which measures white level while ignoring very small, extremely bright objects. Some degree of averaging is used to prevent specular reflections from controlling gain over the entire picture area. The gain control voltage generated by the white P/A detector is fed back to the sensor (vidicon target for example) to control its gain and also to a feed-forward variable gain stage to compensate for imperfection in sensor gain control.

All gain stages through the variable gain stage have linear transfer functions. A peak white/black clipper next eliminates areas of extreme contrast.

A critical factor in the AGC design is the time constant, especially in the slow scan mode where gain adjustment must be predicted from the previous frame.

6.2.1.1.2 Filtering

A low pass filter is required between the sensor and the A/D converter to prevent high frequency variations (especially noise) from being folded over into the video passband.

6.2.1.2 Analog to Digital Converter

An analog to 6-bit-binary digital converter is required to convert the video to a form which is compatible with the digital processing circuits which follow. The conversion rate is approximately 10 MHz when using video from a 30 frame per second camera. If a slow scan camera is used which outputs video at the data processing rate, the sampling rate will be lower, specifically 250 kHz for the parameters selected for the basic system in Section 5.0 of this report.

A/D converters are not common items at 10 MHz sampling rate, partly because popular designs use a successive conversion process and therefore require a sample and hold circuit. A minimal size implementation uses a parallel quantizer approach which compares the video with 63 thresholds and makes a single decision. The quantizer outputs are combined logically to produce a 6 bit binary code. This approach sounds complex on the surface but lends itself to Large Scale Integration due to the fact that simple circuits, with minimal interconnection, are repeated many times.

An A/D converter for operation at 250 kHz is in the realm of commercially available dual inline packages, such as the Micro Networks Corporation MN5120 which is reported to be capable of completing a 6 bit conversion in less than 2uSec. This unit is 1" x 0.5" x 0.15" in size. A possible sample and hold is the Teledyne Philbrick 4856 14 pin dual inline module.

6.2.1.3 Transmitter Frame Memory

The transmitter frame memory is necessary when using presently configured high frame rate cameras. In this sense, the memory is an interim component which is needed to slow down camera video to the Transform/DPCM processing rate. Speeding up the processing rate requires some added hardware volume. It is anticipated that future cameras will be able to output video directly at the processor rate, thus the memory will not be needed. The combination of a low speed Transform/DPCM encoder and a frame memory appears to be an optimum solution for both present and projected sensors.

During system operation, 6 bit video words are written in the memory at a 10 MHz rate until a full frame has been stored (1/30 sec). Unfortunately, cameras presently being used in RPV's use interlaced scanning, therefore it is necessary to organize the memory into two segments so that video is entered first into one half of the memory (Field 1) and then into the second half of the memory (Field 2).

The video data is read out of the memory in a line alternating fashion (line 1 of field 1, line 1 of field 2, line 2 of field 1, etc.) thus converting the data to a non-interlaced format. This is necessary because the DPCM encoder ideally compares adjacent scan lines. Note: the inverse process is performed at the receiver (ground) station to again produce an interlaced display. Design of the memory is straightforward, with the greatest challenge being to minimize memory module count, size and cost. A digital memory using the Fairchild CCD461A module is considered the optimum choice at the present time. This module, a 22 pin dual inline, is capable of storing 16,384 bits. A total of 96 modules is required to store a complete frame. Input and output levels are TTL compatible.

6.2.1.4 Transform Coder

The transform coder block diagram is shown in Figure 6-3. Thirty two picture element groups defined by six bit video words (g_n) are fed to a multiplier register one at a time and held through a processing cycle. The 6 bit video word is successively multiplied by 17 words from the Trig ROM. Each trig word, $\cos(nk)$, represents a value of 17 cosine terms which are harmonically related to the picture element frequency. The resulting words are placed in the Coefficient Storage Register via a summer. (For the first summation, assume that all stages of the coefficient storage register have been reset to zero). Each successive 6 bit picture element is placed in the multiplier register and is multiplied by the next basis vector word. Each of the resulting products is added to the previous products obtained for the corresponding coefficient term. This process continues until all 32 video words of a processing strip have been multiplied by the basis vectors.

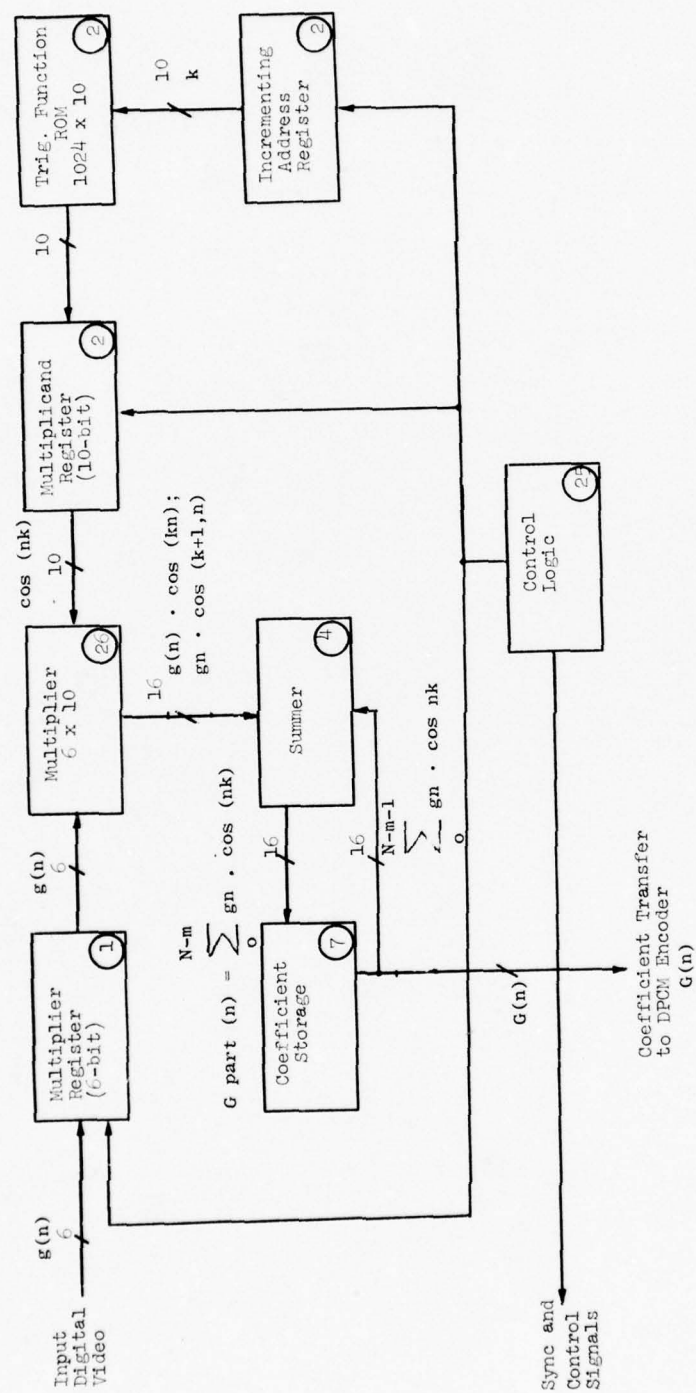


Figure 6-3 Transform Coder Block Diagram

The next group of 32 video words (from the next processing strip) are placed in the multiplier register and the process repeats. During the first iteration, the previous coefficient values in the coefficient storage register are read out of the register and passed on to the DPCM Coder and zeros are inserted in place of the data.

The trig ROM contains all of the basis vectors stored on a point-by-point basis in the sequence in which they multiply the picture element values. A counter, driven by the system clock, addresses the trig values in the proper sequence.

The control logic coordinates the transform coder with the video source and the DPCM coder.

6.2.1.5 Digital DPCM Encoder

The DPCM Coder is shown in Figure 6-4. Sixteen bit coefficients are fed into a coefficient register of the transform coder. It acts as a smoothing buffer for the intermittent coefficient data from the transform coder. The coefficient, G_n , is subtracted in a Binary Adder from a previously determined value from the line memory $G(n)$. (Some average value is assumed for the first line to get the process started). This difference, D_n , is fed to a comparator which determines whether the difference is above or below specific threshold values, Q_n , supplied by a 32×8 ROM. The number and magnitude of thresholds for a given coefficient are determined by the sequence of values determined in the study program and stored in the 32×8 ROM.

The DPCM Code ROM encodes the comparator output B_n as a parallel code suitable for conversion to serial form for transmission and also generates a quantitized magnitude of the comparator output \hat{D}_n . This latter value is added to the predicted value which is a percentage of the value of the same coefficient of the same segment of the previous line, to form a new predicted value $G(n)$. The new predicted value is put into the line memory in place of the old value.

A counter which is interlocked with the transform coder control logic times the operation of the DPCM coder.

Figure 6-4 shows an optional rate buffer structured around a 1024×8 buffer block. This buffer is intended to supply continuous data to the transmission link during the time a new video frame is being captured either by the optional frame memory or by a flash exposed sensor.

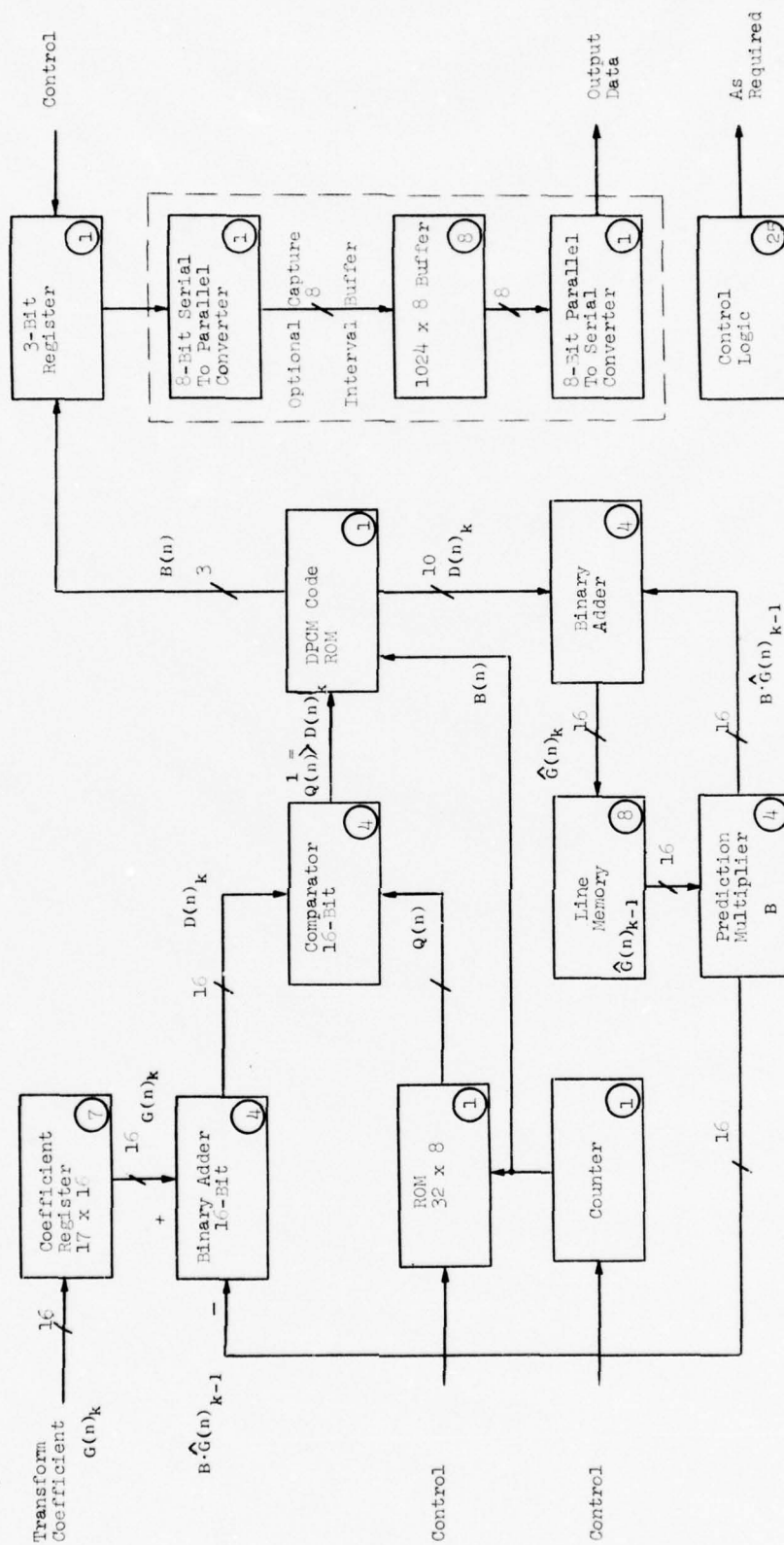


Figure 6-4 Digital DPCM Encoder Block Diagram

6.2.1.6 Sync Addition

Sync bits must be inserted into the video stream prior to transmission. The technique which was developed on the present program inserts a single bit of a sync sequence periodically in the video frame. See Appendix A for a detailed analysis of the synchronization system.

The sequence of sync bits represents a particular word which, when recognized, periodically establishes line sync. These words are phase coded to represent another word which establishes frame sync. The advantage of this technique in a jamming environment is that all sequences are repetitive in a way which permits the use of windows to look only for desired sync data once lock-on has been established.

6.2.1.7 Power Supply

The Aeronutronic Ford Aeronutronic Division in Newport Beach, California has developed power supplies for powering electronics in aircraft and RPV's. The power supply implementation is based on their proven designs for the BGM-34 operating from a 22 to 32 volt DC input range. Based on this design, it is estimated that the equipment described in the present section of this report could be powered by a scaled down version to meet our lower power requirements. Estimated parameters of supplies to be used with and without a frame memory are:

	<u>With Memory</u>	<u>Without Memory</u>
Power Required by Load	43 Watts	20 Watts
Power Input (@65% efficiency)	66 Watts	31 Watts
Power Supply Size	4"x8"x 1"	4"x8"x0.75"
Weight	3 lbs.	2.25 lbs.
Operating Range	-25°C to 90°C	
Input Voltage Range	22 to 32 volts D.C.	

6.2.2 Hardware

Prime considerations in designing RPV hardware are small size, low power consumption and ruggedness, but most of all, highly reliable performance. Of course cost is an ever present factor.

The Aeronutronic Ford implementation was initially modeled with a design using off-the-shelf components to show feasibility. Component groups were next subjected to analysis to determine their suitability for LSI packaging. Factors considered were grouping of components to minimize inter-connecting leads for lower cost assembly, greater reliability, and grouping in functional packages for ease in trouble shooting. Consideration was also given to configuring LSI modules to make them usable in both airborne and ground station implementations.

The circuits are envisioned as being constructed on double sided printed circuit cards approximately $4\frac{1}{2}$ inches wide by 10 inches long. The cards will be mounted in a housing which would be light in weight, yet rigid when fastened to the RPV framework. Cards would be captured along their edges in a manner which affords easy removal from the housing for test and repair. Any high dissipation components (such as the power supply) would be thermally connected to the housing for cooling.

Figure 6-5 shows the board complement for three configurations representing different levels of LSI circuit development. Table 6-1 shows the detailed component organization of the various boards as a result of combining discrete modules in LSI packages.

The package dimensions on Figure 6-5 are compatible with available space indicated on drawings for the BGM34C.

The following list summarized the main characteristics of the airborne RPV equipment.

<u>Compressor Characteristics</u>	No <u>LSI</u>	Level 1 <u>LSI</u>	Level 2 <u>LSI</u>
Size	$3\frac{1}{2} \times 5 \times 12$ "	$3 \times 5 \times 12$ "	$2\frac{1}{2} \times 5 \times 12$ "
Weight		15 lbs.	
Power Input		31 Watts	
<u>Memory Characteristics</u>			
Size	$1\frac{1}{2} \times 5 \times 12$ " (Added to Compressor)		
Weight		5 lbs.	
Input Power		35 Watts	

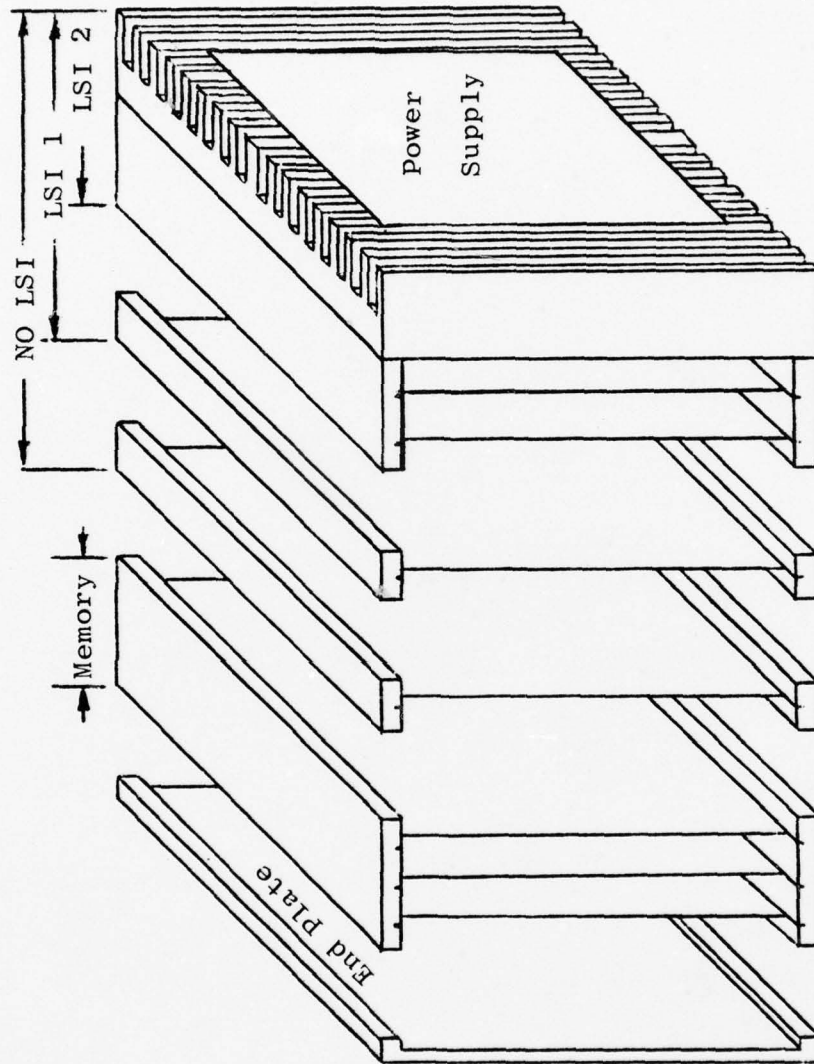


Figure 6-5 Mechanical Configuration of Airborne Compression Equipment (Cover Removed)

Function	No LSI	Board No.		Level 1 LSI		Level 2 LSI		Board No.	
Transform Coder	44-16 Pin Modules	1		43-16 Pin Modules 2-22 pin LSI Mod 1-40 Pin LSI Mod		43-16 Pin Modules 2-22 Pin LSI Mod 1-40 Pin LSI Mod		1	
		2							
DPCM Coder	44-16 Pin Modules								
System Control	50-16 Pin Modules	3		50-16 Pin Modules		40-16 Pin Modules 2-22 pin Modules 1-40 Pin Module		2	
		4							
A/D, Video Proc. Memory Control	40-16 Pin Modules			40-16 Pin Mod		3			

Table 6-1 Transmitter Board Complement

6.2.3 Alternate Approaches

The approach implementing the cosine transform/DPCM encoding technique previously described is the preferred method of implementation. There is at least one alternative approach.

The approach described in previous sections was selected for several reasons.

- a) It is an all digital approach requiring a minimum of adjustment and repair.
- b) It is adaptable; that is, the design can be such that the encoder can be dynamically altered during a mission to accommodate a wide variety of missions and video parameters.
- c) By appropriate application of LSI techniques the hardware implementation can be reduced to acceptable power, weight, and volume.
- d) The performance of the device can be adapted to the sensor by designing the degree of precision desired into the digital processing circuit.

An alternative approach employing analog processing techniques does exist. This approach was developed by the Navy Undersea Center in San Diego. This approach solves the transform coding problem by the use of transversal filters. The implementation of these filters can be either charge coupled devices or surface acoustic wave devices.

For the data sequence

$$g_0, g_1, \dots, g_{n-1}$$

the even discrete cosine transform can be defined as

$$G_k = \exp\left[\frac{-i\pi k}{2N}\right] \sum_{n=-N}^{N-1} g_n \exp\left[\frac{-i2\pi kn}{2N}\right]$$

for $k = 0, 1, \dots, N-1$

and where the data sequence has been extended so that

$$g_{-1-n} = g_n \text{ for } n = 0, 1, \dots, N-1$$

If the mutually complex conjugate terms in the above equation are combined, the following results.

$$G_K = 2 \sum_{n=0}^{N-1} g_n \cos \left[\frac{2\pi(n-\frac{1}{2})K}{2N} \right]$$

This can be put in the Chirp Z Transform format.

$$G_K = 2 \operatorname{Re} \left\{ \exp \left[\frac{-i\pi K}{2N} \right] \exp \left[\frac{-i\pi K^2}{2N} \right] \sum_{n=0}^{N-1} g_n \exp \left[\frac{-i\pi n^2}{2N} \right] \exp \left[\frac{i\pi(n-K)^2}{2N} \right] \right\}$$

In this form the transform can be obtained by a pre-processing multiplication of the discrete signal with a Chirp, convolution with a chirp, and post multiplication with a chirp. Figure 6-6 depicts a block diagram of this implementation.

The analog approach is proposed as a secondary implementation because not enough can be determined about the performance which can be expected. Maintenance and reliability in an operating environment are also unknowns.

It appears that weight, volume, and power requirements will be similar to the digital approach when a moderate amount of circuitry is in LSI form. The previous discussions of frame memory and interface with existing sensors still apply.

For a more detailed description of the analog approach the following references are suggested.

Whitehouse, H.J., Spieser, J.M., and Means, R.W., "High Speed Serial Access Linear Transform Implementations," symposium All Applications Digital Computer, Orlando, Florida.

Means, R.W., Buss D.D., and Whitehouse, H.J., "Real-Time Discrete Fourier Transforms Using Charge Transfer Devices", Proceedings of the CCD Application Conference, Naval Electronics Laboratory Center, San Diego, CA., September 1973.

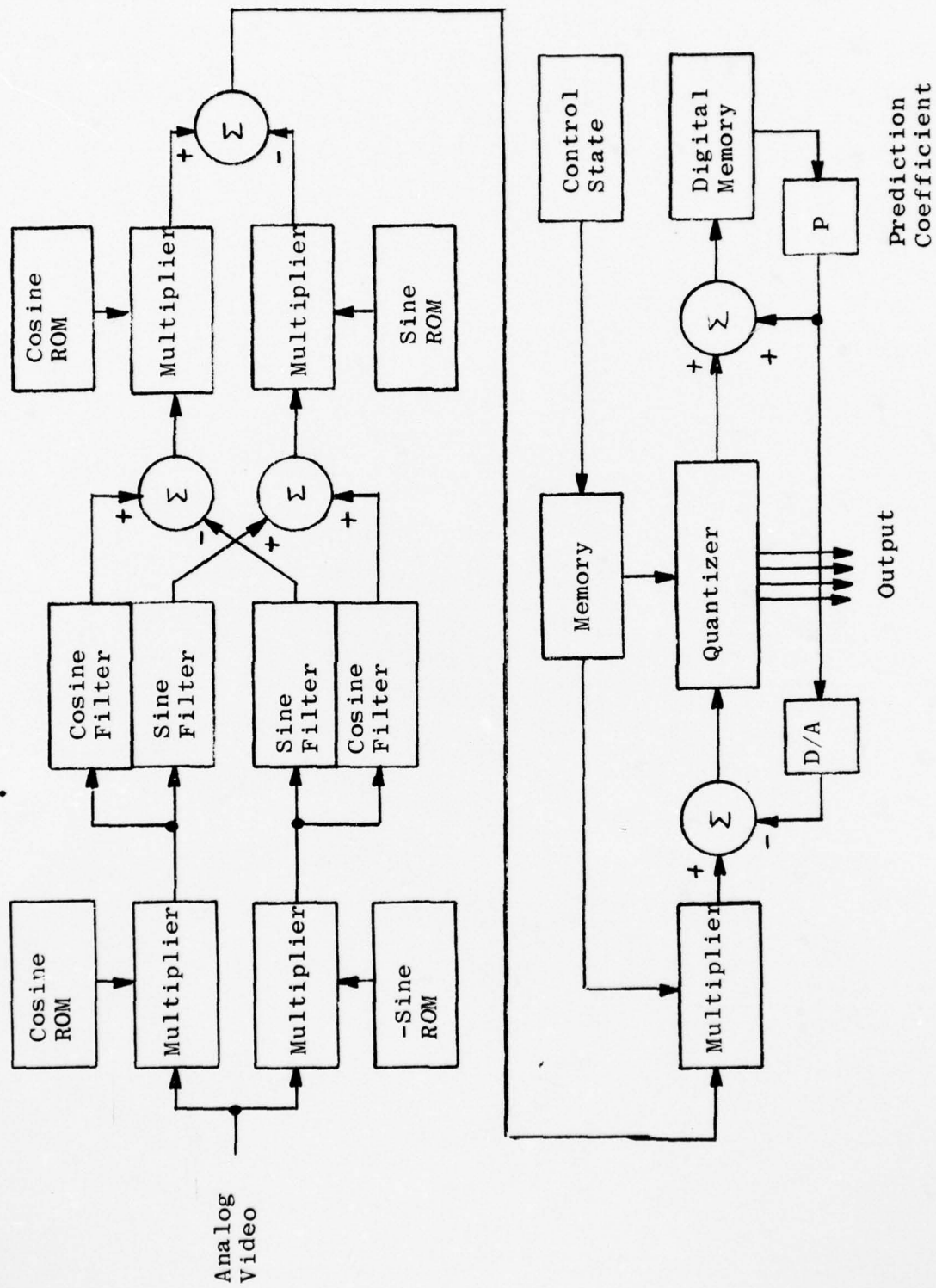


Figure 6-6 Analog Cosine Transform/DPCM Encoder

6.3 Control Center Implementation

6.3.1 Principle of Operation

Figure 6-7 is a block diagram of the video processing equipment in the control center. No special components need to be developed for this center because all functions are within the limits of off-the-shelf components. Also considerably greater space and power is available compared to that which is available in the RPV. It is realized, however, that components developed for RPV use should also be utilized in the control center where there are significant size, power or reliability advantages without cost penalty.

Digital circuits are favored, where practical, because they require no adjustment, have high reliability and permit maintenance at the operational level by simple board substitution without the need for making adjustments.

6.3.1.1 Sync Decoder

In the implementation of the sync system described in Appendix A, video plus sync data bits are clocked into the sync decoder by data link clock pulses from the receive modem. The bit stream is clocked through a register which is tapped at points corresponding to the location of line sync-bits in the data stream.

These taps are tied to a comparator whose second input contains the desired sync code. If the two codes match within a certain number of bits, a line sync detect occurs and a bit counter driven by bit sync is reset and enabled. The bit counter is configured to output a pulse when the next line sync pattern should be available at the output of the comparison register. If a match does occur, the circuit continues to look for the line sync code at the proper location. If a match does not occur on subsequent looks, the circuit examines all comparator outputs until a match does occur. The counter is reset and once again looks at predicted locations for the line sync code. Once the first correct code is detected, this window ignores false codes in the video information. Each detected line code advances a tally counter which saturates after s detects. If a no-detect occurs (due to noise or jamming), the counter is decremented. The state of this counter is used to determine whether line sync has occurred. A count greater than a certain value indicates "in-sync", below another value indicates "out-of-sync".

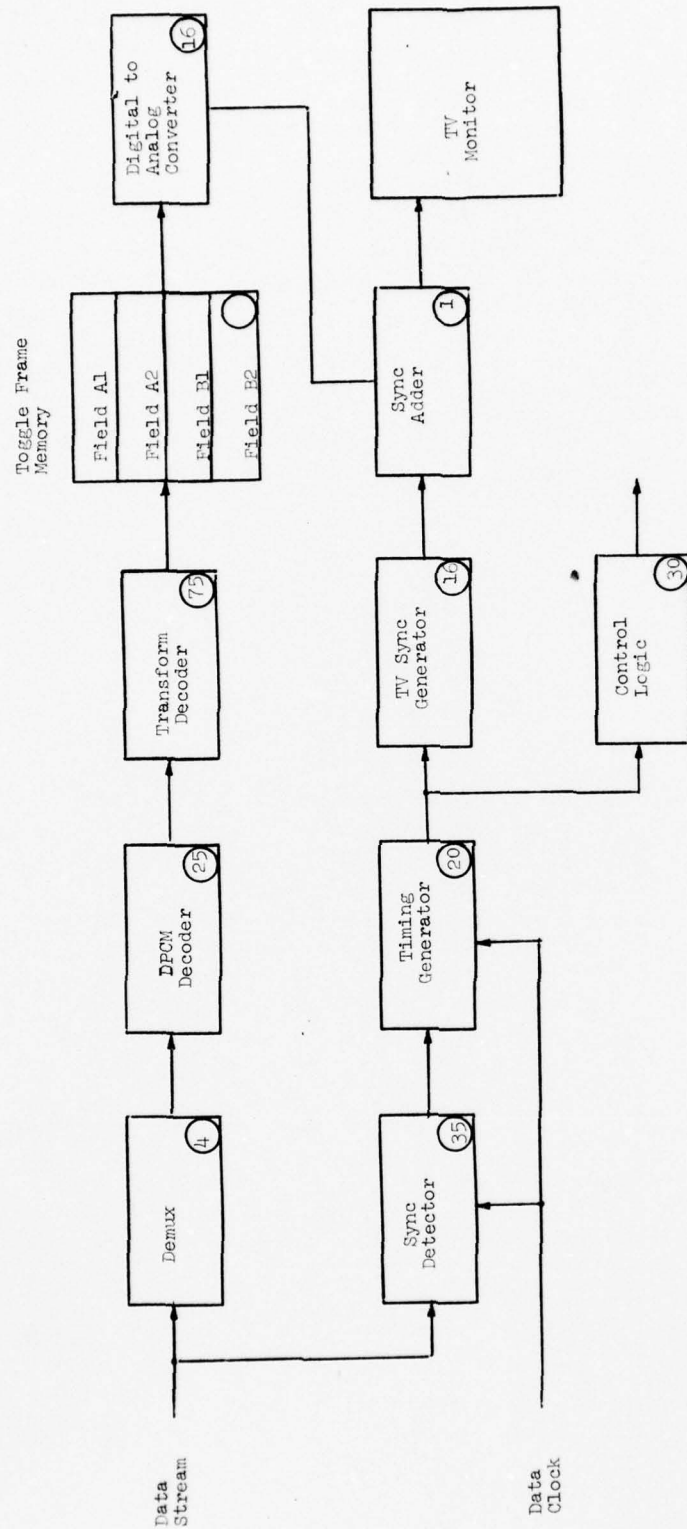


FIGURE 6-7 GROUND CONTROL STATION BLOCK DIAGRAM

Frame sync is determined in a similar manner to line sync. There are actually two line sync codes which represent two senses (1, 0) of the frame sync code elements. The proper sequence of these code senses uniquely defines frame sync. Since line sync must be established before frame sync can be established, there is no need to be concerned with false frame sync.

6.3.1.2 DPCM Decoder

As soon as line sync is established by the sync decoder, video bits can be separated from sync bits and shifted into the DPCM decoder via a three stage shift register. (The 3 corresponds to the maximum number of transmitted DPCM bits per coefficient.) Depending upon which coefficient is in the register, one to three of the bits are transferred into the address ports of a code ROM. A difference value appropriate for the DPCM code for the particular coefficient is applied to one side of a binary adder. The other side of the adder is supplied with a predicted value of the same coefficient from the previous scan line. The prediction coefficient is identical to the one used in the transmitter DPCM encoder. (The predicted value for the first line is the same average value assumed in the transmitter.) The output of the adder is the decoded value of the coefficient. This value is also fed to a one line memory where it is stored until it is needed to decode the same coefficient of the same segment of the next line.

6.3.1.3 Transform Decoder

Operation of the transform decoder is similar to the transform encoder except that the trig ROM stores 17, 32 point cosine terms corresponding to the 17 transform coefficients.

During operation of the transform decoder, coefficient values from the DPCM decoder are fed into a buffer register from which they are transferred into a multiplier register. A coefficient word in the multiplier register is successively multiplied by 32 words from the trig ROM. Each word represents the first value of one of 32 cosine terms which are harmonically related to the picture element frequency. The resulting words are placed in the picture element storage register via a summer. (For the first summation assume that all stages of the PEL storage register have been reset to zero.) The second coefficient value is placed in the multiplier register and is multiplied by 32 words from the trig ROM representing the second value of each of the 32 cosine terms. Each of the resulting products is added to the previous product obtained for the corresponding cosine term. This process continues until all 32 video words of a processing strip have been reconstructed. Processing then proceeds to the next strip.

The reconstructed values of a strip are readout of the PEL storage register as a new strip begins to be processed. These values are held in a buffer until they can be transferred to the frame memory.

6.3.1.4 Dual Frame Memory

The receiver memory is required to convert the low frame rate video transmitted from the RPV to high frame rate video for display to the operator. Capacity for storing two complete video frames must be provided so that one frame can be displayed while the next frame is being received. As a further condition, each frame must be split into 2 fields so that non-interlaced video* from the RPV can be converted to interlaced form for display. The memory is loaded in an alternating line manner, i.e., line 1 is loaded into the field 1 memory, line 2 is loaded into field 2 memory, line 3 is loaded into field 1 memory, etc. During readout, data is read on a standard field alternating basis to produce interlace.

Existing solid state memory devices, such as the Intel IN44 board, can be used for the ground station memory. On a total bit basis, 5 boards are required per frame. RAM devices such as used on the IN44 have an advantage over shift registers in that they can be switched to the read mode as soon as the last received picture element is loaded. The memory which was previously reading can immediately begin to accept new slow scan picture elements. The system need not wait until the end of a field, and so buffering is not required.

6.3.1.5 Digital-to-Analog Converter

A high speed 6 bit D/A is required after the memory to convert the digital video to analog form. The accuracy of this D/A should be equivalent to 8 bits and glitches should be minimized. Composite television sync is added at the DAC output to synchronize the display monitor or any peripheral devices, such as video tape recorders, added to the system for performance evaluation.

* The DPCM encoder in the RPV requires non-interlaced video for its line-to-line comparison.

6.3.1.6 T.V. Monitor

The T.V. monitor should have the following parameters:

- 1) Size - A display area with a diagonal dimension of no more than 14 inches is recommended if the operator sits directly in front of the monitor and operates controls physically located near the viewing screen. This size is a good compromise between being able to quickly scan the entire area when looking for a target and identifying the target if it is small.
- 2) DC restoration to keep the image brightness range constant.

6.3.1.7 System Control and T.V. Sync Generator

The control circuits serve the purpose of timing the DPCM decoder and the cosine transform decoder with respect to input data using bit, line and frame sync derived from the input digital bit stream. Also, the control logic has priority in controlling the writing function of the memory. This is to insure that data is inserted into the memory as soon as it becomes available..

The portion of the memory not receiving data is in the read mode and supplies video bits under control of the T.V. sync generator. Because the memory uses RAMS, write-to-read switching can occur at any time and thus the read and write functions are asynchronous.

6.3.2 Ground Based Control Station Hardware

Because the bandwidth compression equipment is a component part of an overall system, it can be configured as a rack-mountable unit which can be installed in any convenient location. For example, it can be mounted alone or as one unit of a multichannel system in a stand-alone cabinet. The unit can also be mounted in the bottom of an operator console should this be desired by the Mission Control Center designer.

Because the compressor unit is all-digital, it needs no adjustments and therefore can be mounted in a rather inaccessible location. Maintenance, should it be required, is by board replacement on a go-no-go basis. Best of all, no adjustments are required after the defective board is replaced. Mean-time-to repair is minimal even for an inexperienced serviceman using trial-and-error substitution. The ground based hardware is efficiently packaged so that it may be mounted in a small, mobile van with limited space.

The receiver circuits are contained on sixteen 8 inch x 10 $\frac{1}{2}$ inch circuit cards housed in a 10.5 inch card file. The cards are functionally organized as follows:

- 1 Sync Decoder
- 1 DPCM Decoder and Control
- 1 Transform Decoder & Control
- 1 D/A Converter, Sync Adder, Sync Regenerator
- 10 Intel IN44 Memory Cards
- 2 Intel CV40 Control Cards

The above cards occupy about 8 inches of the card file width. The power supplies can be mounted in a standard mounting frame (such as provided by Lambda) or could be mounted in the card file at additional cost if space is critical. Space may be limited in an airborne control station, necessitating additional design cost to mount the supplies in the file.

Power required by the receiver unit is estimated to be 850 watts. The majority of this power is required by the dual frame memory.

The Intel memory cards determine a system operating temperature range of 0°C to +50°C. Storage temperature range is determined by the power supplies as -55°C to +85°C.

6.3.3 Airborne Control Station Hardware

The airborne compressor hardware is functionally identical with the ground based hardware. The major difference is in packaging. The overall unit will be configured to integrate physically with the aircraft structure while maintaining structural rigidity and proper heat conductivity with the aircraft structure and environment.

Printed circuit cards will be the minimum size which is possible with efficient interconnection and will be attached to the mounting structure so as to be unaffected by vibration and shock. Power supplies will have high efficiency and low volume and weight and will be compatible with available aircraft power.

6.4 Airborne Relay Processing

Aeronutronic Ford does not foresee any complications in retransmitting the compressed/reduced video through a relay. The video data in its basic form is a binary bit stream with a 250 kilobit per second rate. Other than maintaining an error rate less than the maximum acceptable level recommended in section 5.0 of this report, there is no constraint placed on the relay. In light of the fact that anti-jam techniques may be used in the link, baseband digit regeneration would be difficult to implement because AJ decoding and reencoding would be required.

6.5 Interface With Maverick and Stubby Hobo

The first requirement for using the video compression system with the Maverick and Stubby Hobo is to provide a sufficiently high frame rate so that the ground station operator can manually acquire the target for the weapon's automatic tracker. The exact frame rate is a function of the weapon velocity, field of view and camera attitude stability. Determining the exact frame rate for target acquisition is not within the scope of the present program, however an example will be given. The Maverick camera has a field of view which is approximately one fourth that of the RPV camera used in the present study. If 256 PEL by 240 line resolution and one bit per PEL compression encoding precision is used, equivalent display resolution will still be 2 times greater than was allowed on the present study and the operator should easily recognize the target. The 450 kHz, 15 dB S/N data link will readily support 7.5 frames per second with a 400 K Bit/Second data rate. Several simple tests on the present program indicated that 7.5 frames per second might be acceptable.

Operating the compression system at 7.5 frames per second with the T.V. cameras presently in the Maverick and Stubby Hobo requires a frame memory to capture every fourth camera frame and slow the video down to the compressor processing rate.

The second requirement for operating with the Maverick and Stubby Hobo is to provide a smooth switchover from the RPV camera to the weapon camera. Failure to do so will cause the operator's display monitor to lose sync momentarily. Under the conditions simulated on the present programs, loss of sync could be disastrous, because on some runs the target is only visible for several seconds. Sync loss with its attendant operator disorientation, could prevent target lockon.

The weapon cameras presently have their own sync generators and cannot be driven by the RPV sync source. It is recommended that the capability of driving the weapon camera with RPV sync be provided. The weapon camera would be slaved to RPV sync when mounted on the RPV, but would free-run after launch.

The third consideration of operation with the Maverick is video scaling and improved AGC. The Maverick AGC presently operates to maintain average video level at about 2 volts. Peak values can reach a level of about 4.3 volts. Without scaling the video will thus greatly exceed the A/D converter dynamic range. The AGC concept described in Section 6.2.1.1.1 of this report is recommended to maximize the amount of useful information transmitted.

6.6 Reliability and Maintainability Estimates

6.6.1 System Mean-Time-Between-Failure (MTBF)

Figure 6-8 shows the reliability math model and MTBF result for the RPV Video System. This model combines the RPV (airborne) portion of the system with the Ground Display portion to provide the total system, air to ground. The Sensor and the air-to-ground video data transmission equipment are not an integral part of this study and therefore are not included in this reliability estimate. The estimated system MTBF of 1100 hours reflects an assumed 100% operational duty-cycle, i.e., 100% of all hours are RPV flight video and ground video display hours. The total estimated system failure rate is 88 failures/ 10^5 hours. The estimated MTBF of the RPV equipment is 1600 hours, or a failure rate of 62 failures/ 10^5 hours. The estimated ground equipment MTBF is 3,900 hours which corresponds to a failure rate of 26 failures/ 10^5 hours.

If the system is implemented using a Sensor having an integral frame memory, the transmitter Frame Memory would be removed and the estimated overall system MTBF would improve from 1,100 hours to 1,200 hours.

6.6.2 Airborne RPV System MTBF

Figure 6-9 presents the reliability math model and MTBF result for the airborne portion of the system. The model elements correspond to the functional sections of the airborne equipment described elsewhere in Section 6.0 of this report. The model estimated failure rate for operating hours only is 62 failures per 10^5 hours. The failure rate and MTBF of a single airborne RPV system, considering an estimated 5% operational (flight) duty cycle, are 3.1 failures per 10^5 hours and 32,000 hours respectively.

AD-A040 033

AERONUTRONIC FORD CORP WILLOW GROVE PA WILLOW GROVE--ETC F/G 17/2
VIDEO IMAGE BANDWIDTH REDUCTION/COMPRESSION STUDY.(U)
FEB 76 E SCHMIDT, W SPICER, H WATKINS F33657-75-C-0353

UNCLASSIFIED

ASD-TR-76-36

NL

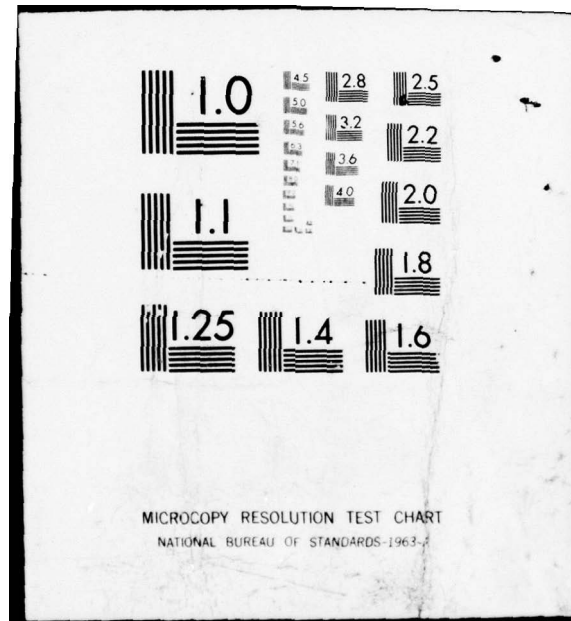
2 OF 2

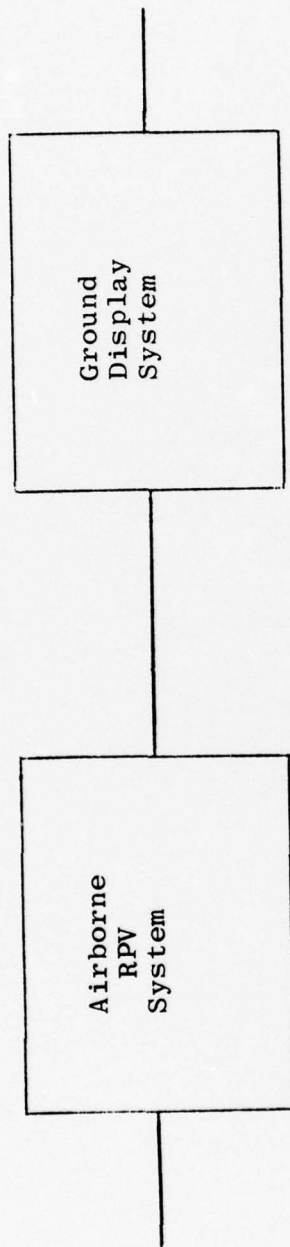
AD
A040033



END

DATE
FILMED
6-77





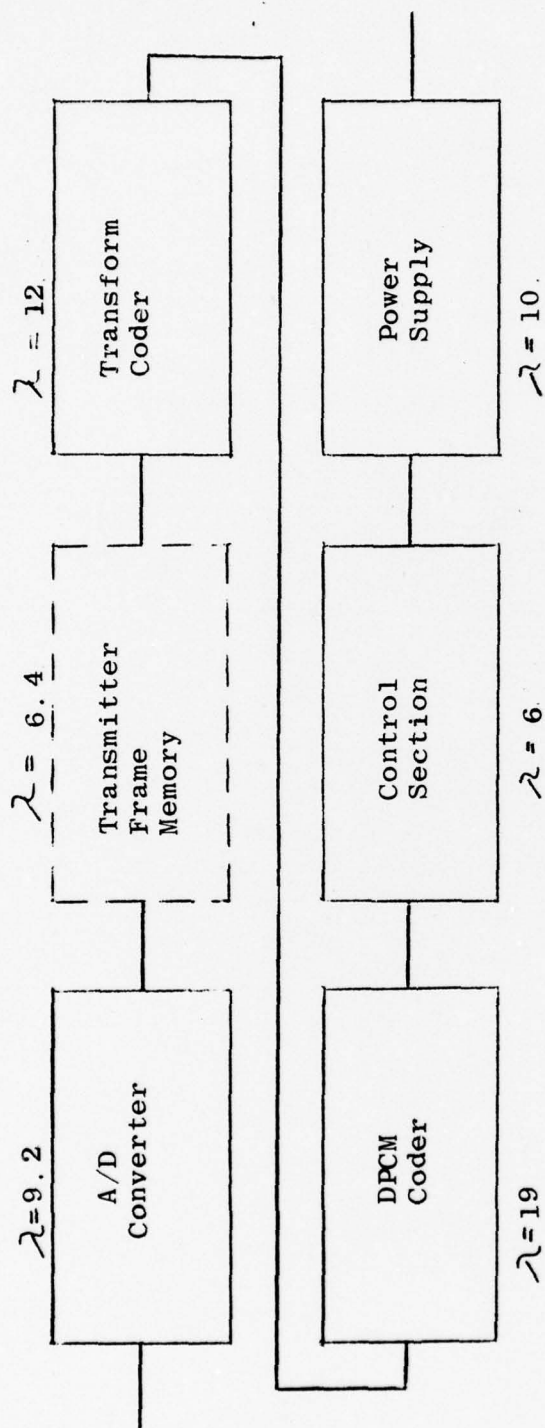
$$\lambda_{OP'G} = 62 \text{ f}/10^5 \text{ hours} \quad \lambda_{OP'G} = 25 \text{ f}/10^5 \text{ hours}$$

$$MTBF_{OP'G} = 1600 \text{ hours/f} \quad MTBF_{OP'G} = 3,900 \text{ hours/f}$$

$$RPV \text{ Video System } MTBF = \left[\frac{1}{\sum_{i=1}^n \lambda_i} \right]^{-1} = 1,140 \text{ hours/f}$$

Figure 6-8 RPV Video System Reliability Math Model

Note: Model element failure rates (λ) are given in $f/10^5$ hrs.



$$\begin{aligned} \text{Operating Failure Rate} &= \sum \lambda = 62/10^5 \text{ hours} \\ \text{Operating MTBF} &= 1600 \text{ hours} \end{aligned}$$

Figure 6-9 Airborne RPV Compression System Reliability Math Model

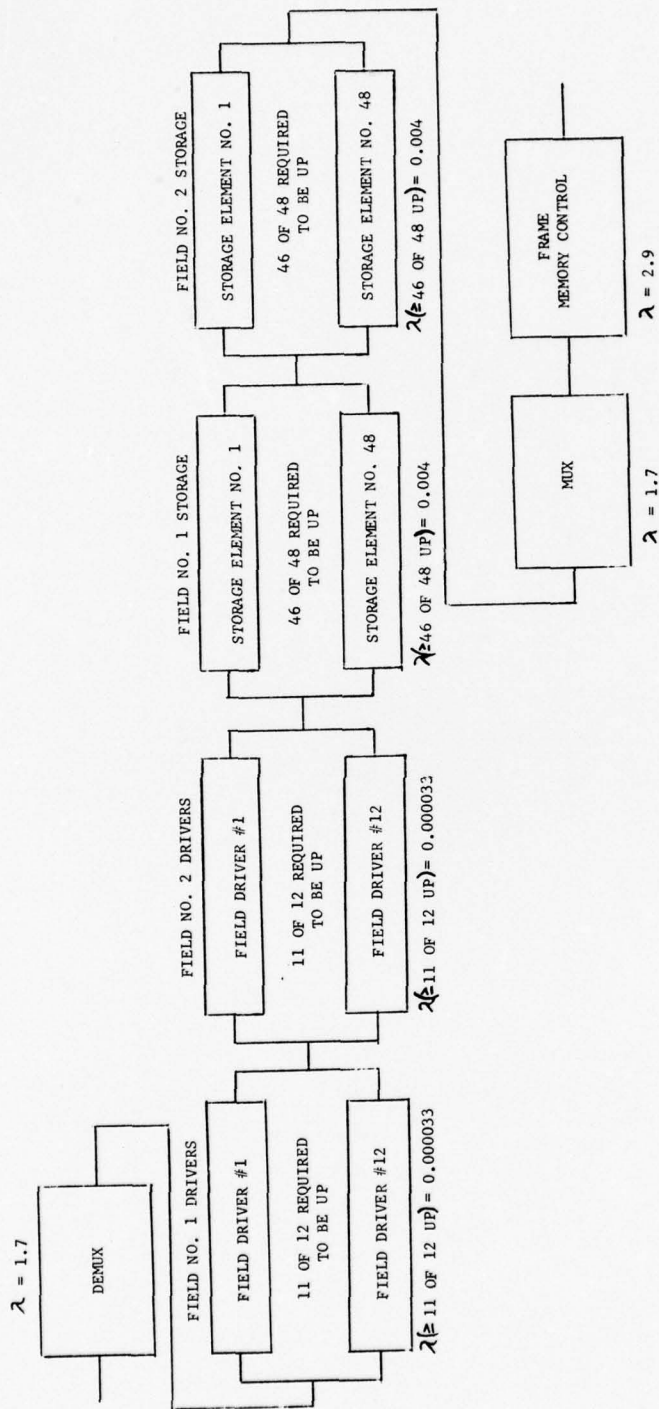
If the system is implemented using a Sensor having an integral frame memory and slow analog output, the digital transmitter Frame Memory will not be necessary and the A/D Converter will become a slower version. In this case, the airborne system would have an operating failure rate of 56 failures per 10^5 hours corresponding to an MTBF of 1800 hours.

6.6.2.1 Frame Memory

Figure 6-10 presents a detailed reliability model of the Transmitter Frame Memory element of the airborne system reliability model. The Frame Memory, in effect, has extensive redundancy in its field storage elements (Field No. 1 Drivers, Field No. 2 Drivers, Field No. 1 Storage and Field No. 2 Storage). The redundancy results from estimating that up to 8 percent of all the drivers can fail and up to 4 percent of all the field storage devices can fail before the operator's performance is significantly affected. This estimate assumes that component failures cause single PEL errors which are randomly distributed throughout the displayed frame. With this redundancy, the Transmitter Frame Memory failure rate is held to 6.4 failures per 10^5 hours.

6.6.3 Ground Display System MTBF

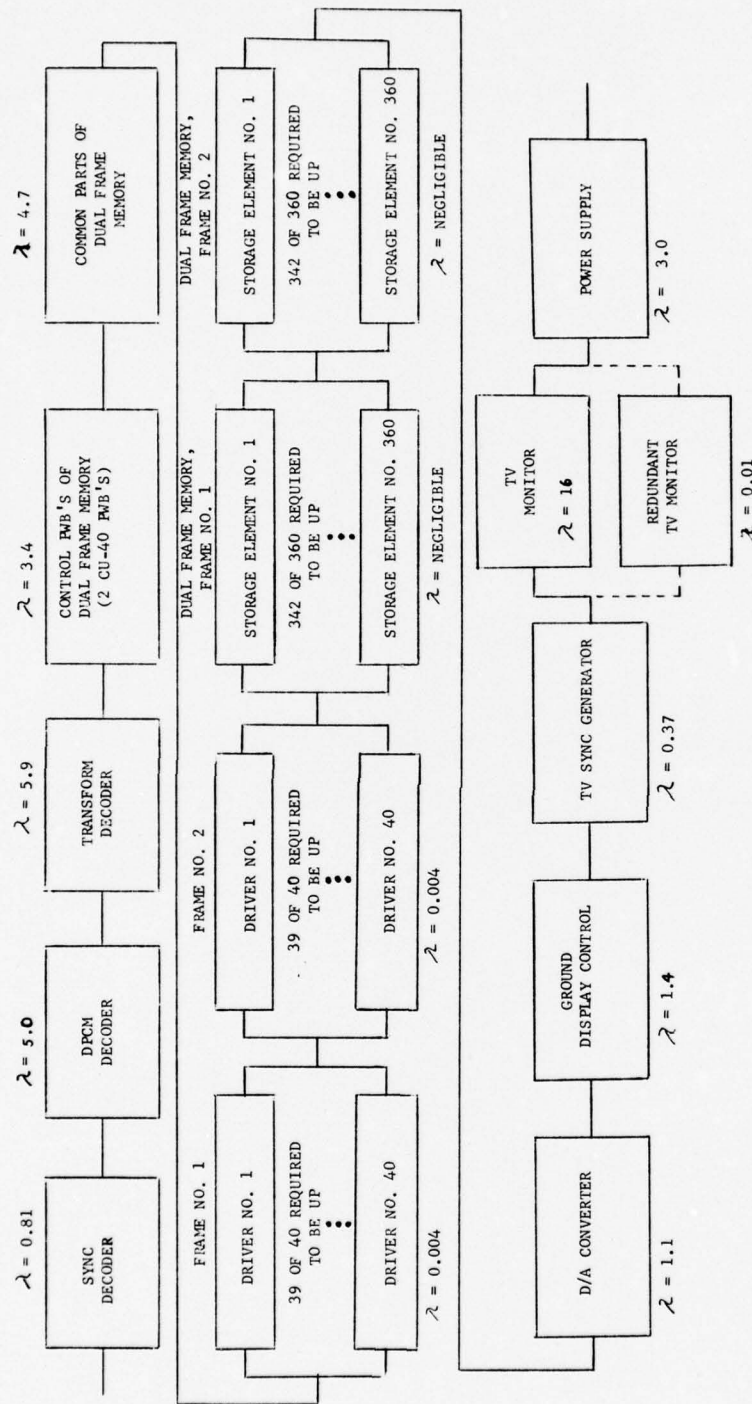
Figure 6-11 shows the Ground Display System reliability math model and MTBF result. The model elements correspond to the functional portions of the ground equipment described elsewhere in the Implementation section of this report. The estimated ground model failure rate for operating hours is 26 failures per 10^5 hours. This estimate is for an individual set of receiver electronics. It is possible to provide one complete receiver unit as standby in the event of prime equipment failure. This redundancy reduces the ground station failure rate to a negligible value. In a multi operator control center one spare could be provided for the entire center. Using reasoning similar to that of Section 6.6.2.1 above, the dual frame memory elements have an effective redundancy in that only 342 out of 360 storage elements and 39 of 40 driver elements of each of two frame memories are required to be "UP". This is based on the assumption that 10% of the storage bits can be lost before operator performance is significantly degraded. By allowing this redundancy, the driver and storage element part of the Dual Frame Memory has almost negligible failure rate.



$$\Sigma \lambda = 6.4$$

Figure 6-10
Transmitter Frame Memory MTBF Math Model

NOTE: FAILURE RATES (λ) ARE GIVEN
FAILURES PER 10^5 HOURS



NOTE: MODEL ELEMENT FAILURE RATES (λ) ARE GIVEN IN F/10⁵ HOURS

OPERATING FAILURE RATE = 25 FAILURES PER 10⁵ HOURS
 OPERATING MTBF = 3,900 HOURS

Figure 6-11
 GROUND COMPRESSION SYSTEM RELIABILITY MATH MODEL

6.6.4 Equipment Failure Rate Estimates

A failure estimate has been obtained for each model element (block) of the airborne system model (Figure 6-9 and 6-10) and the ground system model (Figure 6-11). The failure rates have been obtained by using the failure rate model and failure rate tables of Section 3, MIL-HDBK-217B, Reliability Prediction of Electronic Equipment. Section 3 employs the parts count method of reliability prediction and is applicable (1) to establish feasibility and (2) during early design phases, when only generic part types (including complexity for IC's), part quantities, part quality levels, and the equipment operating environment are known.

The types and quantities of integrated circuits were estimated by circuit design engineers. The part quality level of the IC's is estimated to be MIL-M-38510, Class C. The airborne equipment operating environment is Airborne, Uninhabited; the ground equipment environment is Ground, Fixed. The failure rates employed in the estimates correspond to these conditions.

Since part types, quantities, and quality levels for the ground D/A Converter were not accurately known by Aero-Ford, the supplier's MIL-HDBK-217A failure rate prediction for this assembly was used. Power supply failure rates were estimated based on previous experience with power supplies of similar complexities and output ratings.

It is expected that, in the implementation, all discrete parts will be of the MIL qualified types (JAN) or parts which have been qualified so as to be MIL equivalents, and without special screening tests. These parts, in general, have not been included where they accompany IC's in this overwhelmingly IC-implemented equipment. It is expected that such discrete parts would add less than 5 per cent to model element failure rates, and therefore they have not been included in these feasibility estimates.

Also, for the implementation, it is expected that large volume production will not be achieved for three or more years. By that time, it is estimated that the failure rates for MOS integrated circuits will have decreased to approximately the same values as were achievable for bipolar integrated circuits of comparable complexity and function in 1974. Therefore, bipolar failure rates from MIL-HDBK-217B have been employed for MOS circuits so that the failure rate estimates will reflect the reliability expected at the time of large volume production. The improvement in reliability of integrated circuits with time, experience and maturity is a well known reliability effect and has been demonstrated in the past with bipolar IC's, digital/linear, RTL/DTL/TTL, etc.

6.6.5 Maintainability

6.6.5.1 RPV Equipment Maintainability

The RPV equipment will be designed to facilitate rapid repair on the ground. The power supply will have test points for each of the three output voltages, and a circuit breaker or fuse with indicator lamp for the 28 VDC input. Removal of the circuit board compartment cover will provide quick access to the seven plug-in boards. The power supply will also be removable as a unit. Spares will be provided for each of the seven circuit boards and the power supply. Trouble shooting and equipment function restoral is most readily accomplished by replacing the circuit boards one-by-one until system operation is restored as indicated on the ground TV monitor. The on-ground mean-time-to-restore (MTTR) the airborne equipment to proper operation by circuit board and power supply replacement is estimated to be approximately 0.5 hours.

6.6.5.2 Ground Display System Maintainability

The ground equipment will be packaged on plug-in printed-wiring boards which will be contained in a printed-circuit card cage. There will be approximately 16 circuit boards (including twelve in the dual frame memory) with from 50 to 90 IC's per board. The standard power supplies will be housed in the same card file. It is expected that the TV monitor (and its backup unit, if required) would be mounted in a separate operator's console. This arrangement provides quick access to the equipment assemblies to facilitate timely equipment function restoral. Operating spares would be provided for each circuit card and power supply type; these are all replaceable assemblies. Troubleshooting would be performed to the level of replacing the defective assembly. Test programs or test pattern generators could be provided to aid in trouble verification and diagnosis and in equipment checkout after assembly replacement. Equipment operation, test, and maintenance manuals would be provided to aid the on-site technician. Standard test instruments and tools would also be provided. Under these conditions, it is estimated that the mean-time-to-restore the ground equipment to correct operation would be approximately 0.6 hours.

6.6.5.3 Off-Line Repair

Off-line repair of failed circuit card and power supply assemblies (air and ground) would be accomplished to the piece part level at higher levels of maintenance support. At these levels of support a circuit card tester/trouble-shooter would be necessary, especially for the high-volume airborne circuit-card types, for most efficient maintenance.

6.7 Cost of Implementation

6.7.1 Basis of Cost Analysis

The cost of producing the compression equipment located in the RPV was determined for components of the quality used to compute system reliability in Section 6.6. The quality of these components is near the center of the range of available component quality which extends from limited temperature un-tested parts to fully qualified MIL parts. The chosen level yields reasonable reliability at a moderate cost. In actual practice, quality level could be changed by direct substitution of higher or lower quality components. Table 6-2 lists a range of quality and resultant prices for a typical digital integrated circuit.

The ground station cost was estimated using limited-temperature-range ceramic integrated circuits since it is expected that the ground equipment will be located in a room or van which must maintain a tolerable environment for operating personnel. The ceramic integrated circuit packages will withstand all extremes of temperature and humidity encountered in shipping and storage.

Since the nature of the airborne control center is not known at this time, it can only be stated that its receiver electronics would be similar to the ground equipment if located in a controlled environment in the aircraft. If mounted in an uncontrolled environment, components comparable to those used in the RPV transmitter would be required and special thermal and shock mounting would be necessary.

Table 6-2 Range of Typical IC Quality & Resultant Cost

<u>Part Number</u>	<u>Component Characteristics</u>	<u>Single Unit Price</u>	<u>Cost Factor</u>
SN7400N	Plastic-Commercial 0-70°C	\$ 0.58	1.0
SN7400J	Ceramic 0-70°C	0.86	1.5
SN5400J	Ceramic -55°C to +125°C	3.27	5.6
SNC5400J (TI)	MACH IV/JAN B EQUIV. APPROX. Failure Rate 0.004-0.008/lk Hrs.	4.57 *	7.9
JANSN5400J	JAN M38510 - Fully Qualified	12.50	21.6

* Cost estimates were made with this level of component quality for all parts except the Memory modules which, being new, are presently at a quality level comparable to the SN7400J module. This quality level is expected to be increased in the future, also the memory may not be required with future slow scan cameras.

6.7.2 Non-Recurring Costs

Non-recurring costs of developing the first operational prototype system, and also documentation necessary to produce 50 units, are summarized in Table 6-3. Tasks which would be performed under this effort are; definition of precise system parameters and interface requirements, detailed circuit design, construction and testing of a laboratory breadboard, printed circuit card design, housing design and finally construction and performance testing of the prototype system. Laboratory environmental tests would be performed prior to testing of the equipment in an actual RPV system.

Development cost of the transmitter memory is broken out of the total cost to demonstrate the cost impact of developing cameras with built-in storage.

Two levels of LSI development are described which reduce the transmitter board count from 4 boards to 3 boards and also to 2 boards.

Ancillary items necessary to complete the prototype effort are also listed in Table 6-3.

6.7.3 Per-Unit Production Cost of RPV and Ground Equipment

Table 6-4 lists the cost of producing a quantity of 50 operational equipments based on drawings and experience developed during the development program described in Section 6.7.2 above. The costs must be used cautiously because a quantity of 50 units is small for efficient production of transmitter units, especially if the custom LSI circuits are developed. On the other hand, 50 ground terminals is a large number since one-for-one deployment of RPV's and control stations is unrealistic.

The costs in Table 6-4 are actual production costs on a per unit basis and do not include a factory startup cost of \$100,000 per procurement.

Table 6-3 Non-Recurring Development Costs

	<u>Without Memory</u>	<u>With Memory</u>
1) System Design & Prototype Development	270,000	313,000
A.) Total cost with Level 1 LSI Development	348,000	391,000
B.) Total cost with Level 2 LSI Development	465,000	508,000
2) Documentation for Production	40,000	
3) Instruction Manuals	50,000	
4) Maintenance training including material Preparation and 1 week course	8,000	
5) Spare parts for one year	2,000 per site	
6) Special test equipment consisting of one set of transmitter and receiver electronics	25,000/site	

Table 6-4 Fifty Quantity Production Costs

1.) RPV Equipment Per Unit Cost	<u>Without Memory</u>	<u>With Memory</u>
Basic coder (No LSI)	\$ 4,400	\$ 8,100
Coder with Level 1 LSI	\$ 2,900	\$ 6,600
Coder with Level 2 LSI	\$ 1,900	\$ 5,600
2.) Ground Control Station Equipment Per Unit Cost		
Decoder, Memory, Display		\$19,000

NOTE: The above cost figures are actual production cost. Factory startup is estimated to be \$100,000.

6.8 Potential Hazards

The risk of injury or damage is minimal in the recommended system. The airborne compression equipment is all low power low voltage solid state electronics. There are no moving parts which could come apart during operation. The power supply will be protected to current limit if a circuit component fails, thus preventing heating and a potential fire hazard.

Ground based equipment is also considered quite safe. Again, all processing circuits are constructed with low voltage, low power integrated circuits. Power supplies will be fully short-circuit protected and also will accept unusual line voltage variations without failure.

The T.V. display monitor, by nature, has three potential hazards, however the Manufacturer of the recommended monitor has taken the following precautions to minimize these dangers.

- 1.) CRT Implosion - A laminated safety glass on the CRT increases the faceplate impact resistance and binds fragments together should an unusually heavy blow be struck on the faceplate.
- 2.) X Radiation - Regulation of CRT ultor voltage and faceplate shielding keeps the X radiation below the level allowed by Department of Health, Education and welfare X-Radiation rules, 42 CFR, Part 78.
- 3.) High voltage shock and fire hazard

High voltage components are covered and/or shielded to protect maintenance personnel. Also, flame resistant materials are used in high voltage areas. The operator is further protected by the metal cabinet in which the monitor is housed.

No components with high speed moving parts, such as a video disc recorder, are used in the system, therefore no mechanical hazards are anticipated.

6.9 Operational Constraints

The Aeronutronic Ford Video Bandwidth Compression System is designed to impose minimal constraints on the RPV mission. The truth of this statement was proven during the experimental test phase of the present program. High compression ratios were achieved with no increase in operating complexity over that required for the baseline imagery. For example, the recommended system has full resolution throughout the camera field of view. Therefore, the operator need not slew the camera to place areas he desires to scrutinize in the center of the field of view as he would in a foveal/peripheral system. He merely needs to use his inherent capability of scanning the viewing screen with his eyes.

Retention of full field of view at maximum resolution also makes it possible for the operator to locate targets even in the presence of the rather severe gyrations in the attitude of the camera used to generate the test films for the present program.

Although the recommended basic system operates at one frame per second, it is not necessary to modify the operation of existing cameras. The frame memory permits the camera to operate at its normal 30 frame per second rate.

7 CONCLUSIONS AND RECOMMENDATIONS

The following conclusions are derived from the results of the study program as presented in the preceeding sections.

7.1 Coding Algorithm

The cosine transform/DPCM coding algorithm appears ideally suited to the RPV video compression task. The specific parameters which conservatively appear to provide a satisfactory performance even under high error rate conditions are 512 elements per scan line, 480 scan lines per frame, one frame per second and one bit per picture element. Under these conditions the baseband bandwidth is under 250 kHz using the conservative assumption of one bit per Hertz.

If target tracking is required, the frame rate should be raised to 8 frames per second while a reduction in resolution to 256 x 240 appears satisfactory due to the usual decrease in field of view. Therefore, with the same coding algorithm the baseband bandwidth still remains under 450 kHz.

7.2 Implementation

An all digital implementation of the coder is recommended to provide high reliability and minimize the need for maintenance and adjustment under field conditions. With a reasonable amount of LSI circuitry only two 5 x 10 PC boards and a miniature power supply are required. The anticipated volume is 150 cubic inches and power dissipation is 31 watts.

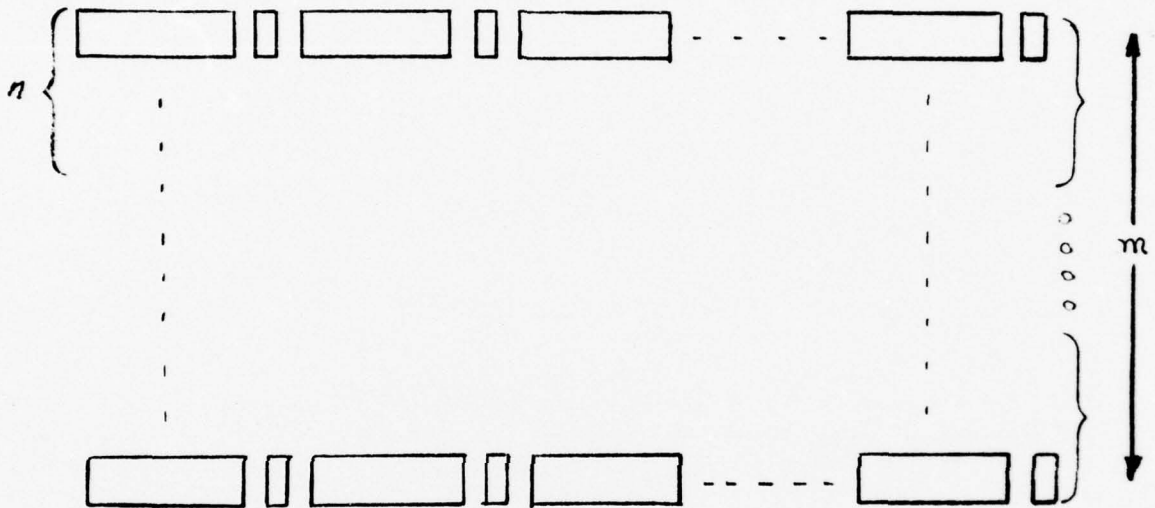
7.3 Sensor

A sensor which can be read out at slow frame rates is recommended, particularly the presently emerging solid state devices. If it is necessary to use the encoder with a conventional TV camera, a frame memory is recommended. This device adds 90 cubic inches and 35 watts to the above estimate.

APPENDIX A

LINE AND FRAME SYNCHRONIZATION ANALYSIS

Consider the following scheme in which a single bit of a sync sequence is inserted periodically* in the video frame. The bits of sync sequence can represent a particular word, say a Barker tuple, which, when recognized, periodically establishes line sync. The tuples, in turn, can be phase coded to represent another word which establishes frame sync. We have the following:



Assume the horizontal word is spread over a sub-frame of size n ; the vertical word over m subframes. The period of the complete framing signal is $N = m \times n$ bits.

Consider first line sync: A sub-frame of size n consists of r sync bits and $n-r$ information bits. If we let p_s denote the probability of correctly recognizing an r bit pattern within a subframe, we have

$$p_s = (1 - p_f)(1 - p_m) \quad (1)$$

- * If the composite data stream is transmitted directly, the periodicity of the sync pattern would be detectable by spectrum analysis and therefore permit the use of sync-correlated jamming. We assume, however, that in the present application, spectrum spreading will be used and as a result the sync pattern will be randomized and therefore difficult to detect.

where

P_f = probability of false recognition of data as sync

p_m = probability of failing to recognize a valid pattern

False sync can occur in any of $n - r$ positions within a sub-frame. Denoting the probability of false sync at any of these positions as p_f , we have:

$$P_f = p_f + (1-p_f)p_f + (1-p_f)^2 p_f + \dots + (1-p_f)^{n-r} p_f$$

or summing

$$P_f = 1 - (1-p_f)^{n-r} \quad (2)$$

where i runs up to $n - r$ and p_f is given by

$$p_f = 2^{-r} \sum_{j=0}^{n-r} \binom{n-r}{j} \quad (3)$$

The upper limit on the summation, t , represents a threshold setting corresponding to the number of errors allowable in an r bit pattern.

The miss probability, p_m , is just the probability of $t+1$ or more errors in a pattern and, assuming a channel characterized by independent errors,

$$p_m = \sum_{j=t+1}^r \binom{r}{j} p^j q^{r-j}$$

or alternatively

$$p_m = 1 - \sum_{j=0}^t \binom{r}{j} p^j q^{r-j} \quad (4)$$

where p , of course, is the bit error rate of the received data stream.

The probability of recognizing a pattern correctly in k subframes is given by

$$P_{sk} = p_s + (1-p_s)p_s + (1-p_s)^2 p_s + \dots + (1-p_s)^{k-1} p_s$$

or

$$P_{sk} = 1 - (1-p_s)^k \quad (5)$$

On the average, we will have to search only one-half of the $n - r + 1$ possible sync positions. The mean time to line synchronization, in subframes, is then given by the expectation of p_s .

$$E[P_s] = \frac{1}{2} p_s + \frac{3}{2} (1-p_s) p_s + \frac{5}{2} (1-p_s)^2 p_s + \dots + \frac{2n-1}{2} (1-p_s)^{n-1} p_s$$

or

$$E[P_s] = \frac{1}{p_s} - \frac{1}{2} \quad (6)$$

If we require l_1 consecutive acceptable patterns before declaring line sync lock, we have

$$p_s' = (1 - P_f)(1 - p_{mi})^{l_1} = p_s (1 - p_{mi})^{l_1-1}$$

and P_{sk} becomes

$$P_{sk}' = (1 - p_{mi})^{l_1-1} P_{sk} \quad (7)$$

Having established line sync, we must look at the phase (sense) of each of the r -tuples carrying the line framing information. The phase information forms an s -tuple, there being one or more s -tuples per frame (N) such that the beginning of the frame is determined uniquely. **Because** line sync is already established, we need not be concerned about false framing, and we can write the probability of vertical framing, p_s' , as

$$p_s' = (1 - p_m') \quad (8)$$

where

p_m' = probability of failing to recognize a valid pattern

This miss probability, p_m' , is the probability of $u + 1$ or more errors in the vertical framing pattern and, again assuming a channel characterized by independent errors,

$$p_m' = 1 - \sum_{j=0}^u \binom{u}{j} p^j q^{u-j} \quad (9)$$

The p in this expression, of course, is the probability that an r -tuple is not accepted because of errors, and $q = 1 - p$. Adjusting u allows p_m' to be made very small at little chance of false framing.

The overall probability of framing in a time equal to $2s$ -tuples, (typically one video frame), P_s , is

$$P_s = \text{Prob} \left\{ \text{vertical framing} / \text{horizontal frequency} \right\} \times \text{Prob} \left\{ \text{acquiring horizontal framing in } 2s-1 \text{ r-tuples} \right\}$$

This latter term is essentially unity, so we can write

$$P_s = p_s' = (1 - p_m') \quad (10)$$

If we further require that the receiver see l_2 consecutive acceptable s-tuples, before advancing from the sync acquisition to the sync lock mode, we have

$$P_s = (1 - p_m')^{l_2} \quad (11)$$

Consider now the probability of loss of framing once framing lock is declared. Loss of framing can occur by failing to recognize the line sync pattern in its expected position j or more times, returning to the sync acquisition mode and falsely recognizing the pattern before correctly recognizing it. Denoting the probability of loss of horizontal framing as p_l , we have

$$p_l = p_m^j (P_f + p_m (1 - P_f) P_f + p_m^2 (1 - P_f)^2 P_f + \dots + p_m^{j-1} (1 - P_f)^{j-1} P_f)$$

or

$$p_l = \frac{p_m^j P_f}{1 - p_m (1 - P_f)} \quad (12)$$

where P_f may or may not be different from that previously defined once reacquisition is attempted. The number of consecutive misses required to initiate sync search is j , and p_m is again the miss probability. For reasonable values of p_m and p_f , p_l becomes

$$p_l \approx p_m^j P_f \quad (13)$$

The probability that loss of line sync occurs on the k th subframe, P_{lk} , is given by

$$P_{lk} = p_l + (1 - p_l) p_l + (1 - p_l)^2 p_l + \dots + (1 - p_l)^{k-1} p_l$$

or

$$P_{lk} = 1 - (1 - p_l)^k \quad (14)$$

The mean time to loss of frame, expressed in subframes, is just the expectation of this expression with k let run to infinity and can be shown to be

$$E[P_L] = \frac{1}{p_L} \quad (15)$$

Alternatively, if we were to require that loss of framing not occur more frequently than once in M subframes, (broadband noise interference) with probability equal to or greater than η , we have

$$1 - P_{L_M} = \eta \quad P_{L_M} = 1 - (1 - p_L)^M = 1 - \eta$$

and

$$p_L = \frac{1 - \eta}{M} \quad (16)$$

Before dismissing the subjected loss of frame performance, one further point warrants consideration. There is the probability of non-recognition of loss of framing. By adjusting t and u once sync lock is declared, p_L can be made almost infinitesimally small, but at the cost of accepting a large class of false framing patterns. Hence, loss of framing can go undetected by the recognition circuits with high probability. This probability of non-recognition is exactly the probability of false sync in any one position, P_f , at the same t and u settings. Denoting this probability of detection of loss of framing by p_d , we can write

$$P_d = 1 - P_f \quad (17)$$

and summing over k subframes, the probability of detection in k subframes, P_{d_k} is

$$P_{d_k} = 1 - (1 - P_d)^k \quad (18)$$

Consider now the performance of a specific framing scheme which utilizes a distributed framing pattern of the type described above. Assume the horizontal pattern to be constructed by augmenting a Barker 7-tuple to an 8-tuple and then forming a 16-bit r -tuple by cascading a pair of 'like sense' (both pos or both neg.) 8-tuples.

Since we must look for both 8-tuples at all times, by eq. (3) we have, allowing no errors ($t = 0$)

$$P_f = (2 \times 2^{-8})^2 = 2^{-14}$$

Depending upon the frequency with which sync bits are inserted into the video stream, we have by eq. (2)

256 x 256 EI Picture				512 x 512 EI Picture		
Sub-Frame Size	$n-r$	% Redundancy	P_f	$n-r$	% Redundancy	P_f
1 Line				512	3	0.0308
2 Lines	512	3	0.0308	1024	1.5	0.0606
4 Lines	1014	1.5	0.0606	2048	0.75	0.1175
8 Lines	2048	0.75	0.1175			

The miss probability, p_m , is given by eq(4) and again for $t = 0$, we have for 10^{-2} and 10^{-5} error rate environments

p	p_m
10^{-2}	.1485
10^{-5}	1.6×10^{-4}

Utilizing eq's (1) and (5), the probability of acquiring horizontal framing in k subframes becomes

		256 x 256 Element Picture				512 x 512 Element Picture			
P_{sk} k		3% Redundancy		0.75% Redundancy		3% Redundancy		0.75% Redundancy	
		$p=10^{-2}$	$p=10^{-5}$	$p=10^{-2}$	$p=10^{-5}$	$p=10^{-2}$	$p=10^{-5}$	$p=10^{-2}$	$p=10^{-5}$
1		0.8252	0.9690	0.7514	0.8824	(SAME)			
2		0.9695	0.9990	0.9382	0.9862				
4		0.9991		0.9962	0.9998				
8				0.99999					

If we were to require 4 consecutive error free patterns before declaring line sync lock, the results in the above table are multiplied by 0.5256 at $p = 10^{-2}$ and 0.9994 at $p = 10^{-5}$. Framing performance at $p = 10^{-5}$ is unaffected, but at $p = 10^{-2}$ the number of subframes required, k , increases by a factor of approximately 2 for a similar performance level.

Having established horizontal framing (line sync), consider now vertical framing. We assume that the phase of horizontal r -tuples has been noted and stored in a shift register as a binary pattern. Actually, because we may miss certain r -tuples after horizontal sync lock is declared due to errors, we record erasures too by using 2 shift registers.

By eq's (8) and (9) we compute p_m' and p_s' as a function of the threshold setting, u , for an s-tuple of length 8.

u	$p = 10^{-2}$		$p = 10^{-5}$	
	p_m'	p_s'	p_m'	p_s'
0	0.7275		0.0013	0.9987
1	0.3428			
2	0.1052	0.8948		
3	0.0214	0.9786		

In the above calculations $q' = 0.8515$ at $p = 10^{-2}$ and $q' = 0.99984$ at $p = 10^{-5}$.

The number of s-tuples of length 8 permissible in a 256 or 512 line picture is determined by the number of lines per sub-frame (1 subframe = 1 bit of verticle s-tuple). These may be tabulated as below.

Sub-Frame Size	256		512	
	% Red	#S-Tuples	% Red	#S-Tuples
1 Line			3	64
2 Lines	3	16	1.5	32
4 Lines	1.5	8	0.75	16
8 Lines	0.75	4		

From the table it is evident that there is ample room to distribute several vertical S-tuples in any frame and hence, both horizontal and vertical framing can be achieved in one frame.

Setting $u = 3$, and by eq (10), we find

	$p = 10^{-2}$	$p = 10^{-5}$
P_{s1}	0.97	0.99

If we choose, as a criterion for declaring loss of framing, the non-recognition of 4 consecutive n-tuples, then by eq. (13) we have, at $p = 10^{-2}$, and largest sub-frame size

$$p_2 = (0.1485)^4 (0.1175) = 5.7 \times 10^{-5}$$

The mean-time to loss of frame by eq (15) is

$$E[P_{e_b}] = \frac{1}{p_2} = 1.75 \times 10^4 \text{ subframes}$$

On, setting $\eta = 0.95$, in eq(16), we can say that loss of framing will not occur more frequently than once in M subframes with probability 0.95 where M is given by

$$M = \frac{5 \times 10^{-2}}{5.7 \times 10^{-5}} = 877 \text{ subframes}$$

Again, this is at $p = 10^{-2}$. Better performance can be obtained by increasing the allowable number of misses or at lower p .

APPENDIX B

SUPPLEMENTAL DATA FOR THE RPV IMAGE BANDWIDTH REDUCTION/COMPRESSION STUDY PROGRAM

The results of the study program have been discussed in the body of this report. The evaluations were based on SLANT RANGE at time of detection with NO DETECTS weighted as SLANT RANGE equal to altitude.

The SLANT RANGE for any film strip with any one of the ten processing methods was determined from the median of the ten observers TIME TO DETECT (time from the beginning of the film strip to target detection). The TIME FROM START TO GROUND ZERO minus the TIME TO DETECT produces the TIME FROM DETECT TO GROUND ZERO from which SLANT RANGE and all other conclusions are drawn. Tables 1 through 10 report this raw data, i.e., TIME FROM DETECT TO GROUND ZERO in the following format.

NO RUN (Film strip number and title)

= X Y (Number of samples (X) not including NO DETECTS
taken in sequence (Y))

= A B C D (TIME FROM DETECT TO GROUND ZERO in seconds)

This is followed by the tabulation of computer processed data including median, mean, variance and deviation. Note that NO DETECTS do not enter into the calculations.

The data presented in Tables B-1 through B-10 is depicted graphically in Figure B-1 showing the mean and deviation for each film strip and each simulation.

Table B-11 presents the computer print out which generated a single mean and deviation for each simulation. This data is tabulated in Table B-12. The last row shows the mean of the 10 previously calculated means for each of the 10 film strips. The deviation of the 10 film strip means for each simulation is also tabulated. This data and the equivalent SLANT RANGE is presented graphically in Figure B-2.

#NO 14 COLD SPRINGS

#13 1

#23.5 24 25.5 22 27 22.5 25 24 19 25 0625 26 22

NUMBER OF OBSERVATIONS 13

MEAN = XBR = SUM(X(I))/N 2.398462E 01
 MEDIAN 2.400000E 01
 RANGE 8.000000E 00
 UNADJUSTED (BIASED) VARIANCE =
 SUM((X(I)-XBR)**2)/N = UVR 4.121302E 00
 UNADJUSTED STANDARD DEVIATION = ... 2.030099E 00

#NO 17 SOUTH PUMPING PLANT

#13 1

#19 20 16 15 16 13.5 10 17 15.5 14.5 19 16 15

NUMBER OF OBSERVATIONS 13

MEAN = XBR = SUM(X(I))/N 1.598462E 01
 MEDIAN 1.600000E 01
 RANGE 1.000000E 01
 UNADJUSTED (BIASED) VARIANCE =
 SUM((X(I)-XBR)**2)/N = UVR 6.275148E 00
 UNADJUSTED STANDARD DEVIATION = ... 2.505025E 00

#NO 7 BUILDING

#13 1

#20 13 14 17 14 10.5 14 17 9 7.5 9 12 12

NUMBER OF OBSERVATIONS 13

MEAN = XBR = SUM(X(I))/N 1.300000E 01
 MEDIAN 1.300000E 01
 RANGE 1.250000E 01
 UNADJUSTED (BIASED) VARIANCE =
 SUM((X(I)-XBR)**2)/N = UVR 1.188462E 01
 UNADJUSTED STANDARD DEVIATION = ... 3.447407E 00

#NO 12 PIRU BRIDGE

#13 1

#35.5 20 36 9.5 19 13 15 25 19.5 17 12 12 17

NUMBER OF OBSERVATIONS 13

MEAN = XBR = SUM(X(I))/N 1.926923E 01
 MEDIAN 1.700000E 01
 RANGE 2.650000E 01
 UNADJUSTED (BIASED) VARIANCE =
 SUM((X(I)-XBR)**2)/N = UVR 6.506213E 01
 UNADJUSTED STANDARD DEVIATION = ... 8.066110E 00

#NO 2 BRIDGE (180°)

#12 1

#3 26.5 12 18 25 7 6 8 11 12 11 11

NUMBER OF OBSERVATIONS 12

MEAN = XBR = SUM(X(I))/N 1.254167E 01
 MEDIAN 1.100000E 01
 RANGE 2.350000E 01
 UNADJUSTED (BIASED) VARIANCE =
 SUM((X(I)-XBR)**2)/N = UVR 4.772743E 01
 UNADJUSTED STANDARD DEVIATION = ... 6.908504E 00

#NO 11 POWER DISTRIBUTION STATION

#13 1

#17 19.5 14 16.5 20.5 21 32 19.5 20.5 20 28 32 25

NUMBER OF OBSERVATIONS 13

MEAN = XBR = SUM(X(I))/N 2.196154E 01
 MEDIAN 2.050000E 01
 RANGE 1.800000E 01
 UNADJUSTED (BIASED) VARIANCE =
 SUM((X(I)-XBR)**2)/N = UVR 2.971006E 01
 UNADJUSTED STANDARD DEVIATION = ... 5.450693E 00

#NO 13 GIBALTAR DAM

#13 1

#20 19.5 23 16 11 19 21 19.5 16 21 21 29 19

NUMBER OF OBSERVATIONS 13

MEAN = XBR = SUM(X(I))/N 1.961539E 01
 MEDIAN 1.950000E 01
 RANGE 1.800000E 01
 UNADJUSTED (BIASED) VARIANCE =
 SUM((X(I)-XBR)**2)/N = UVR 1.589053E 01
 UNADJUSTED STANDARD DEVIATION = ... 3.986293E 00

#NO 3 SAMSITE (350°)

#13 1

#17 11 18 13 21 11 12 12 12 10 18 22 18

NUMBER OF OBSERVATIONS 13

MEAN = XBR = SUM(X(I))/N 1.500000E 01
 MEDIAN 1.300000E 01
 RANGE 1.200000E 01
 UNADJUSTED (BIASED) VARIANCE =
 SUM((X(I)-XBR)**2)/N = UVR 1.569231E 01
 UNADJUSTED STANDARD DEVIATION = ... 3.961352E 00

#NO 5 SAMSITE (75°)

#13 1

#12.5 15 11.5 9 20 17 12 18.5 23 12 14 15 16

NUMBER OF OBSERVATIONS 13

MEAN = XBR = SUM(X(I))/N 1.503946E 01
 MEDIAN 1.500000E 01
 RANGE 1.400000E 01
 UNADJUSTED (BIASED) VARIANCE =
 SUM((X(I)-XBR)**2)/N = UVR 1.382544E 01
 UNADJUSTED STANDARD DEVIATION = ... 3.718258E 00

#NO 16 INDUSTRIAL BLDG.

#12 1

#26.5 16 20 24.5 21 29 26 31 22 29 31 29

NUMBER OF OBSERVATIONS 12

MEAN = XBR = SUM(X(I))/N 2.541667E 01
 MEDIAN 2.650000E 01
 RANGE 1.500000E 01
 UNADJUSTED (BIASED) VARIANCE =
 SUM((X(I)-XBR)**2)/N = UVR 2.103472E 01
 UNADJUSTED STANDARD DEVIATION = ... 4.586363E 00

NO 14 COLD SPRINGS CANYON BRIDGE

=3 1
=22 22 24 21 24 26 26 24

NUMBER OF OBSERVATIONS 8
MEAN = $\bar{XBR} = \text{SUM}(X(I))/N$ 2.362500E 01
MEDIAN 2.400000E 01
RANGE 5.000000E 00
UNADJUSTED (BIASED) VARIANCE =
SUM((X(I)- \bar{XBR})**2)/N = UVR 2.934375E 00
UNADJUSTED STANDARD DEVIATION = ... 1.727534E 00

=NO 17 SOUTH PUMPING PLANT

=3 1
=15 13 12 15 17 15 14 13

NUMBER OF OBSERVATIONS 8
MEAN = $\bar{XBR} = \text{SUM}(X(I))/N$ 1.425000E 01
MEDIAN 1.500000E 01
RANGE 5.000000E 00
UNADJUSTED (BIASED) VARIANCE =
SUM((X(I)- \bar{XBR})**2)/N = UVR 2.137500E 00
UNADJUSTED STANDARD DEVIATION = ... 1.477020E 00

=NO 7 BUILDING

=7 1
=13 13 14 9 13 10 13

NUMBER OF OBSERVATIONS 7
MEAN = $\bar{XBR} = \text{SUM}(X(I))/N$ 1.214236E 01
MEDIAN 1.300000E 01
RANGE 5.000000E 00
UNADJUSTED (BIASED) VARIANCE =
SUM((X(I)- \bar{XBR})**2)/N = UVR 2.77592E 00
UNADJUSTED STANDARD DEVIATION = ... 1.726149E 00

=NO 12 PIRO BRIDGE

=3 1
=17 13 14 13 15 15 12 15

NUMBER OF OBSERVATIONS 8
MEAN = $\bar{XBR} = \text{SUM}(X(I))/N$ 1.437500E 01
MEDIAN 1.500000E 01
RANGE 6.000000E 00
UNADJUSTED (BIASED) VARIANCE =
SUM((X(I)- \bar{XBR})**2)/N = UVR 3.359375E 00
UNADJUSTED STANDARD DEVIATION = ... 1.832860E 00

=NO 2 BRIDGE (180°)

=3 1
=10 9 3 9 10 3 9 9

NUMBER OF OBSERVATIONS 8
MEAN = $\bar{XBR} = \text{SUM}(X(I))/N$ 9.000000E 00
MEDIAN 9.000000E 00
RANGE 2.000000E 00
UNADJUSTED (BIASED) VARIANCE =
SUM((X(I)- \bar{XBR})**2)/N = UVR 5.000000E 01
UNADJUSTED STANDARD DEVIATION = ... 7.071063E 01

=NO 11 POWER DISTRIBUTION STATION

=8 1
=19 15 20 19 27 18 10 25

NUMBER OF OBSERVATIONS 8
MEAN = $\bar{XBR} = \text{SUM}(X(I))/N$ 1.912500E 01
MEDIAN 1.700000E 01
RANGE 1.700000E 01
UNADJUSTED (BIASED) VARIANCE =
SUM((X(I)- \bar{XBR})**2)/N = UVR 2.485937E 01
UNADJUSTED STANDARD DEVIATION = ... 4.935913E 00

=NO 13 GIBRALTAR DAM

=3 1
=14 15 13 13 17 18 19 16

NUMBER OF OBSERVATIONS 8
MEAN = $\bar{XBR} = \text{SUM}(X(I))/N$ 1.625000E 01
MEDIAN 1.700000E 01
RANGE 6.000000E 00
UNADJUSTED (BIASED) VARIANCE =
SUM((X(I)- \bar{XBR})**2)/N = UVR 3.937500E 00
UNADJUSTED STANDARD DEVIATION = ... 1.934313E 00

=NO 3 SAMSITE (350°)

=7 1
=16 12 11 17 16 10 17

NUMBER OF OBSERVATIONS 7
MEAN = $\bar{XBR} = \text{SUM}(X(I))/N$ 1.414236E 01
MEDIAN 1.600000E 01
RANGE 7.000000E 00
UNADJUSTED (BIASED) VARIANCE =
SUM((X(I)- \bar{XBR})**2)/N = UVR 7.336735E 00
UNADJUSTED STANDARD DEVIATION = ... 2.777417E 00

=NO 5 SAMSITE (75°)

=3 1
=14 11 22 11 13 14 11 14

NUMBER OF OBSERVATIONS 8
MEAN = $\bar{XBR} = \text{SUM}(X(I))/N$ 1.437500E 01
MEDIAN 1.400000E 01
RANGE 1.100000E 01
UNADJUSTED (BIASED) VARIANCE =
SUM((X(I)- \bar{XBR})**2)/N = UVR 1.323433E 01
UNADJUSTED STANDARD DEVIATION = ... 3.637903E 00

=NO 16 INDUSTRIAL BLDG.

=3 1
=24 19 26 26 22 20 12 10

NUMBER OF OBSERVATIONS 8
MEAN = $\bar{XBR} = \text{SUM}(X(I))/N$ 1.787500E 01
MEDIAN 2.200000E 01
RANGE 1.600000E 01
UNADJUSTED (BIASED) VARIANCE =
SUM((X(I)- \bar{XBR})**2)/N = UVR 3.210938E 01
UNADJUSTED STANDARD DEVIATION = ... 5.666514E 00

Table B-3 Data for 512 x 1, BER = 10⁻⁴ Simulation

=NO 14 COLD SPRINGS CANYON BRIDGE
=3 1
=20 23 25 22 26 24 20 21

NUMBER OF OBSERVATIONS 3
MEAN = $\bar{X}_B = \text{SUM}(X(I))/N$ 2.325000E 01
MEDIAN 2.400000E 01
RANGE 4.000000E 00
UNADJUSTED (BIASED) VARIANCE =
SUM((X(I)- \bar{X}_B)*2)/N = UVR 7.637500E 00
UNADJUSTED STANDARD DEVIATION = ... 2.772634E 00

=NO 17 SOUTH PUMPING PLANT
=3 1
=13 13 13 11 16 15 14 16

NUMBER OF OBSERVATIONS 3
MEAN = $\bar{X}_B = \text{SUM}(X(I))/N$ 1.337500E 01
MEDIAN 1.400000E 01
RANGE 5.000000E 00
UNADJUSTED (BIASED) VARIANCE =
SUM((X(I)- \bar{X}_B)*2)/N = UVR 2.607375E 00
UNADJUSTED STANDARD DEVIATION = ... 1.615356E 00

=NO 7 BUILDING
=3 1
=12 11 14 14 12 12 11 12

NUMBER OF OBSERVATIONS 3
MEAN = $\bar{X}_B = \text{SUM}(X(I))/N$ 1.225000E 01
MEDIAN 1.200000E 01
RANGE 3.000000E 00
UNADJUSTED (BIASED) VARIANCE =
SUM((X(I)- \bar{X}_B)*2)/N = UVR 1.137500E 00
UNADJUSTED STANDARD DEVIATION = ... 1.063725E 00

=NO 12 PIRU BRIDGE
=3 1
=17 14 13 9 19 15 9 11

NUMBER OF OBSERVATIONS 3
MEAN = $\bar{X}_B = \text{SUM}(X(I))/N$ 1.337500E 01
MEDIAN 1.400000E 01
RANGE 1.000000E 01
UNADJUSTED (BIASED) VARIANCE =
SUM((X(I)- \bar{X}_B)*2)/N = UVR 1.144433E 01
UNADJUSTED STANDARD DEVIATION = ... 3.383360E 00

=NO 2 BRIDGE (180°)
=3 1
=6 3 3 7 3 3 9 2

NUMBER OF OBSERVATIONS 3
MEAN = $\bar{X}_B = \text{SUM}(X(I))/N$ 7.375000E 00
MEDIAN 8.000000E 00
RANGE 3.000000E 00
UNADJUSTED (BIASED) VARIANCE =
SUM((X(I)- \bar{X}_B)*2)/N = UVR 3.523750E 01
UNADJUSTED STANDARD DEVIATION = ... 3.270243E 01

=NO 11 POWER DISTRIBUTION STATION
=3 1
=13 12 19 16 13 23 13 15

NUMBER OF OBSERVATIONS 3
MEAN = $\bar{X}_B = \text{SUM}(X(I))/N$ 1.325000E 01
MEDIAN 1.300000E 01
RANGE 5.000000E 00
UNADJUSTED (BIASED) VARIANCE =
SUM((X(I)- \bar{X}_B)*2)/N = UVR 4.937500E 00
UNADJUSTED STANDARD DEVIATION = ... 2.222049E 00

=NO 13 GIBRALTAR DAM
=3 1
=11 16 13 14 17 23 13 17

NUMBER OF OBSERVATIONS 3
MEAN = $\bar{X}_B = \text{SUM}(X(I))/N$ 1.612500E 01
MEDIAN 1.700000E 01
RANGE 1.200000E 01
UNADJUSTED (BIASED) VARIANCE =
SUM((X(I)- \bar{X}_B)*2)/N = UVR 1.160933E 01
UNADJUSTED STANDARD DEVIATION = ... 3.407253E 00

=NO 3 SAM SITE (350°)
=3 1
=3 12 13 12 16 23 12 3

NUMBER OF OBSERVATIONS 3
MEAN = $\bar{X}_B = \text{SUM}(X(I))/N$ 1.237500E 01
MEDIAN 1.200000E 01
RANGE 2.000000E 01
UNADJUSTED (BIASED) VARIANCE =
SUM((X(I)- \bar{X}_B)*2)/N = UVR 2.923433E 01
UNADJUSTED STANDARD DEVIATION = ... 5.406332E 00

=NO 5 SAM SITE (75°)
=3 1
=3 12 12 12 13 15 3 13

NUMBER OF OBSERVATIONS 3
MEAN = $\bar{X}_B = \text{SUM}(X(I))/N$ 1.225000E 01
MEDIAN 1.200000E 01
RANGE 1.000000E 01
UNADJUSTED (BIASED) VARIANCE =
SUM((X(I)- \bar{X}_B)*2)/N = UVR 9.637500E 00
UNADJUSTED STANDARD DEVIATION = ... 3.112475E 00

=NO 16 INDUSTRIAL BLDG.
=3 1
=25 27 17 17 19 13 15 24

NUMBER OF OBSERVATIONS 3
MEAN = $\bar{X}_B = \text{SUM}(X(I))/N$ 2.025000E 01
MEDIAN 1.700000E 01
RANGE 1.200000E 01
UNADJUSTED (BIASED) VARIANCE =
SUM((X(I)- \bar{X}_B)*2)/N = UVR 1.718750E 01
UNADJUSTED STANDARD DEVIATION = ... 4.145731E 00

Table B-4 Data for 512 x 1, BER = 10⁻³ Simulation

NO 14 COLD SPRINGS CANYON BRIDGE
=3 1
=26 24 24 23 23 17 19 27

NUMBER OF OBSERVATIONS 3
MEAN = XBR = SUM(X(I))/N 2.287500E 01
MEDIAN 2.400000E 01
RANGE 1.000000E 01
UNADJUSTED (BIASED) VARIANCE =
SUM((X(I)-XBR)**2)/N = UVR 9.859375E 00
UNADJUSTED STANDARD DEVIATION = ... 3.139964E 00

=NO 17 SOUTH PUMPING PLANT
=3 1
=10 14 10 3 3 7 13 16

NUMBER OF OBSERVATIONS 3
MEAN = XBR = SUM(X(I))/N 1.137500E 01
MEDIAN 1.000000E 01
RANGE 1.100000E 01
UNADJUSTED (BIASED) VARIANCE =
SUM((X(I)-XBR)**2)/N = UVR 1.473437E 01
UNADJUSTED STANDARD DEVIATION = ... 3.833533E 00

=NO 7 BUILDING
=3 1
=13 12 11 15 12 14 12 14

NUMBER OF OBSERVATIONS 3
MEAN = XBR = SUM(X(I))/N 1.287500E 01
MEDIAN 1.300000E 01
RANGE 4.000000E 00
UNADJUSTED (BIASED) VARIANCE =
SUM((X(I)-XBR)**2)/N = UVR 1.609375E 00
UNADJUSTED STANDARD DEVIATION = ... 1.268611E 00

=NO 12 PIRU BRIDGE
=5 1
=10 3 20 12 16

NUMBER OF OBSERVATIONS 5
MEAN = XBR = SUM(X(I))/N 1.320000E 01
MEDIAN 1.200000E 01
RANGE 1.200000E 01
UNADJUSTED (BIASED) VARIANCE =
SUM((X(I)-XBR)**2)/N = UVR 1.356000E 01
UNADJUSTED STANDARD DEVIATION = ... 4.303132E 00

=NO 2 BRIDGE (180°)
=7 1
=3 3 3 9 2 3 12

NUMBER OF OBSERVATIONS 7
MEAN = XBR = SUM(X(I))/N 9.857143E 00
MEDIAN 8.000000E 00
RANGE 4.000000E 00
UNADJUSTED (BIASED) VARIANCE =
SUM((X(I)-XBR)**2)/N = UVR 1.836735E 00
UNADJUSTED STANDARD DEVIATION = ... 1.355262E 00

=NO 11 POWER DISTRIBUTION STATION
=3 1
=16 19 13 16 13 11 16 20

NUMBER OF OBSERVATIONS 3
MEAN = XBR = SUM(X(I))/N 1.675000E 01
MEDIAN 1.800000E 01
RANGE 2.000000E 00
UNADJUSTED (BIASED) VARIANCE =
SUM((X(I)-XBR)**2)/N = UVR 6.687500E 00
UNADJUSTED STANDARD DEVIATION = ... 2.586020E 00

=NO 13 GIBRALTAR DAM
=8 1
=14 14 17 10 14 15 13 13

NUMBER OF OBSERVATIONS 3
MEAN = XBR = SUM(X(I))/N 1.437500E 01
MEDIAN 1.400000E 01
RANGE 3.000000E 00
UNADJUSTED (BIASED) VARIANCE =
SUM((X(I)-XBR)**2)/N = UVR 5.234375E 00
UNADJUSTED STANDARD DEVIATION = ... 2.287376E 00

=NO 3 SAM SITE (350°)
=3 1
=10 11 11 11 13 19 16 17

NUMBER OF OBSERVATIONS 3
MEAN = XBR = SUM(X(I))/N 1.350000E 01
MEDIAN 1.300000E 01
RANGE 2.000000E 00
UNADJUSTED (BIASED) VARIANCE =
SUM((X(I)-XBR)**2)/N = UVR 1.000000E 01
UNADJUSTED STANDARD DEVIATION = ... 3.162278E 00

=NO 5 SAM SITE (75°)
=7 1
=15 13 12 7 19 16 22

NUMBER OF OBSERVATIONS 7
MEAN = XBR = SUM(X(I))/N 1.557143E 01
MEDIAN 1.600000E 01
RANGE 1.500000E 01
UNADJUSTED (BIASED) VARIANCE =
SUM((X(I)-XBR)**2)/N = UVR 2.081633E 01
UNADJUSTED STANDARD DEVIATION = ... 4.562491E 00

=NO 16 INDUSTRIAL BLDG.
=3 1
=14 9 16 14 23 13 17 16

NUMBER OF OBSERVATIONS 3
MEAN = XBR = SUM(X(I))/N 1.525000E 01
MEDIAN 1.600000E 01
RANGE 1.400000E 01
UNADJUSTED (BIASED) VARIANCE =
SUM((X(I)-XBR)**2)/N = UVR 1.373750E 01
UNADJUSTED STANDARD DEVIATION = ... 3.733296E 00

Table B-5 Data for 512 x 1, BER = 10⁻² Simulation

=NO 14 COLD SPRINGS CANYON BRIDGE
=8 1
=22 12 11 19 21 21 13 15

NUMBER OF OBSERVATIONS 8
MEAN = $\bar{X} = \text{SUM}(X(I))/N$ 1.675000E 01
MEDIAN 1.900000E 01
RANGE 1.100000E 01
UNADJUSTED (BIASED) VARIANCE =
SUM((X(I)- \bar{X})**2)/N = UVR 1.768750E 01
UNADJUSTED STANDARD DEVIATION = ... 4.205651E 00

=NO 17 SOUTH PUMPING PLANT
=8 1
=15 10 11 15 14 12 14 13

NUMBER OF OBSERVATIONS 8
MEAN = $\bar{X} = \text{SUM}(X(I))/N$ 1.300000E 01
MEDIAN 1.400000E 01
RANGE 5.000000E 00
UNADJUSTED (BIASED) VARIANCE =
SUM((X(I)- \bar{X})**2)/N = UVR 3.000000E 00
UNADJUSTED STANDARD DEVIATION = ... 1.732051E 00

=NO 7 BUILDING
=3 1
=11 3 2 7 11 19 9 11

NUMBER OF OBSERVATIONS 8
MEAN = $\bar{X} = \text{SUM}(X(I))/N$ 1.062500E 01
MEDIAN 1.100000E 01
RANGE 1.200000E 01
UNADJUSTED (BIASED) VARIANCE =
SUM((X(I)- \bar{X})**2)/N = UVR 1.198438E 01
UNADJUSTED STANDARD DEVIATION = ... 3.461346E 00

=NO 12 PIRU BRIDGE
=6 1
=11 12 22 14 11 12

NUMBER OF OBSERVATIONS 6
MEAN = $\bar{X} = \text{SUM}(X(I))/N$ 1.366667E 01
MEDIAN 1.200000E 01
RANGE 1.100000E 01
UNADJUSTED (BIASED) VARIANCE =
SUM((X(I)- \bar{X})**2)/N = UVR 1.488389E 01
UNADJUSTED STANDARD DEVIATION = ... 3.853612E 00

=NO 2 BRIDGE (180°)
=3 1
=5 7 7 9 7 6 9

NUMBER OF OBSERVATIONS 8
MEAN = $\bar{X} = \text{SUM}(X(I))/N$ 7.750000E 00
MEDIAN 3.000000E 00
RANGE 3.000000E 00
UNADJUSTED (BIASED) VARIANCE =
SUM((X(I)- \bar{X})**2)/N = UVR 1.187500E 00
UNADJUSTED STANDARD DEVIATION = ... 1.089725E 00

=NO 11 POWER DISTRIBUTION STATION
=8 1
=13 11 17 15 11 14 15 14

NUMBER OF OBSERVATIONS 8
MEAN = $\bar{X} = \text{SUM}(X(I))/N$ 1.375000E 01
MEDIAN 1.400000E 01
RANGE 6.000000E 00
UNADJUSTED (BIASED) VARIANCE =
SUM((X(I)- \bar{X})**2)/N = UVR 3.637500E 00
UNADJUSTED STANDARD DEVIATION = ... 1.920236E 00

=NO 13 GIBRALTAR DAM
=8 1
=13 15 16 19 14 17 16 14

NUMBER OF OBSERVATIONS 8
MEAN = $\bar{X} = \text{SUM}(X(I))/N$ 1.612500E 01
MEDIAN 1.600000E 01
RANGE 5.000000E 00
UNADJUSTED (BIASED) VARIANCE =
SUM((X(I)- \bar{X})**2)/N = UVR 2.359375E 00
UNADJUSTED STANDARD DEVIATION = ... 1.690969E 00

=NO 3 SAM SITE (350°)
=7 1
=10 10 12 13 12 10 9

NUMBER OF OBSERVATIONS 7
MEAN = $\bar{X} = \text{SUM}(X(I))/N$ 1.085714E 01
MEDIAN 1.000000E 01
RANGE 4.000000E 00
UNADJUSTED (BIASED) VARIANCE =
SUM((X(I)- \bar{X})**2)/N = UVR 1.836735E 00
UNADJUSTED STANDARD DEVIATION = ... 1.355262E 00

=NO 5 SAM SITE (75°)
=8 1
=14 9 11 15 8 8 13 9

NUMBER OF OBSERVATIONS 8
MEAN = $\bar{X} = \text{SUM}(X(I))/N$ 1.037500E 01
MEDIAN 1.100000E 01
RANGE 7.000000E 00
UNADJUSTED (BIASED) VARIANCE =
SUM((X(I)- \bar{X})**2)/N = UVR 6.959375E 00
UNADJUSTED STANDARD DEVIATION = ... 2.619041E 00

=NO 16 INDUSTRIAL BLDG.
=8 1
=14 16 11 15 13 17 21 15

NUMBER OF OBSERVATIONS 8
MEAN = $\bar{X} = \text{SUM}(X(I))/N$ 1.587500E 01
MEDIAN 1.600000E 01
RANGE 1.000000E 01
UNADJUSTED (BIASED) VARIANCE =
SUM((X(I)- \bar{X})**2)/N = UVR 7.609375E 00
UNADJUSTED STANDARD DEVIATION = ... 2.753510E 00

NO 14 COLD SPRINGS CANYON BRIDGE
=3 1
=24 20 25 26 24 18 28 21

NUMBER OF OBSERVATIONS 8
MEAN = $\bar{X} = \text{SUM}(X(I))/N$ 2.325000E 01
MEDIAN 2.400000E 01
RANGE 1.000000E 01
UNADJUSTED (BIASED) VARIANCE =
SUM((X(I)- \bar{X})**2)/N = UVR 9.687500E 00
UNADJUSTED STANDARD DEVIATION = ... 3.112475E 00

=NO 17 SOUTH PUMPING PLANT
=3 1
=13 14 15 13 13 14 12 12

NUMBER OF OBSERVATIONS 8
MEAN = $\bar{X} = \text{SUM}(X(I))/N$ 1.325000E 01
MEDIAN 1.300000E 01
RANGE 3.000000E 00
UNADJUSTED (BIASED) VARIANCE =
SUM((X(I)- \bar{X})**2)/N = UVR 9.375000E-01
UNADJUSTED STANDARD DEVIATION = ... 9.682458E-01

=NO 7 BUILDING
=3 1
=13 13 1 1 19 13 13 14 11

NUMBER OF OBSERVATIONS 8
MEAN = $\bar{X} = \text{SUM}(X(I))/N$ 1.462500E 01
MEDIAN 1.400000E 01
RANGE 8.000000E 00
UNADJUSTED (BIASED) VARIANCE =
SUM((X(I)- \bar{X})**2)/N = UVR 9.234375E 00
UNADJUSTED STANDARD DEVIATION = ... 3.038811E 00

=NO 12 PIRU BRIDGE
=3 1
=11 14 11 11 12 14 15 14

NUMBER OF OBSERVATIONS 8
MEAN = $\bar{X} = \text{SUM}(X(I))/N$ 1.275000E 01
MEDIAN 1.400000E 01
RANGE 4.000000E 00
UNADJUSTED (BIASED) VARIANCE =
SUM((X(I)- \bar{X})**2)/N = UVR 2.437500E 00
UNADJUSTED STANDARD DEVIATION = ... 1.561249E 00

=NO 2 BRIDGE (180°)
=7 1
=3 12 3 9 9 3 3

NUMBER OF OBSERVATIONS 7
MEAN = $\bar{X} = \text{SUM}(X(I))/N$ 8.357143E 00
MEDIAN 8.000000E 00
RANGE 4.000000E 00
UNADJUSTED (BIASED) VARIANCE =
SUM((X(I)- \bar{X})**2)/N = UVR 1.336735E 00
UNADJUSTED STANDARD DEVIATION = ... 1.355262E 00

=NO 11 POWER DISTRIBUTION STATION
=8 1
=26 15 20 25 19 22 25 26

NUMBER OF OBSERVATIONS 8
MEAN = $\bar{X} = \text{SUM}(X(I))/N$ 2.225000E 01
MEDIAN 2.500000E 01
RANGE 1.100000E 01
UNADJUSTED (BIASED) VARIANCE =
SUM((X(I)- \bar{X})**2)/N = UVR 1.393750E 01
UNADJUSTED STANDARD DEVIATION = ... 3.733296E 00

=NO 13 GIBALTAR DAM
=7 1
=18 14 27 26 18 14 16

NUMBER OF OBSERVATIONS 7
MEAN = $\bar{X} = \text{SUM}(X(I))/N$ 1.900000E 01
MEDIAN 1.300000E 01
RANGE 1.300000E 01
UNADJUSTED (BIASED) VARIANCE =
SUM((X(I)- \bar{X})**2)/N = UVR 2.455714E 01
UNADJUSTED STANDARD DEVIATION = ... 4.955694E 00

=NO 3 SAM SITE (75°)
=3 1
=12 12 19 16 13 14 25 12

NUMBER OF OBSERVATIONS 8
MEAN = $\bar{X} = \text{SUM}(X(I))/N$ 1.687500E 01
MEDIAN 1.300000E 01
RANGE 1.300000E 01
UNADJUSTED (BIASED) VARIANCE =
SUM((X(I)- \bar{X})**2)/N = UVR 1.660937E 01
UNADJUSTED STANDARD DEVIATION = ... 4.075460E 00

=NO 5 SAM SITE (75°)
=7 1
=16 15 22 14 13 26 9

NUMBER OF OBSERVATIONS 7
MEAN = $\bar{X} = \text{SUM}(X(I))/N$ 1.642857E 01
MEDIAN 1.500000E 01
RANGE 1.700000E 01
UNADJUSTED (BIASED) VARIANCE =
SUM((X(I)- \bar{X})**2)/N = UVR 2.824490E 01
UNADJUSTED STANDARD DEVIATION = ... 5.314593E 00

=NO 16 INDUSTRIAL BLDG.
=8 1
=22 20 24 24 19 20 23 20

NUMBER OF OBSERVATIONS 8
MEAN = $\bar{X} = \text{SUM}(X(I))/N$ 2.150000E 01
MEDIAN 2.200000E 01
RANGE 5.000000E 00
UNADJUSTED (BIASED) VARIANCE =
SUM((X(I)- \bar{X})**2)/N = UVR 3.500000E 00
UNADJUSTED STANDARD DEVIATION = ... 1.870829E 00

NO 14 COLD SPRINGS

=3 1

=30 17 23 22 23 24 17 20

NUMBER OF OBSERVATIONS 3

MEAN = XBR = SUM(X(I))/N 2.262500E 01

MEDIAN 2.300000E 01

RANGE 1.300000E 01

UNADJUSTED (BIASED) VARIANCE =

SUM((X(I)-XBR)**2)/N = UVR 1.943438E 01

UNADJUSTED STANDARD DEVIATION = ... 4.414111E 00

=NO 17 SOUTH PUMPING PLANT

=3 1

=14 11 13 13 12 11 12 17

NUMBER OF OBSERVATIONS 3

MEAN = XBR = SUM(X(I))/N 1.287500E 01

MEDIAN 1.300000E 01

RANGE 6.000000E 00

UNADJUSTED (BIASED) VARIANCE =

SUM((X(I)-XBR)**2)/N = UVR 3.357375E 00

UNADJUSTED STANDARD DEVIATION = ... 1.832860E 00

=NO 7 BUILDING

=3 1

=12 9 11 14 14 10 9 8

NUMBER OF OBSERVATIONS 3

MEAN = XBR = SUM(X(I))/N 1.087500E 01

MEDIAN 1.100000E 01

RANGE 6.000000E 00

UNADJUSTED (BIASED) VARIANCE =

SUM((X(I)-XBR)**2)/N = UVR 4.609375E 00

UNADJUSTED STANDARD DEVIATION = ... 2.146946E 00

=NO 12 PIRU BRIDGE

=7 1

=11 10 6 10 12 11 8

NUMBER OF OBSERVATIONS 7

MEAN = XBR = SUM(X(I))/N 2.714286E 00

MEDIAN 1.000000E 01

RANGE 6.000000E 00

UNADJUSTED (BIASED) VARIANCE =

SUM((X(I)-XBR)**2)/N = UVR 3.632653E 00

UNADJUSTED STANDARD DEVIATION = ... 1.905952E 00

=NO 2 BRIDGE (180°)

=3 1

=3 3 3 9 10 7 8 7

NUMBER OF OBSERVATIONS 3

MEAN = XBR = SUM(X(I))/N 3.250000E 00

MEDIAN 3.000000E 00

RANGE 3.000000E 00

UNADJUSTED (BIASED) VARIANCE =

SUM((X(I)-XBR)**2)/N = UVR 9.375000E 01

UNADJUSTED STANDARD DEVIATION = ... 9.682458E 01

=NO 11 POWER DISTRIBUTION STATION

=7 1

=15 13 24 19 18 20 16

NUMBER OF OBSERVATIONS 7

MEAN = XBR = SUM(X(I))/N 1.357143E 01

MEDIAN 1.300000E 01

RANGE 9.000000E 00

UNADJUSTED (BIASED) VARIANCE =

SUM((X(I)-XBR)**2)/N = UVR 7.337755E 00

UNADJUSTED STANDARD DEVIATION = ... 2.718042E 00

=NO 13 GIBRALTAR DAM

=3 1

=17 16 24 22 15 16 16 17

NUMBER OF OBSERVATIONS 3

MEAN = XBR = SUM(X(I))/N 1.737500E 01

MEDIAN 1.700000E 01

RANGE 9.000000E 00

UNADJUSTED (BIASED) VARIANCE =

SUM((X(I)-XBR)**2)/N = UVR 2.359375E 00

UNADJUSTED STANDARD DEVIATION = ... 3.059310E 00

=NO 3 SAM SITE (350°)

=3 1

=9 15 13 16 13 8 11 10

NUMBER OF OBSERVATIONS 3

MEAN = XBR = SUM(X(I))/N 1.312500E 01

MEDIAN 1.500000E 01

RANGE 1.000000E 01

UNADJUSTED (BIASED) VARIANCE =

SUM((X(I)-XBR)**2)/N = UVR 1.460937E 01

UNADJUSTED STANDARD DEVIATION = ... 3.322221E 00

=NO 5 SAM SITE (75°)

=3 1

=19 6 22 18 14 12 10 3

NUMBER OF OBSERVATIONS 3

MEAN = XBR = SUM(X(I))/N 1.362500E 01

MEDIAN 1.400000E 01

RANGE 1.600000E 01

UNADJUSTED (BIASED) VARIANCE =

SUM((X(I)-XBR)**2)/N = UVR 2.793437E 01

UNADJUSTED STANDARD DEVIATION = ... 5.290026E 00

=NO 16 INDUSTRIAL BLDG.

=7 1

=15 17 20 12 13 20 11

NUMBER OF OBSERVATIONS 7

MEAN = XBR = SUM(X(I))/N 1.542857E 01

MEDIAN 1.500000E 01

RANGE 9.000000E 00

UNADJUSTED (BIASED) VARIANCE =

SUM((X(I)-XBR)**2)/N = UVR 1.157347E 01

UNADJUSTED STANDARD DEVIATION = ... 3.416646E 00

NO 14 COLD SPRINGS
=7 1
=22 20 27 22 22 13 20

NUMBER OF OBSERVATIONS 7
MEAN = $\bar{XBR} = \text{SUM}(X(I))/N$ 2.085714E 01
MEDIAN 2.200000E 01
RANGE 1.400000E 01
UNADJUSTED (BIASED) VARIANCE =
SUM((X(I)- \bar{XBR})**2)/N = UVR 1.497959E 01
UNADJUSTED STANDARD DEVIATION = ... 3.870348E 00

NO 17 SOUTH PUMPING PLANT
=6 1
=14 23 20 20 22 13

NUMBER OF OBSERVATIONS 6
MEAN = $\bar{XBR} = \text{SUM}(X(I))/N$ 1.950000E 01
MEDIAN 2.000000E 01
RANGE 2.000000E 00
UNADJUSTED (BIASED) VARIANCE =
SUM((X(I)- \bar{XBR})**2)/N = UVR 3.583333E 00
UNADJUSTED STANDARD DEVIATION = ... 2.929733E 00

NO 7 BUILDING
=6 1
=14 12 13 13 10 21

NUMBER OF OBSERVATIONS 6
MEAN = $\bar{XBR} = \text{SUM}(X(I))/N$ 1.383333E 01
MEDIAN 1.300000E 01
RANGE 1.100000E 01
UNADJUSTED (BIASED) VARIANCE =
SUM((X(I)- \bar{XBR})**2)/N = UVR 1.130556E 01
UNADJUSTED STANDARD DEVIATION = ... 3.435921E 00

NO 12 PIRU BRIDGE
=3 1
=9 11 12 10 11 11 9

NUMBER OF OBSERVATIONS 8
MEAN = $\bar{XBR} = \text{SUM}(X(I))/N$ 1.050000E 01
MEDIAN 1.100000E 01
RANGE 3.000000E 00
UNADJUSTED (BIASED) VARIANCE =
SUM((X(I)- \bar{XBR})**2)/N = UVR 1.000000E 00
UNADJUSTED STANDARD DEVIATION = ... 1.000000E 00

NO 2 BRIDGE (180°)
=3 06 1
=9 9 10 3 11 3

NUMBER OF OBSERVATIONS 6
MEAN = $\bar{XBR} = \text{SUM}(X(I))/N$ 9.166667E 00
MEDIAN 9.000000E 00
RANGE 3.000000E 00
UNADJUSTED (BIASED) VARIANCE =
SUM((X(I)- \bar{XBR})**2)/N = UVR 1.138889E 00
UNADJUSTED STANDARD DEVIATION = ... 1.067187E 00

NO 11 POWER DISTRIBUTION STATION
=6 1
=15 13 13 13 14 20

NUMBER OF OBSERVATIONS 6
MEAN = $\bar{XBR} = \text{SUM}(X(I))/N$ 1.633333E 01
MEDIAN 1.800000E 01
RANGE 7.000000E 00
UNADJUSTED (BIASED) VARIANCE =
SUM((X(I)- \bar{XBR})**2)/N = UVR 6.222222E 00
UNADJUSTED STANDARD DEVIATION = ... 2.494438E 00

NO 13 GIBRALTAR DAM
=3 1
=17 17 11 15 11 20 25 3 00

NUMBER OF OBSERVATIONS 3
MEAN = $\bar{XBR} = \text{SUM}(X(I))/N$ 1.825000E 01
MEDIAN 1.700000E 01
RANGE 1.900000E 01
UNADJUSTED (BIASED) VARIANCE =
SUM((X(I)- \bar{XBR})**2)/N = UVR 3.318750E 01
UNADJUSTED STANDARD DEVIATION = ... 6.179604E 00

NO 3 SAM SITE (350°)
=3 1
=10 3 21 9 9 11 3 12

NUMBER OF OBSERVATIONS 8
MEAN = $\bar{XBR} = \text{SUM}(X(I))/N$ 1.100000E 01
MEDIAN 1.000000E 01
RANGE 1.300000E 01
UNADJUSTED (BIASED) VARIANCE =
SUM((X(I)- \bar{XBR})**2)/N = UVR 1.600000E 01
UNADJUSTED STANDARD DEVIATION = ... 4.000000E 00

NO 5 SAM SITE (75°)
=7 1
=9 3 22 8 14 12 16

NUMBER OF OBSERVATIONS 7
MEAN = $\bar{XBR} = \text{SUM}(X(I))/N$ 1.271429E 01
MEDIAN 1.200000E 01
RANGE 1.400000E 01
UNADJUSTED (BIASED) VARIANCE =
SUM((X(I)- \bar{XBR})**2)/N = UVR 2.243930E 01
UNADJUSTED STANDARD DEVIATION = ... 4.742341E 00

NO 16 INDUSTRIAL BLDG.
=3 1
=14 17 24 15 14 15 15 25

NUMBER OF OBSERVATIONS 9
MEAN = $\bar{XBR} = \text{SUM}(X(I))/N$ 1.737500E 01
MEDIAN 1.500000E 01
RANGE 1.100000E 01
UNADJUSTED (BIASED) VARIANCE =
SUM((X(I)- \bar{XBR})**2)/N = UVR 1.773437E 01
UNADJUSTED STANDARD DEVIATION = ... 4.211226E 00

Table B-9 Data for 256 x 2, BER = 10⁻³ Simulation

=NO 14 COLD SPRINGS CANYON BRIDGE

=3 1

=14 24 24 25 23 22 25 19

NUMBER OF OBSERVATIONS 3

MEAN = $\bar{X} = \text{SUM}(X(I))/N$ 2.200000E 01

MEDIAN 2.400000E 01

RANGE 1.100000E 01

UNADJUSTED (BIASED) VARIANCE =

$\text{SUM}((X(I)-\bar{X})^2)/N = \text{UVR}$ 1.250000E 01

UNADJUSTED STANDARD DEVIATION = ... 3.535534E 00

=NO 17 SOUTH PUMPING PLANT

=3 1

=12 17 11 13 15 16 16 7

NUMBER OF OBSERVATIONS 3

MEAN = $\bar{X} = \text{SUM}(X(I))/N$ 1.337500E 01

MEDIAN 1.500000E 01

RANGE 1.000000E 01

UNADJUSTED (BIASED) VARIANCE =

$\text{SUM}((X(I)-\bar{X})^2)/N = \text{UVR}$ 9.734375E 00

UNADJUSTED STANDARD DEVIATION = ... 3.119996E 00

=NO 7 BUILDING

=7 1

=10 10 12 10 6 11

=10

NUMBER OF OBSERVATIONS 7

MEAN = $\bar{X} = \text{SUM}(X(I))/N$ 9.857143E 00

MEDIAN 1.000000E 01

RANGE 6.000000E 00

UNADJUSTED (BIASED) VARIANCE =

$\text{SUM}((X(I)-\bar{X})^2)/N = \text{UVR}$ 2.979592E 00

UNADJUSTED STANDARD DEVIATION = ... 1.726149E 00

=NO 12 PIRU BRIDGE

=4 1

=9 11 12 13

NUMBER OF OBSERVATIONS 4

MEAN = $\bar{X} = \text{SUM}(X(I))/N$ 1.125000E 01

MEDIAN 1.200000E 01

RANGE 4.000000E 00

UNADJUSTED (BIASED) VARIANCE =

$\text{SUM}((X(I)-\bar{X})^2)/N = \text{UVR}$ 2.187500E 00

UNADJUSTED STANDARD DEVIATION = ... 1.479020E 00

=NO 2 BRIDGE (180°)

=5 1

=16 3 9 11 11

NUMBER OF OBSERVATIONS 5

MEAN = $\bar{X} = \text{SUM}(X(I))/N$ 1.100000E 01

MEDIAN 1.100000E 01

RANGE 3.000000E 00

UNADJUSTED (BIASED) VARIANCE =

$\text{SUM}((X(I)-\bar{X})^2)/N = \text{UVR}$ 7.600000E 00

UNADJUSTED STANDARD DEVIATION = ... 2.756310E 00

NO 11 POWER DISTRIBUTION STATION

=9 1

=13 21 13 16 13 22 21 19 15

NUMBER OF OBSERVATIONS 9

MEAN = $\bar{X} = \text{SUM}(X(I))/N$ 1.311111E 01

MEDIAN 1.300000E 01

RANGE 2.000000E 00

UNADJUSTED (BIASED) VARIANCE =

$\text{SUM}((X(I)-\bar{X})^2)/N = \text{UVR}$ 3.098765E 00

UNADJUSTED STANDARD DEVIATION = ... 2.445433E 00

=NO 13 GIBRALTAR DAM

=9 1

=19 12 24 15 14 22 13 14 15

NUMBER OF OBSERVATIONS 9

MEAN = $\bar{X} = \text{SUM}(X(I))/N$ 1.644444E 01

MEDIAN 1.500000E 01

RANGE 1.200000E 01

UNADJUSTED (BIASED) VARIANCE =

$\text{SUM}((X(I)-\bar{X})^2)/N = \text{UVR}$ 1.530247E 01

UNADJUSTED STANDARD DEVIATION = ... 3.975232E 00

=NO 3 SAM SITE (350°)

=9 1

=3 9 14 13 13 10 10 10 16

NUMBER OF OBSERVATIONS 9

MEAN = $\bar{X} = \text{SUM}(X(I))/N$ 1.144444E 01

MEDIAN 1.000000E 01

RANGE 3.000000E 00

UNADJUSTED (BIASED) VARIANCE =

$\text{SUM}((X(I)-\bar{X})^2)/N = \text{UVR}$ 6.246914E 00

UNADJUSTED STANDARD DEVIATION = ... 2.499333E 00

=NO 5 SAM SITE (75°)

=9 1

=14 3 10 3 28 10 11 11 8

NUMBER OF OBSERVATIONS 9

MEAN = $\bar{X} = \text{SUM}(X(I))/N$ 1.200000E 01

MEDIAN 1.000000E 01

RANGE 2.000000E 01

UNADJUSTED (BIASED) VARIANCE =

$\text{SUM}((X(I)-\bar{X})^2)/N = \text{UVR}$ 3.533333E 01

UNADJUSTED STANDARD DEVIATION = ... 5.944195E 00

=NO 16 INDUSTRIAL BLDG.

=9 1

=17 25 22 22 27 22 16 27 15

NUMBER OF OBSERVATIONS 9

MEAN = $\bar{X} = \text{SUM}(X(I))/N$ 2.144444E 01

MEDIAN 2.200000E 01

RANGE 1.200000E 01

UNADJUSTED (BIASED) VARIANCE =

$\text{SUM}((X(I)-\bar{X})^2)/N = \text{UVR}$ 1.346914E 01

UNADJUSTED STANDARD DEVIATION = ... 4.297573E 00

=NO 14 COLD SPRINGS
=3 1
=23 19 23 24 19 22 22 24

NUMBER OF OBSERVATIONS 3
MEAN = $\bar{X} = \text{SUM}(X(I))/N$ 2.200000E 01
MEDIAN 2.300000E 01
RANGE 5.000000E 00
UNADJUSTED (BIASED) VARIANCE =
 $\text{SUM}((X(I)-\bar{X})^2)/N = UVR$ 3.500000E 00
UNADJUSTED STANDARD DEVIATION = ... 1.870829E 00

=NO 17 SOUTH PUMPING PLANT
=3 1
=16 16 15 15 11 13 12 14

NUMBER OF OBSERVATIONS 3
MEAN = $\bar{X} = \text{SUM}(X(I))/N$ 1.400000E 01
MEDIAN 1.500000E 01
RANGE 5.000000E 00
UNADJUSTED (BIASED) VARIANCE =
 $\text{SUM}((X(I)-\bar{X})^2)/N = UVR$ 3.000000E 00
UNADJUSTED STANDARD DEVIATION = ... 1.732051E 00

=NO 7 BUILDING
=7 1
=12 10 10 13 7 12 12

NUMBER OF OBSERVATIONS 7
MEAN = $\bar{X} = \text{SUM}(X(I))/N$ 1.114236E 01
MEDIAN 1.200000E 01
RANGE 4.000000E 00
UNADJUSTED (BIASED) VARIANCE =
 $\text{SUM}((X(I)-\bar{X})^2)/N = UVR$ 1.836735E 00
UNADJUSTED STANDARD DEVIATION = ... 1.355262E 00

=NO 12 PIRU BRIDGE
=6 1
=9 8 9 10 9 11

NUMBER OF OBSERVATIONS 6
MEAN = $\bar{X} = \text{SUM}(X(I))/N$ 9.333333E 00
MEDIAN 9.000000E 00
RANGE 3.000000E 00
UNADJUSTED (BIASED) VARIANCE =
 $\text{SUM}((X(I)-\bar{X})^2)/N = UVR$ 8.333333E 01
UNADJUSTED STANDARD DEVIATION = ... 9.428090E 01

=NO 2 BRIDGE (180°)
=3 1
=9 8 10

NUMBER OF OBSERVATIONS 3
MEAN = $\bar{X} = \text{SUM}(X(I))/N$ 9.000000E 00
MEDIAN 9.000000E 00
RANGE 2.000000E 00
UNADJUSTED (BIASED) VARIANCE =
 $\text{SUM}((X(I)-\bar{X})^2)/N = UVR$ 6.666667E 01
UNADJUSTED STANDARD DEVIATION = ... 3.164966E 01

=NO 11 POWER DISTRIBUTION STATION
=7 1
=14 20 23 26 12 25 28

NUMBER OF OBSERVATIONS 7
MEAN = $\bar{X} = \text{SUM}(X(I))/N$ 2.114236E 01
MEDIAN 2.300000E 01
RANGE 1.600000E 01
UNADJUSTED (BIASED) VARIANCE =
 $\text{SUM}((X(I)-\bar{X})^2)/N = UVR$ 3.212245E 01
UNADJUSTED STANDARD DEVIATION = ... 5.667667E 00

=NO 13 GIBRALTAR DAM
=7 1
=13 16 13 15 14 20 22

NUMBER OF OBSERVATIONS 7
MEAN = $\bar{X} = \text{SUM}(X(I))/N$ 1.685714E 01
MEDIAN 1.600000E 01
RANGE 9.000000E 00
UNADJUSTED (BIASED) VARIANCE =
 $\text{SUM}((X(I)-\bar{X})^2)/N = UVR$ 9.265306E 00
UNADJUSTED STANDARD DEVIATION = ... 3.043979E 00

=NN#0 3 SAM SITE (350°)
=8 1
=11 10 12 24 8 9 16 17

NUMBER OF OBSERVATIONS 8
MEAN = $\bar{X} = \text{SUM}(X(I))/N$ 1.337500E 01
MEDIAN 1.200000E 01
RANGE 1.600000E 01
UNADJUSTED (BIASED) VARIANCE =
 $\text{SUM}((X(I)-\bar{X})^2)/N = UVR$ 2.493437E 01
UNADJUSTED STANDARD DEVIATION = ... 4.998437E 00

=NO 5 SAM SITE (75°)
=3 1
=10 10 26 16 12 10 23 20

NUMBER OF OBSERVATIONS 8
MEAN = $\bar{X} = \text{SUM}(X(I))/N$ 1.650000E 01
MEDIAN 1.600000E 01
RANGE 1.300000E 01
UNADJUSTED (BIASED) VARIANCE =
 $\text{SUM}((X(I)-\bar{X})^2)/N = UVR$ 4.775000E 01
UNADJUSTED STANDARD DEVIATION = ... 6.910137E 00

=NO 16 INDUSTRIAL BLDG.
=7 1
=15 12 23 8 23 16 26

NUMBER OF OBSERVATIONS 7
MEAN = $\bar{X} = \text{SUM}(X(I))/N$ 1.757143E 01
MEDIAN 1.600000E 01
RANGE 1.800000E 01
UNADJUSTED (BIASED) VARIANCE =
 $\text{SUM}((X(I)-\bar{X})^2)/N = UVR$ 3.738776E 01
UNADJUSTED STANDARD DEVIATION = ... 6.114553E 00

BEST AVAILABLE COPY

#NO 1 Baseline

#3 1

#17.2 13.5 17 16.1 17.5 16.4 17.4 17 16.2 19.5
20.6 17.4 16.2

NUMBER OF OBSERVATIONS 13

MEAN = $\bar{XBR} = \text{SUM}(X(I))/N$ 1.307692E 01

MEDIAN 1.350000E 01

RANGE 4.500000E 00

UNADJUSTED (BIASED) VARIANCE =
 $\text{SUM}(X(I)-\bar{XBR})^2/N = UVR$ 2.172504E 00

UNADJUSTED STANDARD DEVIATION = ... 1.473355E 00

#NO 2 512 x 1; BER = 0

#3 1

#16.4 14.7 16.7 17.5 15.7 13.7 15.6 16

NUMBER OF OBSERVATIONS 3

MEAN = $\bar{XBR} = \text{SUM}(X(I))/N$ 1.531250E 01

MEDIAN 1.600000E 01

RANGE 3.300000E 00

UNADJUSTED (BIASED) VARIANCE =
 $\text{SUM}(X(I)-\bar{XBR})^2/N = UVR$ 1.271094E 00

UNADJUSTED STANDARD DEVIATION = ... 1.127428E 00

#NO 3 512 x 1; BER = 10^{-4}

#3 1

#13.3 16 15.2 13.4 16.4 17.6 12.7 15.6

NUMBER OF OBSERVATIONS 3

MEAN = $\bar{XBR} = \text{SUM}(X(I))/N$ 1.511250E 01

MEDIAN 1.560000E 01

RANGE 4.700000E 00

UNADJUSTED (BIASED) VARIANCE =
 $\text{SUM}(X(I)-\bar{XBR})^2/N = UVR$ 2.303594E 00

UNADJUSTED STANDARD DEVIATION = ... 1.517759E 00

#NO 4 512 x 1; BER = 10^{-3}

#3 1

#13.7 13.6 14.3 13.6 13.5 14.4 15.7 17.3

NUMBER OF OBSERVATIONS 3

MEAN = $\bar{XBR} = \text{SUM}(X(I))/N$ 1.466250E 01

MEDIAN 1.440000E 01

RANGE 4.300000E 00

UNADJUSTED (BIASED) VARIANCE =
 $\text{SUM}(X(I)-\bar{XBR})^2/N = UVR$ 1.399344E 00

UNADJUSTED STANDARD DEVIATION = ... 1.179349E 00

#NO 5 512 x 1; BER = 10^{-2}

#3 1

#12.6 11 12.3 14 13.2 14.1 12.3 12.1

NUMBER OF OBSERVATIONS 3

MEAN = $\bar{XBR} = \text{SUM}(X(I))/N$ 1.275000E 01

MEDIAN 1.320000E 01

RANGE 3.100000E 00

UNADJUSTED (BIASED) VARIANCE =
 $\text{SUM}(X(I)-\bar{XBR})^2/N = UVR$ 2.350000E 01

UNADJUSTED STANDARD DEVIATION = ... 2.669540E 01

#NO 6 512 x 0.75; BER = 0

#3 1

#15.1 12.7 16.6 16.3 15.3 13.2 13.2 11.3

NUMBER OF OBSERVATIONS 3

MEAN = $\bar{XBR} = \text{SUM}(X(I))/N$ 1.427500E 01

MEDIAN 1.510000E 01

RANGE 4.300000E 00

UNADJUSTED (BIASED) VARIANCE =
 $\text{SUM}(X(I)-\bar{XBR})^2/N = UVR$ 2.769375E 00

UNADJUSTED STANDARD DEVIATION = ... 1.664144E 00

#NO 7 512 x 0.75; BER = 10^{-3}

#3 1

#17.5 14.9 13.2 19.3 16.3 15.5 19 14.7

NUMBER OF OBSERVATIONS 3

MEAN = $\bar{XBR} = \text{SUM}(X(I))/N$ 1.625000E 01

MEDIAN 1.750000E 01

RANGE 4.400000E 00

UNADJUSTED (BIASED) VARIANCE =
 $\text{SUM}(X(I)-\bar{XBR})^2/N = UVR$ 2.315000E 00

UNADJUSTED STANDARD DEVIATION = ... 1.677766E 00

#NO 8 256 x 2; BER = 0

#3 1

#13.3 14 13.6 12.5 13.7 15.3 12.7 12.1

NUMBER OF OBSERVATIONS 3

MEAN = $\bar{XBR} = \text{SUM}(X(I))/N$ 1.475000E 01

MEDIAN 1.400000E 01

RANGE 6.600000E 00

UNADJUSTED (BIASED) VARIANCE =
 $\text{SUM}(X(I)-\bar{XBR})^2/N = UVR$ 5.700000E 00

UNADJUSTED STANDARD DEVIATION = ... 2.387457E 00

#NO 9 256 x 2; BER = 10^{-3}

#3 1

#13.3 15 16.4 13.3 17.7 15.7 14.7 15.2 12.3

NUMBER OF OBSERVATIONS 3

MEAN = $\bar{XBR} = \text{SUM}(X(I))/N$ 1.503339E 01

MEDIAN 1.500000E 01

RANGE 4.400000E 00

UNADJUSTED (BIASED) VARIANCE =
 $\text{SUM}(X(I)-\bar{XBR})^2/N = UVR$ 1.720933E 00

UNADJUSTED STANDARD DEVIATION = ... 1.311864E 00

#NO 10 256 x 2; BER = 0

#3 1

#13.7 13.4 17.7 15.7 13.2 12.3 13.7 13.4

NUMBER OF OBSERVATIONS 3

MEAN = $\bar{XBR} = \text{SUM}(X(I))/N$ 1.550000E 01

MEDIAN 1.570000E 01

RANGE 6.100000E 00

UNADJUSTED (BIASED) VARIANCE =
 $\text{SUM}(X(I)-\bar{XBR})^2/N = UVR$ 5.650000E 00

UNADJUSTED STANDARD DEVIATION = ... 2.376972E 00

		DATA ON TIME FROM DETECT TO GROUND ZERO										STANDARD DEVIATION													
		MEAN																							
		Baseline	512 × 1; BER = 0	512 × 1; BER = 10 ⁻⁴	512 × 1; BER = 10 ⁻³	512 × 1; BER = 10 ⁻²	512 × 0.75; BER = 0	512 × 0.75; BER = 10 ⁻³	256 × 2; BER = 0	256 × 2; BER = 10 ⁻³	256 × 2; BER = 0	256 × 2; BER = 10 ⁻³	Overall	Baseline	512 × 1; BER = 0	512 × 1; BER = 10 ⁻⁴	512 × 1; BER = 10 ⁻³	512 × 1; BER = 10 ⁻²	512 × 0.75; BER = 0	512 × 0.75; BER = 10 ⁻³	256 × 2; BER = 0	256 × 2; BER = 10 ⁻³	256 × 2; BER = 0	256 × 2; BER = 10 ⁻³	Overall
14	Cold Springs Canyon Bridge	23.9	23.6	23.3	22.9	16.8	23.3	22.6	20.9	22.0	22.0	22.0	22.0	2.03	1.73	2.78	3.14	4.20	3.11	4.41	3.87	3.54	1.87		
17	South Pumping Plant	15.9	14.3	13.9	11.4	13.0	13.3	12.9	19.5	13.4	14.0		2.51	1.48	1.62	3.84	1.73	0.97	1.83	2.93	3.12	1.73			
7	Building	13.0	12.1	12.3	12.9	10.6	14.6	10.9	13.8	9.86	11.1		3.45	1.73	1.09	1.27	3.46	3.04	2.15	3.44	1.73	1.36			
12	Piru Bridge	19.3	14.9	13.4	13.2	13.7	12.8	9.71	10.5	11.3	9.33		8.07	1.83	3.39	4.31	3.86	1.56	1.91	1.00	1.48	0.94			
2	Bridge (180°)	12.5	9.00	7.88	8.86	7.75	8.86	8.25	9.17	11.0	9.00		6.91	0.71	0.93	1.36	1.09	1.36	0.97	1.07	2.76	0.82			
11	Power Distribution Station	22.0	19.1	18.3	16.8	13.8	22.3	18.57	16.3	18.1	21.1		5.45	4.99	2.22	2.59	1.92	3.73	2.72	2.49	2.85	5.67			
13	Gibraltar Dam	19.6	16.3	16.1	14.4	16.1	19.0	17.9	18.3	16.4	16.9		3.99	1.98	3.41	2.29	1.69	4.99	3.06	6.18	3.98	3.04			
3	Sam Site (350°)	15.0	14.1	12.4	13.5	10.9	16.9	13.1	11.0	11.4	13.4		3.96	2.80	5.41	3.16	1.36	4.08	3.82	4.00	2.50	5.00			
5	Sam Site (75°)	15.0	14.4	12.3	15.6	10.9	16.4	13.6	12.7	12.0	16.5		3.72	3.64	3.11	4.56	2.62	5.31	5.29	4.74	5.94	6.91			
16	Industrial Building	25.4	19.9	20.4	15.3	15.9	21.5	15.4	17.4	21.4	17.6		4.59	5.67	4.15	3.73	2.76	1.87	3.42	4.21	4.30	6.11			
Summation by Compression Parameter		18.1	15.8	15.1	14.7	13.0	17.0	14.3	15.0	15.1	15.5		1.47	1.13	1.52	1.38	0.97	1.66	1.68	2.39	1.32	2.38			

NOTE: Horizontal data indicates deviation due to subjects only
Vertical calculations delete deviation due to film strips

Table B-12 Tabulation of Mean and Deviation for All Simulations

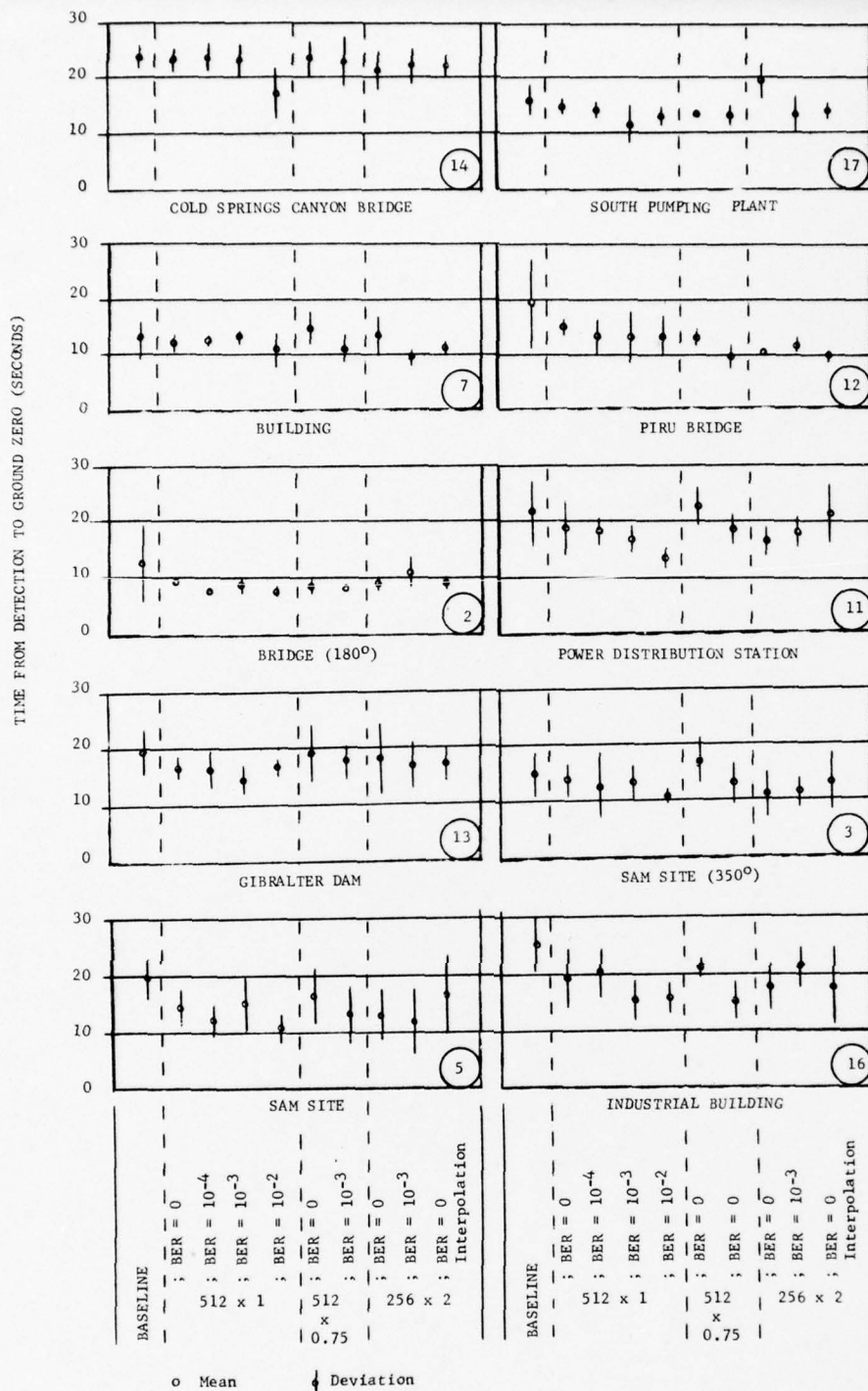


Figure B-1 Graphical Presentation of Mean and Deviation for All Simulations

STATISTICAL SUMMARY OF SIMULATION RESULTS				
SIMULATION	MEAN		DEVIATION	
	TIME (SEC)	SLANT RANGE (FT)	TIME (SEC)	DISTANCE (FT)
Baseline	15.1	12,579	1.47	1,014
512 x 1; BER = 0	15.8	11,005	1.13	780
512 x 1; BER = 10 ⁻⁴	15.1	10,526	1.52	1,049
512 x 1; BER = 10 ⁻³	14.7	10,253	1.38	952
512 x 1; BER = 10 ⁻²	13.0	9,095	0.97	669
512 x 0.75; BER = 0	14.3	9,980	1.66	1,145
512 x 0.75; BER = 10 ⁻³	17.0	11,836	1.68	1,159
256 x 2; BER = 0	15.0	10,458	2.39	1,649
256 x 2; BER = 10 ⁻³	15.1	10,526	1.31	904
256 x 2; BER = 0 with interpolation	15.5	10,800	2.38	1,642

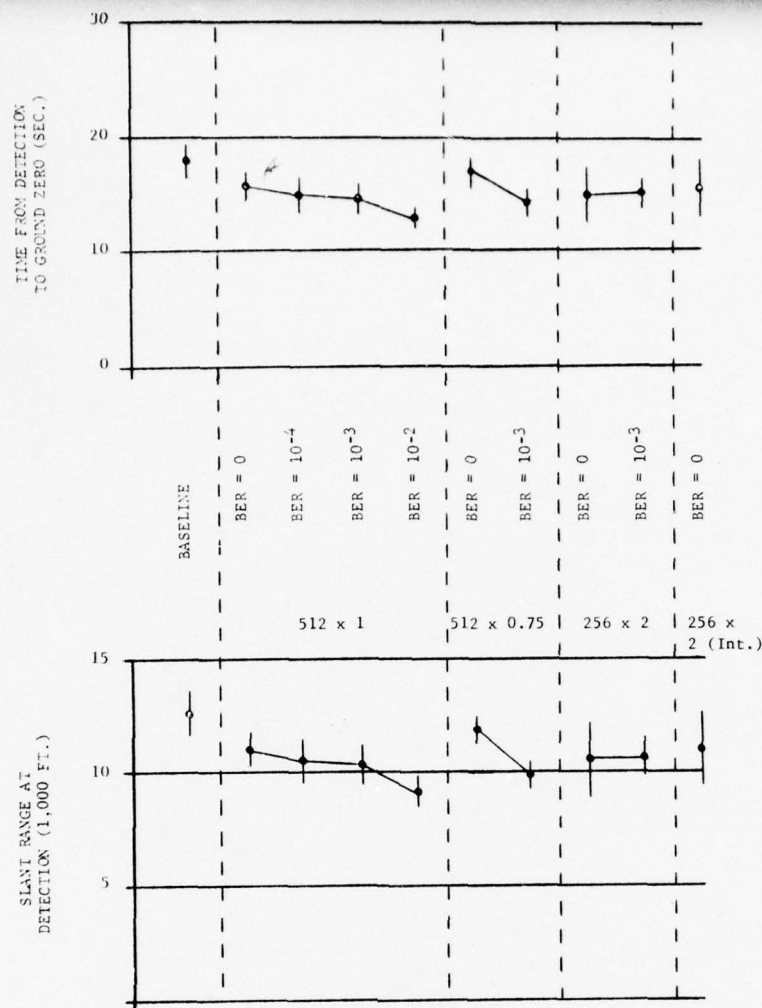


Figure B-2 Statistical Summary of Simulation Results

APPENDIX C

VIDEO COMPRESSION EVALUATION ORIENTATION

This appendix contains the text of a standard Air Force-supplied briefing chart given to each test subject to read prior to performing test runs. This chart was intended to ensure that all subjects had the same understanding of the purpose of and method of performing the tests. Each subject was given as much time as he required to read and understand the text.

- TEXT -

"You are an observer in a study whose purpose is to determine the maximum distance at which most observers can reliably locate each of a variety of known man-made objects. You will be viewing a television screen (or CRT) which displays the moving scene included in the field of view of a television camera aimed far ahead of the aircraft in which it is mounted. The aircraft that took the pictures flew level at a low altitude and at a speed of over 400 knots. At the start of the TV picture the object to be found is five to six miles away from the aircraft. It will sometimes be considerably off center of the TV display. It rapidly moves closer, enlarging in size and clarity of details as its image moves down the display. Usually, but not always, not even a "blob" (an unresolved or featureless blur) of the object of your search is seen for awhile. In less than a minute from the start of the run the image of the object to be found has moved off of the picture at the bottom of the TV screen. The objects on the terrain that you will be seeking include bridges, buildings, a dam, etc. Some of the objects are large and conspicuous, being easily designated at long ranges, while others are not easily found until they are quite close to the aircraft. Different groups of observers will all view the same TV pictures, but some groups will have clearer pictures than others, some will have noisy and/or very jerky pictures, etc., i.e., different groups will be tested under different conditions.

Your task is to find and designate objects with which you have become familiar before you start viewing the television display. You will know in advance what the object sought looks like, where it is located on a map and where it is in relation to terrain features, i.e., in the televised scene. To gain this advanced familiarity with the appearance and location of the objects, it will be necessary for you to carefully examine in detail each of three briefing aids: a map and two glossy 8" x 10" photographs. One of the photos was taken by a hand-held camera at a distance of about three miles from the ground object of interest, while the other was taken from a distance of about one mile. Keep in mind the fact that the photographs were not taken from the same flight path as were the TV "movies", so, while they present the same side, etc., do not expect the object for which you are searching to appear at the same location on the TV display as on the photos. Thus, on the photo the bridge, etc., may be in the center of the picture, but on the TV screen it may appear well to one side of center, or it may not.

The present study is not concerned with the range at which an object is so clearly shown on the TV screen that you can be certain, from the image of only the object (without regard to location), that it is the object that you seek. You should be able to point to the object, with some confidence, well before it is so close to the aircraft that it is depicted as a large and highly-detailed image on the TV screen. Your aim is to point to the object while it is far away from the aircraft. Point to it, if you can, while it is so far away that its image is only an unresolved blob on the screen, a blob that has to be the object that you seek because it is in the right location on the ground. However, do not point to a place where not even a "blur" or "blob" can be seen simply because it appears in the correct position: you must see something at the location, even if no distinguishing details are present.

During the test runs the photographs of the object of your search will be on display along side of the TV display so that you can refer to them as frequently as necessary. However, do not expect the TV picture to be as "clear" as the photographs nor to be taken from exactly the same place in space.

On each of the briefing aids the object to be found is designated by an arrow and the briefing aid's label includes the name of the object. Carefully study the map and the pictures so that you can quickly locate the object that you seek by use of other objects and terrain features that precede and/or surround it in the scene. The context is important: reliable long range designation is highly dependent upon knowing where the object is in the scene, i.e., in context."

Appendix D

Statistical Analysis of Test Data

D.1 General

This appendix analyzes the data collected during the experimental program and attempts to determine its significance. This task is somewhat difficult because of the way the tests were specified. Because each group of observers performed tests on only one set of parameters, these parameters are correlated with group capability differences which may have existed even though an attempt was made to select observers at random from what was considered to be one population (viz. airmen).

If each group could have performed one test on each set of parameters, the capability of a given operator would have affected each system in a like manner.

The procedures and assumptions which will be described were arrived at through discussions with Aeronutronic Ford employees who have had experience in statistical analysis and testing. All agreed that results are confounded by the observer variability.

Several basic rules were followed throughout the tests. They are:

1. Slant range-to-target values at the time of detection were normalized to give them equal weight in determining the overall performance of a given system. The rationale for this procedure is that a target which is only visible for a short time at the end of a run cannot be detected at as great a range as one which is visible for a long time. If compared on an absolute basis, short range targets would contribute very little to the analysis. Therefore, a detection slant range for a certain system and for a particular target was normalized by dividing it by the mean observer detection slant range determined for the same target during the baseline test. The baseline was used because intuition suggested that the baseline would be the "best" system tested. The data which will be presented later in this appendix tends to bear out this conclusion.

The normalized values are interpreted as the "slant range at the time of detection for a given set of parameters relative to what would be obtained for a given target with a baseline system."

The above criterion is used in lieu of a definition of target detection difficulty or a criterion for absolute detection time in terms of how much time must be allowed after detection for the remainder of the RPV mission to be a success. If such an absolute time existed, it is realized that much data and indeed some targets would have to be banned from the study because they cannot be detected in time, even by the "perfect" baseline system.

2. No-detects were treated as targets detected at zero slant range. An alternative would have been to ignore the no-detects and base computations only on the number of actual detections. The decision to assign a zero value to no-detects resulted from the observation that the number of no-detects increased with decreasing resolution and to a slight degree with increasing error rate.

Targets which most often caused no-detects were the Piru Bridge (#12) and the Bridge 180 Degrees (#2). This is not surprising since these targets are small and have low contrast with their surround. Since no-detects showed a definite trend, it was decided that they represented real data and their effects should be included in the statistical calculations.

Assuming zero slant range results in a stiff penalty, this assumption may be justified if missing the target constitutes a mission failure.

3. Comparisons were based on calculated means. The mean was used because*
 - a. It is a commonly accepted quantity.
 - b. It lends itself to further statistical treatment. For example, the means of several sets of data can always be combined into an overall mean for all the data. Also, means can be compared statistically for the significance of obtained difference.
 - c. It is relatively reliable in the sense that for sample data, it is generally not strongly affected by chance as some of the other measures of location.

D.2 Basic Calculations

The values of Time-to-Detect-to-Ground-Zero reported in Appendix B of this report were converted to slant range and are shown in Tables D-1 through D-10. For each target, a mean and standard deviation were calculated according to the formulas:

Mean $\bar{X} = \frac{\sum X}{n}$ where each X is a slant range value and n is the number of observations.

Unbiased Sample Standard Deviation S = $\sqrt{\frac{\sum X^2 - \frac{(\sum X)^2}{n}}{n-1}}$ This is the form used by the Hewlett Packard HP25 on which the S values were computed.

D.3 Normalization

All values of \bar{X} and S in Tables D-1 through D-10 were normalized to the mean for the corresponding target of the baseline runs. Thus all baseline

* Freund, John E., "Statistics, A First Course", Englewood Cliffs, New Jersey, Prentice-Hall, 1970.

Table D-1 Slant Range at Detection for Baseline - Data from Table B-1

Observer	Target No.											
	14	17	7	12	2	11	13	3	5	16		
1	16284	13195	13881	24541	2556	11826	13881	11826	8754	18346		
2	16628	13881	9095	13881	18346	13538	13538	7737	10458	11141		
3	17659	11141	9776	24885	8415	9776	15940	12510	8076	13881		
4	15254	10458	11826	6724	12510	11483	11141	9095	6389	16971		
5	18690	11141	9776	13195	17315	14224	7737	14567	13881	14567		
6	15597	9435	7399	9095	5058	14567	13195	7737	11826	20066		
7	17315	7061	9776	10458	4403	22131	14567	8415	8415	18003		
8	16628	11826	11826	17315	5720	13538	13538	8415	12853	21442		
9	13195	10800	6389	13538	7737	14224	11141	8415	15940	*		
10	17315	10117	5388	11826	8415	13881	14567	7061	8415	15254		
11	17315	13195	6389	8415	*	19378	14567	12510	9776	20066		
12	18003	11141	8415	8415	7737	22131	20066	15254	10458	21442		
13	15254	10458	8415	11826	7737	17315	13195	12510	11141	20066		

No Detects Slant
Range = Zero

Mean
(\bar{X})

Sample
Std. Dev.
(S)

16549 11065 9104 13393 8150 15223 13621 10466 10490 16250

% Correct
Identification

100 100 100 100 92 100 100 100 100 92

Mean
(\bar{X})

8829

17604

Sample
Std. Dev.
(S)

4889

3290

* No Detect

Table D-2 Slant Range at Detection for 512 x 1, BER = 0 - Data from Table B-2

Observer	Target No.															
	14	17	7	12	2	1	13	3	5	16						
1	15254	10458	9095	11826	7061	13195	9776	11141	9776	16628						
2	15254	9095	9095	12510	6389	10458	10458	8415	7737	13195						
3	16628	8415	9776	9776	5720	13881	12510	7737	15254	18003						
4	14567	10458	*	9095	6389	13195	9095	11826	7737	18003						
5	16628	11826	6389	10458	7061	18690	11826	11141	12510	15254						
6	18003	10458	9095	10458	5720	12510	12510	7061	9776	13881						
7	18003	9776	7061	8415	6389	7061	13195	*	7737	8415						
8	16628	9095	9095	10458	6389	17315	11141	11826	9776	7061						
Mean (\bar{X})	16370	9946	7448	10373	6389	13281	11312	8639	10032	13796						
Sample Std. Dev. (S)	1324	1107	3277	1339	652	3654	1498	3977	2623	4225						
% Correct Identification	100	100	88	100	100	100	100	88	100	100						
Mean (\bar{X})	8515										9878					
Sample Std. Dev. (S)	1263										2059					

No Detect Slant
Range = Zero

No Detects
Ignored

* No Detect

Table D-3 Slant Range at Detection for 512 X 1, BER = 10^{-4} - Data from Table B-3

Observer	Target No.															
	14	17	7	12	2	11	13	3	5	16						
1	13881	9095	8415	11826	4403	12510	7737	5720	5720	17315						
2	19378	9095	7737	9776	5720	13195	11141	8415	8415	18690						
3	17315	9095	9776	9095	5720	13195	12510	9095	8415	11826						
4	15254	7737	9776	6389	5058	11141	9776	8415	8415	11826						
5	18003	11141	8415	13195	5720	12510	11826	11141	9095	13195						
6	16628	10458	8415	10458	5720	15940	15940	15940	10458	12510						
7	13881	9776	7737	6389	6389	12510	9095	8415	5720	10458						
8	14567	11141	8415	7737	6389	10458	11826	2556	12510	16628						
No Detect Slant Range = Zero																
Mean (\bar{X})	16112	9691	8585	9350	5637	12682	11227	8670	8585	14053						
Sample Std. Dev. (S)	1986	1217	819	2411	2445	1675	2452	3872	2308	3088						
% Correct Identification	100	100	100	100	100	100	100	100	100	100						
No Detects Ignored																
Mean (\bar{X})																
Sample Std. Dev. (S)																

No Detect Slant
Range = Zero

No Detects
Ignored

Table D-4 Slant Range at Detection for 512 X 1, BER = 10^{-3} - Data from Table B-4

Observer	Target No.										
	14	17	7	12	2	11	13	3	5	16	
1	18003	7061	9095	*	5720	11141	9776	7061	*	9776	
2	16628	9776	8415	7061	5720	13195	9776	7737	10458	6389	
3	16628	7061	7737	*	5720	12510	11826	7737	12510	11141	
4	15940	5720	10458	*	*	11141	7061	7737	8415	9776	
5	15940	5720	8415	5720	6389	12510	9776	9095	5058	15940	
6	11826	5058	9776	13881	6389	7737	10458	13195	13195	9095	
7	13195	12510	8415	8415	5720	11141	9095	11141	11141	11826	
8	18690	11141	9776	11141	8415	13881	12510	11826	15254	11141	
Mean (\bar{X})	15855	7991	9010	5769	5506	11654	10032	9435	9492	10629	
Sample Std. Dev. (S)	2317	2766	910	5357	815	1827	1635	2303	4930	2763	
% Correct Identification	100	100	100	63	88	100	100	100	88	100	
Mean (\bar{X})				9244	6296				10862		
Sample Std. Dev. (S)				3278	986				3351		

No Detect Slant
Range = Zero

No Detects
Ignored

* No Detect

Table D-5 Slant Range at Detection for 512 X 1, BER = 10^{-2} - Data from Table B-5

Observer	Target No.										
	14	17	7	12	2	11	13	3	5	16	
1	15254	10458	7737	7737	5720	9095	12510	7061	9776	9776	
2	8415	7061	5720	8415	5058	7737	10458	7061	6389	11141	
3	7737	7737	6389	15254	5058	11826	11141	*	7737	7737	
4	13195	10458	5058	*	6389	10458	13195	8415	10458	10458	
5	14567	9776	7737	*	6389	7737	9776	9095	5720	12510	
6	14567	8415	13195	9776	5058	9776	11826	8415	5720	11826	
7	9095	9776	6389	7737	4403	10458	11141	7061	9095	14567	
8	10458	9095	7737	8415	6389	9776	9776	6389	6389	10458	
Mean (\bar{X})	11654	9095	7483	7162	5554	9605	11227	6685	7652	11056	
Sample Std. Dev. (S)	3144	1217	2549	5089	815	1370	1226	2826	1888	1950	
% Correct Identification	100	100	100	75	100	100	100	88	100	100	
Mean (\bar{X})				9556				7642			
Sample Std. Dev. (S)				2889				991			

No Detect Slant
Range = Zero

No Detects
Ignored

* No Detect

Table D-6 Slant Range at Detection for 512 X 0.75, BER = 0 - Data from Table B-6

Observer	Target No.										
	14	17	7	12	2	11	13	3	5	16	
1	16628	9095	12510	7737	5720	18003	12510	13195	11141	15254	
2	13888	9776	9095	9776	8415	10458	9776	8415	10458	13881	
3	17315	10458	7737	7737	5720	13881	18690	13195	15254	16628	
4	18003	9095	13195	7737	*	17315	18003	11141	9776	16628	
5	16628	9095	12510	8415	6389	13195	12510	12510	9095	13195	
6	12510	9776	9095	9776	6389	15254	*	9776	*	13881	
7	19378	8415	9776	10458	5720	17315	9776	17315	18003	15940	
8	14567	8415	7737	9776	5720	18003	11141	8415	6389	13881	
Mean (\bar{X})	16112	9265	10202	8925	5509	15426	11546	11740	10006	14911	
Sample Std. Dev. (S)	3144	664	2185	1071	2445	2740	5721	3035	5455	1300	
No Detect Slant Range = Zero											
% Correct Identification	100	100	100	100	88	100	88	100	88	100	
Mean (\bar{X})					6296		13201		11445		
Sample Std. Dev. (S)					986		3693		3925		
No Detects Ignored											

* No Detect

Table D-7 Slant Range at Detection for 512 X 0.75, BER = 10^{-3} - Data from Table B-7

Observer	Target No.									
	14	17	7	12	2	11	13	3	5	16
1	20754	9776	8415	7737	6389	10458	11826	6389	13195	10458
2	11826	7737	6389	7061	5720	12510	11141	10458	4403	11826
3	15940	9095	7737	4403	5720	16628	16628	12510	15254	*
4	15254	9095	9776	7061	6389	13195	15254	11141	12510	13881
5	19378	8415	9776	8415	7061	12510	10458	12510	9776	8415
6	16628	7737	7061	7737	5058	13881	11141	5720	8415	9095
7	11826	8415	6389	*	5720	11141	11141	7737	7061	13881
8	13881	11826	5720	5720	5058	*	11826	7061	5720	7737
Mean (\bar{X})	15683	9010	7652	6010	5887	11289	12425	9180	9520	9407
Sample Std. Dev. (S)	3310	1328	1548	2813	734	4871	2179	2826	3881	4388
No Detect Slant Range = Zero										
% Correct Identification	100	100	100	88	100	88	100	100	100	88
Mean (\bar{X})				6876		12903				10756
Sample Std. Dev. (S)				1377		2013				2521
No Detects Ignored										

* No Detect

Table D-8 Slant Range at Detection for 256 X 2, BER = 0 - Data from Table B-8

Observer	Target No.									
	14	17	7	12	2	1	13	3	5	16
1	15254	9776	9776	6389	6389	10458	11826	7061	6389	9776
2	13881	15940	*	7737	6389	9095	11826	5720	5720	11826
3	18690	13881	8415	8415	*	12510	7737	14567	15254	16628
4	*	13881	9095	7061	7061	*	10458	6389	5720	10458
5	15254	15254	*	7737	5720	*	7737	6389	*	9776
6	15254	12510	9095	7737	7737	12510	13881	7737	9776	10458
7	9095	*	7061	7737	5720	9776	17315	5720	8415	10458
8	13881	*	14567	6389	*	13881	20754	8415	11141	17315
Mean (\bar{X})	12660	10154	7247	7399	4875	8527	12682	7737	7788	12082
Sample Std. Dev. (S)	5792	6528	5007	670	3097	5480	4495	2930	4510	3088
% Correct Identification	88	75	75	100	75	75	100	100	88	100
Mean (\bar{X})	14473	13540	9668		6503	11372			8916	
Sample Std. Dev. (S)	2865	2198	2570		786	1868			3486	

No Detect Slant
Range = Zero

No Detects
Ignored

* No Detect

Table D-9 Slant Range at Detection for 256 X 2, BER = 10^{-3} - Data from Table B-9

Observer	Target No.									
	14	17	7	12	2	11	13	3	5	16
1	*	8415	*	*	*	9095	13195	5720	9776	11826
2	9776	*	*	*	11141	14567	8415	6389	5720	17315
3	16628	11826	7061	6389	*	12510	16628	9776	7061	15254
4	16628	7737	7061	7737	5720	11141	10458	9095	5720	15254
5	17315	9095	8415	*	6389	12510	9776	9095	19378	18690
6	15940	10458	7061	8415	7737	15254	15254	7061	7061	15254
7	15254	11141	7061	*	*	14567	9095	7061	7737	11141
8	17315	11141	4403	9095	7737	13195	9776	7061	7737	18690
9	13195	5058	7737	*	*	10458	10458	11141	5720	10458
Mean (\bar{X})	13559	8311	5417	3514	4298	12586	11445	8038	8415	14873
Sample Std. Dev. (S)	5627	3762	3277	4286	4401	2131	2860	1779	4301	3088
No Detect Slant Range = Zero										
% Correct Identification	89	89	78	44	56	100	100	100	100	100
Mean (\bar{X})	15256	9359	6971	7909	7745					
Sample Std. Dev. (S)	2591	2259	1245	1155	2090					
No Detects Ignored										

* No Detect

Table D-10 Slant Range at Detection for 256 X 2, BER = 0, Interpolation Data from Table B-10

Observer	Target No.										
	14	17	7	12	2	11	13	3	5	16	
1	15940	11141	8415	6389	*	9776	9095	7737	7061	10458	
2	13195	11141	7061	5720	*	13881	11141	7061	7061	8415	
3	15940	10458	7061	*	6389	15940	12510	8415	18003	15940	
4	16628	10458	9095	6389	5720	18003	*	16628	11141	5720	
5	13195	7737	6389	7061	*	8415	10458	5720	8415	15940	
6	15254	9095	*	6389	*	*	9776	6389	7061	*	
7	15254	8415	8415	*	*	17315	13881	11141	19378	11141	
8	16628	9776	8415	7737	7061	19378	15254	11826	13881	18003	
Mean (\bar{X})	15254	9776	6855	4959	2396	12839	10264	9350	11483	10702	
Sample Std. Dev. (S)	1324	1217	2913	3117	3342	6546	4631	3663	5035	3088	
No Detect Slant Range = Zero											
% Correct Identification	100	100	88	75	38	88	88	100	100	88	
Mean (\bar{X})			7836	6614	6390	14672	11731			12231	
Sample Std. Dev. (S)			990	695	671	4195	2250			4511	
No Detects Ignored											

* No Detect

targets have a mean detection-slant range of 1.00 or 100%. Values for \bar{X} and \bar{X}^2 for each target of each system were calculated and saved. Normalized results, although not expressed in absolute slant range, show the relative performance of the various systems.

D.4 System Comparison

Using the \bar{X} and \bar{X}^2 values calculated in D.3 above, a Grand Mean and Sample Standard Deviation was computed for each of the ten sets of parameters (including the baseline). These results are plotted in Figure D-1. The values are positioned so that sets of parameters representing a given system are grouped together. The dot in the center represents the normalized grand mean for the particular set of parameters. The vertical bars represent the range included by \pm one sample standard deviation. The circled numerals are the number of no-detects for each set of parameters. The dotted bars on the 512 x 1 x OBER and 256 x 2 x OBER are discussed in Section D.5 of this appendix.

The mean values follow a trend which might be expected in an intuitive sense, namely:

1. The 512 sample density, 1 bit per sample, 1 frame per second system, has a mean detection slant range which is only 14% shorter than the baseline system; its data rate, however, is $24 \times 6 = 144$ times lower than the 24 frame per second, 6 bit PCM baseline system.
2. The mean values of the detection slant ranges for the three compressed systems (512 x 1, 512 x 0.75 and 256 x 2) decrease with increasing transmission error rate.
3. The performance of the 512 x 1 and 512 x 0.75 systems are essentially the same. NOTE: The zero BER points of the two systems are somewhat different, however, the 10^{-3} mean values are similar. There is no intuitive explanation for the difference so additional tests of the 512 x 0.75 system with zero BER were run using laboratory personnel. These tests produced an overall mean value approximately equal to that of the 512 x 1 system. This limited sample result suggests that the observers used in the original 512 x 0.75 test may have all been exceptionally good. It should be pointed out that the 512 x 1 system produces better subjective quality than the 512 x 0.75 system.
4. The 256 x 2 system (with and without interpolation) produces lower mean detection slant ranges and greater deviations than the 512 systems. The large numbers of no-detects are particularly disturbing because, in a sense, they indicate complete mission failure.

D.5 Determination of Data Significance

Analysis of the results shown in Section D.4 was complicated by the organization which was specified for the test program. It would be desirable to determine the degree of confidence in a hypothesis that the distribution of means is due to different system parameters and not merely to chance. It would be desirable to know what portion of the variances (actually standard deviations are plotted) is due to operator differences, what portion is due to

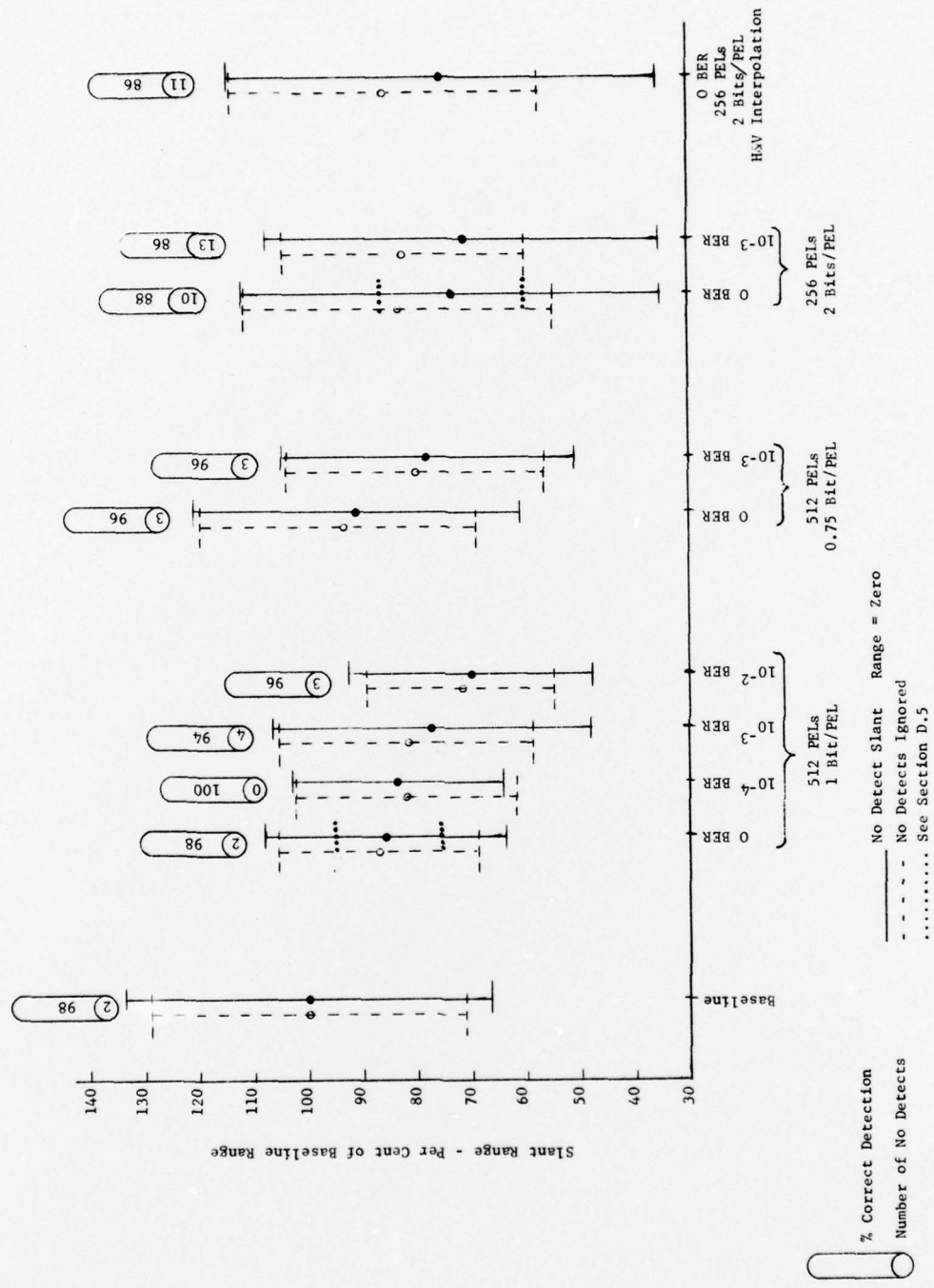


Figure D-1 Plot of Means and Sample Standard Deviations

target differences, what portion is due to operator learning, and finally, what portion is due to system parameter differences. Unfortunately, although many data points were taken, only small groups of data can be tested. The following tests and analyses were conducted, mainly to compare 512 and 256 performance:

1. The first step was to compute the standard error of the mean for each set of system parameters. This was accomplished by dividing each sample standard deviation by \sqrt{n} , where n = number of observers x number of targets for a given set of parameters. Hence:

$$\sigma_{\bar{x}} = \frac{S}{\sqrt{n}}$$

The values which are plotted as bars around the mean value in Figure D-2 represent the expected standard deviation of the mean if a large number of samples had been taken with other observers and targets (all taken from the same populations of observers and targets). The significance given to the results of Figure D-2 is that the degree of overlap between two bars is indicative of the degree of confidence that true system differences are shown by the data. No-overlap suggests large real differences, large overlap might suggest that random effects are significant. The results generally show that differences are significant except between the 256 x 2 system with interpolation and the 256 x 2 system without interpolation. Interpolation does not seem to be worthwhile from a target detection point of view. Its merit would have to be determined strictly from an aesthetic point of view.

2. A χ^2 (chi squared) test was performed on the data points of the 512 x 1 system with zero BER and on the 256 x 2 system with zero BER to test the hypothesis:

H: there is no significant difference between the 512 and 256 results, the result confounded by operator variability.

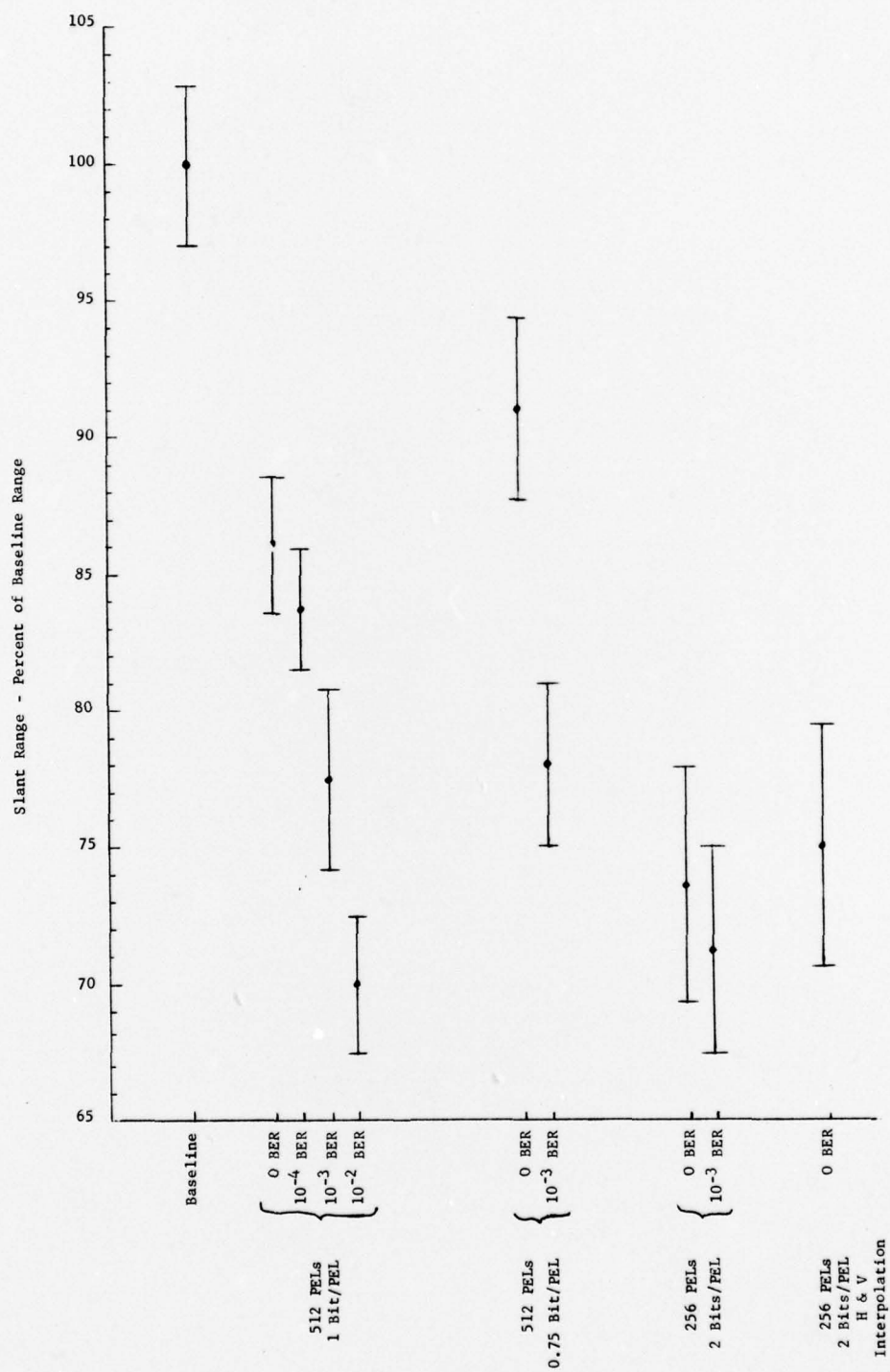


Figure D-2 Means and Estimates of Standard Deviation of Means

The following table was constructed listing the number of data points which fall within each range:

Normalized Range Interval (%)	512 x 1 x 0 BER	256 x 2x 0 BER	$P_i = \frac{1}{n} \sum_j V_{ij}$
> 105	$V_{11} = 14$	$V_{12} = 14$	$P_1 = 0.175$
90-105	$V_{21} = 20$	$V_{22} = 11$	$P_2 = 0.194$
80-90	$V_{31} = 17$	$V_{32} = 10$	$P_3 = 0.169$
65-80	$V_{41} = 23$	$V_{42} = 11$	$P_4 = 0.213$
< 65	$V_{51} = 6$	$V_{52} = 34$	$P_5 = 0.250$

$$\chi^2 = \sum_{i,j} (V_{i,j} - N_j P_i)^2 / N_j P_i \quad (D1)*$$

$$n_1 = 80, n_2 = 80, n = 160$$

Solving equation D1,

$$\chi^2 = 28.25$$

For this example

$$m = (r-1)(s-1) = 4$$

since:

$$s = 2, r = 5$$

From a χ^2 probability table*, a value of $E = 10^{-5}$ was determined for 4 degrees of freedom and $\chi^2 = 28.25$. Therefore, the probability of the hypothesis being true that "there is no significant difference between the 512 x 1 system with zero BER and the 256 x 2 system with zero BER, the result confounded by operator variability" is one chance in 10^5 . Or stated differently, the probability of differences between the systems being due to chance is one in 10^5 .

3. The general trend of the test results was as expected. For example, the detection range decreased as bit error rate increased, and also decreased as resolution decreased. Because of the independent groups experimental design, group capability

* Handbook of Mathematical Functions with Formulas, Graphs, and Mathematical Tables," AM S55, National Bureau of Standards, March 1965.

is correlated with sets of parameters and it is not possible to obtain "hard" evidence that the trends are free from observer differences. However, "soft" evidence that groups of observers have similar capability can be inferred by showing that observers within a group are similar. Since all observers were taken from a single population of "airmen" and no attempt was made to screen or organize the observers into groups with similar talent, a low observer standard deviation would suggest that general operator variability was low and, therefore, had little effect on the comparison of systems.

To make an observer comparison, the slant range measurements of each observer were averaged over all ten targets for a given set of conditions. These means represent the performance of each observer since all observers viewed the same targets, in the same order, under similar test conditions. The eight means thus determined for each set of parameters were averaged and their sample deviation was calculated. The results are shown as dashed lines in Figure D-1. For the 512 system, the observer standard deviation is 0.41 of the total deviation, for the 256 system it is 0.34 of the total deviation.

Since the standard deviation among observers for each set of parameters is moderate compared to the total standard deviation for the parameter set, it can be inferred that observer variability between sets of parameters is small, and does not significantly influence test results.